DOKUZ EYLÜL UNIVERSITY
GRADUATE SCHOOL OF NATURAL AND APPLIED SCIENCES

A DETAILED ANALYSIS OF THE EFFECTS OF VARIOUS COMBINATIONS OF HEART RATE VARIABILITY INDICES IN CONGESTIVE HEART FAILURE

by
Yalçın İŞLER

October, 2009
İZMİR

A DETAILED ANALYSIS OF THE EFFECTS OF VARIOUS COMBINATIONS OF HEART RATE VARIABILITY INDICES IN CONGESTIVE HEART FAILURE

A Thesis Submitted to the
Graduate School of Natural and Applied Sciences of Dokuz Eylül University
In Partial Fulfillment of the Requirements for the Degree of Doctor of Philosophy in Electrical and Electronics Engineering Program

by
Yalçın İŞLER

October, 2009
İZMİR

Ph.D. THESIS EXAMINATION RESULT FORM

We have read the thesis entitled "**A DETAILED ANALYSIS OF THE EFFECTS OF VARIOUS COMBINATIONS OF HEART RATE VARIABILITY INDICES IN CONGESTIVE HEART FAILURE**" completed by **YALÇIN İŞLER** under supervision of **ASSOC.PROF.DR. MEHMET KUNTALP** and we certify that in our opinion it is fully adequate, in scope and in quality, as a thesis for the degree of Doctor of Philosophy.

Assoc. Prof. Dr. Mehmet KUNTALP

Supervisor

Prof. Dr. Cüneyt GÜZELİŞ	Assoc. Prof. Dr. Özgür ASLAN
Thesis Committee Member	Thesis Committee Member
Prof. Dr. Musa Hakan ASYALI	Asst. Prof. Dr. Olcay AKAY
Examining Committee Member	Examining Committee Member

Prof. Dr. Cahit HELVACI
Director

ACKNOWLEDGMENTS

I would like to thank to my supervisor, Assoc. Prof. Dr. Mehmet Kuntalp, for his undying patience, confidence, encouragement, and valuable suggestions. Thank you for giving tirelessly of your time, expertise, smart ideas, and guiding hand in helping me achieve my goal.

I would like to thank my committee members, Prof. Dr. Cüneyt Güzeliş and Assoc. Prof. Dr. Özgür Aslan, for the benefit of their collective wisdom, helpful comments, and generously sharing their time and talents to guide me through the doctoral program.

I would like to give thanks to my colleagues, Murat Şen, Yakup Kutlu, M. Alper Selver, and Savaş Şahin, for their assistance, encouragement and tolerance.

Also, I would like to thank Assoc. Prof. Dr. Mahmut Özer for leading me into this wonderful biomedical world, in which I would love to develop my future career.

I would like to thank my parents for their constant love and support. I have never been able to find suitable words that describe their trust.

Last but not least, I would like to thank my wife and my son, for their support, love, trust and especially for keeping the house running and me alive during the thesis.

Yalçın İŞLER

A DETAILED ANALYSIS OF THE EFFECTS OF VARIOUS COMBINATIONS OF HEART RATE VARIABILITY INDICES IN CONGESTIVE HEART FAILURE

ABSTRACT

The major purpose of the heart is to circulate blood, which carries oxygen and nutrients to the body. Heart Failure is a decreased ability of the heart to either fill itself with blood or emptying it. Because the congestion, which is the fluid accumulation in various parts of the body, is common in the patients with heart failure, this disease is also named as Congestive Heart Failure (CHF). Although, at times, the diagnosis of heart failure is straightforward, it often challenges physicians because particular aspects of the syndrome lead to confusion. When heart failure is suspected, certain elements of the physical examination aid in the diagnosis. Unfortunately, the examination often does not yield enough information for confirmation. Although several diagnostic criteria schemes are available, their clinical utility is questionable, and their concordance is poor.

The physicians have long relied as a gold standard on echocardiography for the diagnosis of CHF patients. It has not been possible to use a simple method as ECG for this purpose because of the many difficulties in interpreting the ECG output. Therefore, it would be very helpful both for physicians and patients alike if it is possible to diagnose CHF from an ECG record. The main purpose of this thesis is accomplishing such a purpose, i.e. detecting CHF from an ECG output.

Heart Rate Variability (HRV) analysis has been the subject of many studies of clinical origin. Majority of these studies have used HRV measures as predictors of the risk of mortality (prognosis) for cardiac patients. Only a few studies have been focused on using HRV measures for diagnostic purpose. This thesis is focused on exploring advanced techniques of HRV analysis in an attempt to develop robust methods for diagnosing patients with CHF from an ECG records. This study considers presenting new feature extraction method, developing new preprocessing techniques, and finding an optimal k-Nearest Neighbors classifier to discriminate the patients with CHF from

the normals and to discriminate systolic versus diastolic dysfunction in CHF patients. The wavelet entropy, which has been used in the other biomedical signal classification schemes like EEG spike detection, is also used as an HRV measure to enhance the performance of the classifier. Furthermore, lagged Poincare plot measures are also included in the study. A new preprocessing technique, called as heart rate normalization, is also used to enhance the performance in discriminating the CHF patients from normals and determining the type of dysfunctionality as systolic or diastolic in CHF patients. In addition, Genetic Algorithm is used to select the optimal features from among a large set. The whole process is summarized as a single flowchart, which will be a useful guide for novice researchers.

In order to conduct these studies, open-source databases from MIT/BIH are used to discriminate the patients with CHF from normal subjects and ECG records from the Faculty of Medicine in Dokuz Eylül University to discriminate systolic CHF patients from diastolic ones. The results show that heart rate normalized analysis of HRV can be used to achieve more accurate results for diagnosing the patients with CHF. In addition, wavelet-entropy based frequency-domain measures seem to be useful in the diagnosis. On the other hand, higher-lagged Poincare plot measures seem to be useless in the diagnosis. As a result, this study achieves the overall accuracies of 93.98% in discriminating the CHF patients from normal subjects and 100% in discriminating systolic versus diastolic dysfunctionality in CHF patients, which are the highest values in the literature.

Keywords: Electrocardiogram, Heart rate variability, Congestive Heart Failure, Normalization, Pattern recognition.

KONJESTİF KALP YETMEZLİĞİNDE KALP HIZI DEĞİŞKENLİĞİ İNDİSLERİNİN ÇEŞİTLİ VARYASYONLARININ ETKİLERİNİN AYRINTILI ANALİZİ

ÖZ

Kalbin asıl görevi vücut için gerekli oksijen ve besinleri taşıyan kanı dolaştırmaktır. Kalp Yetmezliği, kalbin doldurma veya boşaltma ile ilgili yeteneklerinin azalması durumudur. Konjestiflik (vücudun çeşitli yerlerinde sıvı birikmesi durumu) bu rahatsızlığa sahip hastalarda çok yaygın olduğu için bu rahatsızlığa Konjestif Kalp Yetmezliği (KKY) ismi de verilmektedir. Kalp yetmezliğinin teşhisi günümüzde basit olmasına rağmen, hastalık belirtilerinin çoğu diğer hastalıkların belirtileri ile karıştırıldığı için özellikle pratisyen hekimler teşhiste zorlanmaktadırlar. Kalp yetmezliğinden şüphelenildiğinde, teşhiste bazı belli başlı fiziksel inceleme unsurları uygulanmaktadır. Ne yazık ki, bu inceleme sık sık yeterli bilgiyi vermemektedir. Her ne kadar birçok teşhis ölçütleri mevcut olsa da, bunların klinik geçerlikleri hala sorgulanmakta ve birbirleri ile uyumlu sonuç verememektedirler.

Özellikle veri madenciliği ve karar verme teknikleri üzerine çok gelişmiş teknikler sunulmuş olmasına rağmen, tıp doktorları uzun zamandır sınırlı sayıdaki yöntemlerden yararlanmaktadırlar. Kalbin patolojik değişimlerinin erken tespitinde kullanılan elektrokardiyogram (EKG) en yaygın ve en başarılı teşhis yöntemidir. Ne yazık ki, EKG çıktısının değerlendirilmesinde EKG'nin yapısı ve kayıt yöntemleri nedeniyle bazı güçlüklerle karşılaşılmaktadır.

KKY kalp hızı değişkenliği (KHD) üzerine yapılan bir çok çalışmaya konu olmuştur. Bu çalışmaların çoğunluğu KKY ölçümlerini ölüm riskinin kestirilmesi için kullanmaktadır. Buna rağmen, sadece birkaç çalışma teşhis amacıyla KHD ölçümlerinin kullanılması üzerinedir. Bu çalışmada, KKY hastalarının teşhisi için daha iyi sonuç verecek KHD analizi ileri tekniklerin geliştirilmesi için yeni yöntemler araştırılması üzerine odaklanmıştır. Bu çalışma hem KKY hastalarının normal kişilerden hem de sistolik KKY hastalarının diastolik KKY hastalarından ayrılması için yeni öznitelik

çıkarma yöntemleri önerilmesi, ön işlem teknikleri geliştirilmesi ve en iyi k-Yakın Komşuluk sınıflandırıcının bulunması üzerine yapılan araştırmaları sunmaktadır. Daha önce EEG'den iğcik tespiti gibi diğer biyomedikal işaretlerinde başarı ile uygulanmış olan Dalgacık entropisi sınıflandırıcı performansını iyileştirmek için yeni bir KHD özniteliği olarak önerilmiştir. Ayrıca, farklı adımlardaki Poincare çizimi ölçümleri de çalışmaya dâhil edilmiştir. Kalp hızı normalleştirme işlemi olarak bilinen yeni bir ön işleme yöntemi de sınıflandırıcı başarımını arttırmak için kullanılmıştır. Üstelik en uygun öznitelik kombinasyonunu seçmek için Genetik Algoritma kullanılmıştır. Son olarak, tüm çalışma yeni başlayan araştırmacılara faydalı bir rehber olacak şekilde tek bir akış şeması olarak özetlenmiştir.

Bu çalışmaları yürütmek için, KKY hastalarının normal kişilerden ayırt edilmesinde MIT/BIH tarafından sağlanan ve herkesin erişimine açık olan veritabanları ve sistolik KKY hastalarının diastolik KKY hastalarından ayırt edilmesinde ise Dokuz Eylül Üniversitesi Tıp Fakültesi tarafından sağlanan EKG kayıtları kullanılmıştır. Elde edilen sonuçlar, kalp hızı normalleştirilmiş KHD analizinin KKY hastalarının teşhisinde daha başarılı sonuçlara ulaşılabileceğini göstermektedir. Üstelik dalgacık entropisi tabanlı frekans alanı ölçümlerinin kullanılmasının teşhiste faydalı olabileceği görülmektedir. Diğer yandan, yüksek adımlı Poincare çizimi ölçümlerinin teşhiste faydalı olduğu görülmemiştir. Sonuç olarak, bu çalışma ile KKY hastalarının normal kişilerden ayrılmasında %93,98 ve sistolik KKY hastalarının diastolik KKY hastalarından ayrılmasında %100 genel başarım sonuçlarına ulaşılmıştır. Bu değerler literatürdeki en yüksek değerlerdir.

Anahtar sözcükler: Elektrokardiyogram, Kalp hızı değişkenliği, Konjestif kalp yetmezliği, Normalleştirme, Örüntü tanıma.

CONTENTS

CHAPTER ONE
INTRODUCTION

1.1 General Goals

The heart has been one of the most studied subjects since 400 B.C. The pump function of the heart was stated by Plato as "it pumps particles as from a fountain into the channels of the veins, and makes the stream of the veins flow through the body as through a conduit" (Berne & Levy, 1997). Since that time, information about the heart and various diseases that may affect its functioning has increased (Langer, Frank, & Brady, 1976).

To circulate blood, which carries oxygen and nutrients to the body, is the major purpose of the heart. In a normal heart, 50% to 70% of the blood in the pumping chambers is ejected out to the body with each contraction of the heart muscle, which is called ***ejection fraction*** (EF). The normal heart has strength far beyond what we need every day. Hence, even when the EF is low, the heart can often pump well enough for us to enjoy the usual activities in our lives (Berne & Levy, 1997).

Heart Failure is a decreased ability of the heart to either fill or empty (Eberhart-Phillips, Fenaughty, & Rarig, 2003; Flavell & Stevenson, 2001). Because the congestion, fluid accumulation in various parts of the body, is common in the patients with heart failure, this disease is also named as Congestive Heart Failure (CHF) (Wilbur & James, 2005). CHF is the end stage of chronic cardiovascular disease and is one of the leading causes of death in the United States (Albert, 2000; Zambroski, 2003). An estimated five million patients with approximately 500,000 newly diagnosed cases and 250,000 deaths annually are affected (American Heart Association, 2006; Gura & Foreman, 2004). Death of approximately 50 percent of patients is observed within five years of their diagnosis (American Heart Association, 2006). But many of them could be healed, especially if the disease could be detected at early stages.

Afterwards, it is one of the most disabling and lethal medical conditions of cardiovascular disease (Adams et al., 2000). It is the primary cause of hospitalizations, which translate into seven million hospital days annually with a 44 percent incidence

rate of readmission within six months (Gura & Foreman, 2004). It is a long-term chronic condition that gradually gets worse and requires more treatment to manage symptoms and control complications (Levy et al., 2001). CHF is the primary indication for three million physician visits each year. Although the symptoms can be treated, the disease cannot be cured (Boyd et al., 2004). Estimated annual expenditures for hospitalization costs are in excess of twenty billion dollars (Clark, Tu, Weiner, & Murray, 2003). Therefore, it is a costly cardiovascular condition (Albert, 2000).

Although the diagnosis of heart failure is straightforward, physicians are often challenged because particular aspects of the syndrome lead to confusion. For instance, a patient presenting with dyspnea, which is the most common symptom of heart failure, will have a comorbid condition that may also cause this symptom (e.g., chronic obstructive pulmonary disease, COPD). Additionally, a patient may present anywhere along a spectrum from asymptomatic to florid failure. Although the syndrome of heart failure is progressive, there are peaks and valleys along the way, and the point in time when a patient is likely to have an impact on the time to diagnosis. Simple clinical tests are generally unhelpful in confirming heart failure. In addition, because heart failure is a clinical diagnosis, physicians sometimes disagree about it, resulting in delayed interventions. In elderly patients, making the diagnosis is more treacherous, because of a relative absence of typical signs and symptoms and the possibility of attributing heart failure symptoms to other conditions (Gillespie, 2006).

The first step in diagnosing heart failure is to obtain a complete clinical history (Shamsham & Mitchell, 2000). Although heart failure cannot be predicted using single historical record (Wilbur & James, 2005), dyspnea, fatigue, or decreased exercise tolerance are generally present. Less commonly, fluid retention is present as the primary complaint. Dyspnea with exertion is present in most patients who have heart failure, and its complete absence should cause the clinician to reconsider the diagnosis (Davie, Francis, Caruana, Sutherland, & McMurray, 1997). However, dyspnea and other symptoms of heart failure are unreliable especially in the elderly; therefore, these have poor specificity for heart failure (Dosh, 2004; Gillespie, 2006). A previous history of myocardial infarction (MI) may be the most useful element, because it appears to be more strongly associated with the diagnosis of heart failure than other historical items,

and it is a known risk for developing heart failure (Davie et al., 1997). Other historical factors should include risk factors for heart failure, such as hypertension and diabetes, because these are associated with the ultimate development of the syndrome and have implications for its management.

When heart failure is suspected, certain elements of the physical examination aid in the diagnosis (Wilbur & James, 2005). Unfortunately, enough information for confirmation is not yielded by the examination. Although there are several diagnostic criteria schemes (e.g., Framingham, Boston, and others), their clinical utility is still questionable and their concordance is poor (Di Bari et al., 2004).

Clinical assessment is mandatory before detailed investigations are conducted in patients with suspected heart failure, although specific clinical features are often absent and the condition can be diagnosed accurately only in conjunction with more objective investigation, particularly echocardiography (Davies, Gibbs, & Lip, 2000). In the last decades, many clinical guidelines have been published on the diagnosis and treatment of heart failure. The assessment of the value diagnostic tests, e.g. electrocardiography, echocardiography, chest X-ray, in addition to readily available diagnostic parameters from the clinical assessment has been used (Fig. 1.1) (Chiarugi, Colantonio, Emmanouilidou, Moroni, & Salvetti, 2008). Nonetheless, the optimal diagnostic strategy to detect heart failure in suspected patients remains largely unknown, notably in the every-day practice. Since heart failure is mostly managed and the hesitation in making use of echocardiography is especially observed, it is of interest to develop an optimal diagnosis technique in heart failure.

The medical doctors have relied on limited variable combination methods for much too long, especially while there are advanced methods of data mining and decision-making to be harnessed. The electrocardiogram (ECG) is the most common and most successful diagnostic method to detect early pathological changes of the heart. For several decades, computerized ECG interpretation has been used by clinicians and cardiologists as a much needed supplement (Macfarlane, 1992).

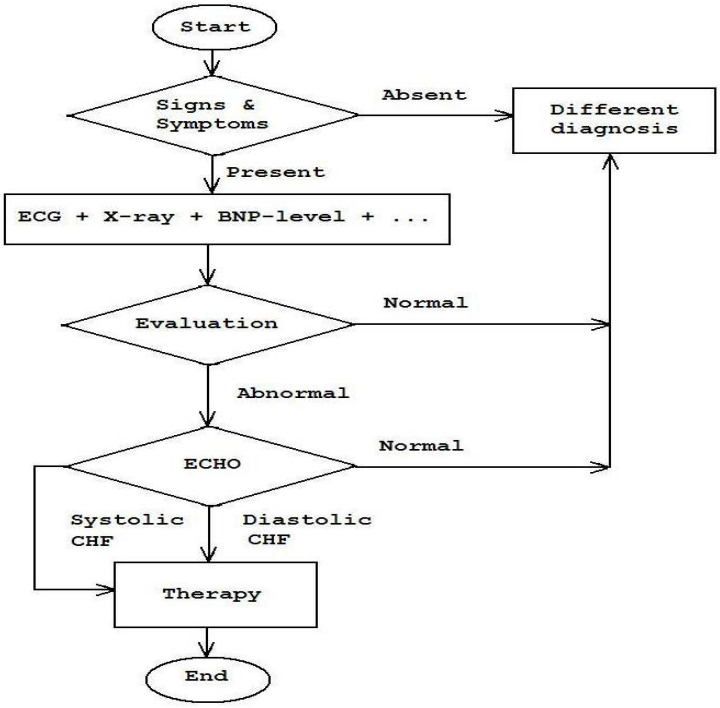

Figure 1.1 The flowchart of the general diagnosis process of CHF.

Unfortunately, because of the mechanisms of ECG and the recording methods, there are many difficulties in interpreting the ECG output. Because an ECG is the recorded potential difference at the body surface, the shape of the wave will be altered by any movement of sensors or anything influencing the electrical signals. Also since the physiological structures of humans vary, different people have different shapes of ECG. Therefore, the wave shape of the same disease may have many different versions. For some diseases, the clinical symptoms are seen in the ECG only when the disease is first apparent, whereas many cardiac diseases develop over a long time, e.g., heart failure. It may take time to make a diagnosis for such diseases. Sometimes, patients are told to carry a Holter ambulatory monitor which can record their ECG for about 24 hours. During a period of 24 hours, the number of ECG waves will be over 100,000. It is unreasonable to expect cardiologists to read all the waves and make a diagnosis in a short time.

Currently there are many integrated commercial ECG analysis systems, especially Holter analysis (Tompkins, 2000), to help cardiologists make a diagnosis. After several decades of development, some components of pattern recognition that improve their

performances are included by the major brands of the current generation of ECG interpretation systems (General Electric Company, 2009). However, none of them provide the function of detecting CHF yet.

In addition to discriminate the patients with CHF, from normal subjects, to distinguish diastolic heart failure from systolic heart failure based on physical findings or symptoms is also an important issue. Echocardiography has been used as a primary tool in the noninvasive assessment of cardiac systolic and diastolic dysfunctioning and is used to confirm the diagnosis of CHF (Gutierrez & Blanchard, 2004).

An essential element for treatment success is the reliable and precise diagnosis of CHF. Nonetheless, systolic dysfunction was determined in only 50% of cases. On questioning, distinguishing between systolic and diastolic heart failure, regarded echocardiography as crucial in diagnosis, followed by clinical signs and symptoms was reported routinely by only 46% of physicians (Hobbs, Korewicki, Cleland, Eastaugh, & Freemantle, 2005). According to their study, which is called IMPROVEMENT study, ECG tests in patients with CHF were performed by the most of the physicians (about 90%). In most of the cases, ECG study was performed at a local hospital with a usual waiting time of 48h. On the other hand, average waiting time for echocardiography was 1 month. Only in Belgium, it was performed within 48h from referral. In some countries including Spain, Sweden, and the UK, most patients with CHF (40%) could be waited to have the study done for 1-3 months. Thus, simple and reliable diagnostic procedures are very important for primary care physicians, who are responsible for the early diagnosis of CHF and implementation of an adequate therapy.

1.2 Specific Aims

The specific aims of this research are listed below in order to improve the performance of the diagnosis of patients with CHF from the normal subjects and discriminating whether the systolic dysfunction or the diastolic dysfunction in CHF patients using Heart Rate Variability Analysis:

1. to offer an ECG preprocessing technique to assess more accurate HRV data,
2. to explore effects of heart rate normalization process,

3. to find out the possible use of Wavelet entropy based measures,
4. to use the lagged Poincare plots' measures,
5. to use traditional patient information data, like age, and
6. to find out the optimal feature subset(s).

1.3 Significance

Heart diseases are the leading killers of Americans today. Over 60 million Americans have one or more heart diseases. In 1993, more than 950,000 people died from them-over 42 percent of all deaths in the United States. CHF is the major chronic disease among the elderly, accounting for 88 percent of heart failure deaths. In addition, older age is associated with a worse prognosis, and fewer than 20 percent of octogenarians with heart failure remain alive after five years (Clark et al., 2003). The mortality rate, two years following symptom onset, is about 35 percent with 80 percent mortality for men and 65 percent for women over the next six years (Artinian et al., 2003). Although these statistics are given for only US, these are also valid for other countries including Turkey. In addition, discriminating the systolic versus diastolic CHF patients is another challenge to determine adequate therapy and only 50% of patients are distinguished as their dysfunctionality according the recent survey (Hobbs et al., 2005), reducing the rate of early diagnosis. Early diagnosis of CHF will reduce the mortality rate and enhance the life quality of the patients.

1.4 Methods

The attempts of designing a k-Nearest Neighbors (KNN) classifier based automated ECG analysis system for early detection of heart failure is the main focus of this dissertation. The objective of this thesis is to present an integrated automated ECG diagnosing method which can be used with clinical Holter ECG data, with the capacity to be included in other ECG interpretation systems which do not detect heart failure. The KNN classifier and the Genetic Algorithm are the selected methods to conduct this study. Routine ECG data from lead II is used for the study. All the data, obtained from the well-known open databases in MIT/BIH websites (Goldberger et al., 2000) and recorded in Faculty of Medicine in Dokuz Eylül University, were annotated by experienced cardiologist(s).

CHAPTER TWO
PHYSIOLOGICAL BACKGROUND

In order to understand the function of the heart and heart diseases well, basic knowledge of the functional anatomy of the heart is necessary. In the following sections, the general terms on the circulatory system, the electrocardiogram, the heart rate variability concept, heart problems, and the brief information about the congestive heart failure are described with the related literature review.

2.1 The Circulatory System

The circulatory system carries nourishment and oxygen (O_2) to, and waste and carbon dioxide (CO_2) from, the tissues and organs of the body. The system can be considered as a closed loop hydraulic system (Webster, 1998).

2.1.1 Elementary Circulatory System

The simplified form of the human circulatory system is shown in Fig. 2.1. The heart can be considered as a pump to move blood through vessels called arteries and veins. Blood is carried away from the heart in arteries and is brought back to the heart in veins.

When blood is circulated through the body, it carries O_2 and nutrients to the organs and tissues and returns carrying CO_2 to be excreted through the lungs and various waste products to be excreted through the kidneys. The deoxygenated blood is returned to the right side of the heart via the venous system.

2.1.2 The Heart

The heart contains four chambers, which are used to form two separate pumps. Each pump consists of an upper chamber (atrium) and a lower chamber (ventricle). The high pressure output side of each pump is the ventricle, so the myocardium thickness in the ventricular region is considerably greater than it is in the atrial region (Webster, 1998).

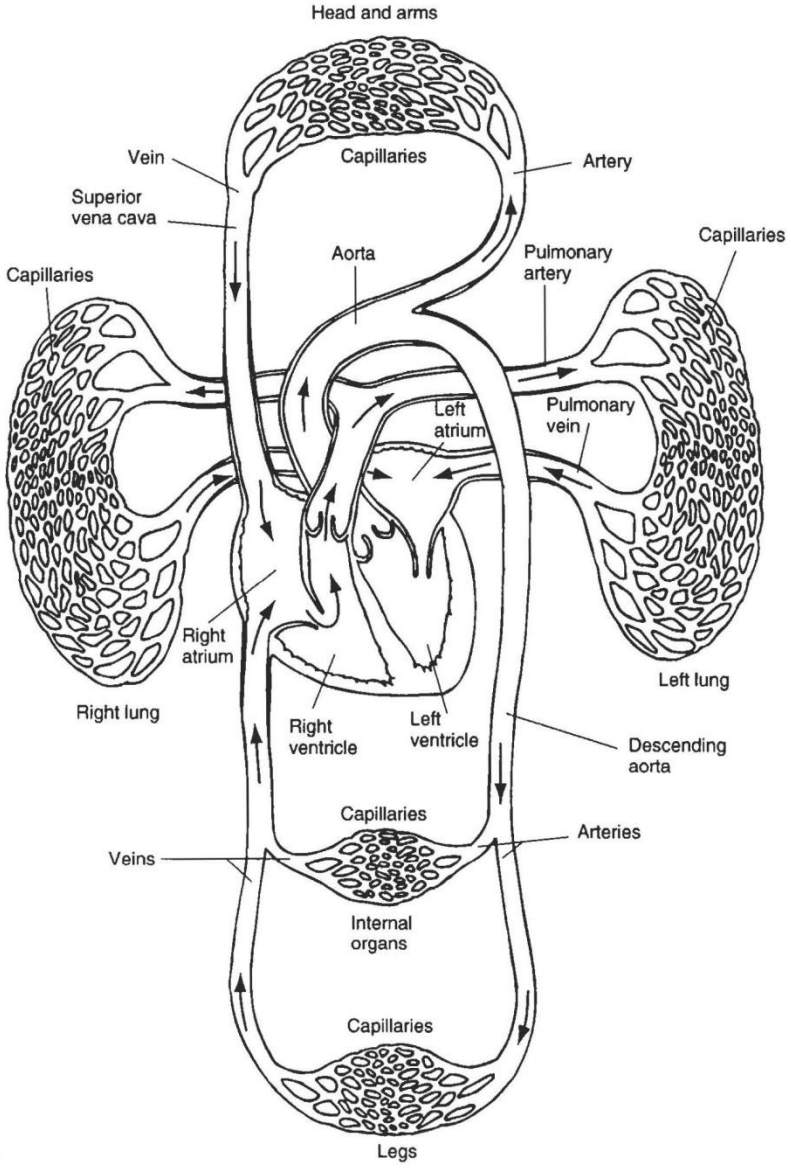

Figure 2.1 Human circulatory system (Webster, 1998).

The basic structure of the heart and the blood flow direction in the heart as well as the connected blood vessels are shown in Fig. 2.2. The unidirectional blood flow is realized by the sequential contraction of the heart chambers and the orientation of the cardiac valves. Reversal of blood flow causes the cusps of the valves to shut so as to prevent back-flow.

There are four valves in the human heart. The valve between the right atrium and the right ventricle is known as the tricuspid valve. It gets its name from the fact that it is formed of three cusp-shaped flaps of tissue arranged so that they will shut off and block

passage of blood in the reverse direction (from ventricles back to the atrium). The second valve, which is between the right ventricle and the pulmonary artery, is named for its shape: semilunar (half moon) valve. It prevents reverse flow (regurgitaion) of blood from the pulmonary artery to the right ventricle. Next, blood returning to the heart from the lungs must pass through the left atrium and the mitral valve (also known as a bicuspid valve for its shape) to the left ventricle. The last valve is the aortic-valve. Its shape is similar to the pulmonary valve and prevents regurgitation of blood from the aorta back to the left ventricle.

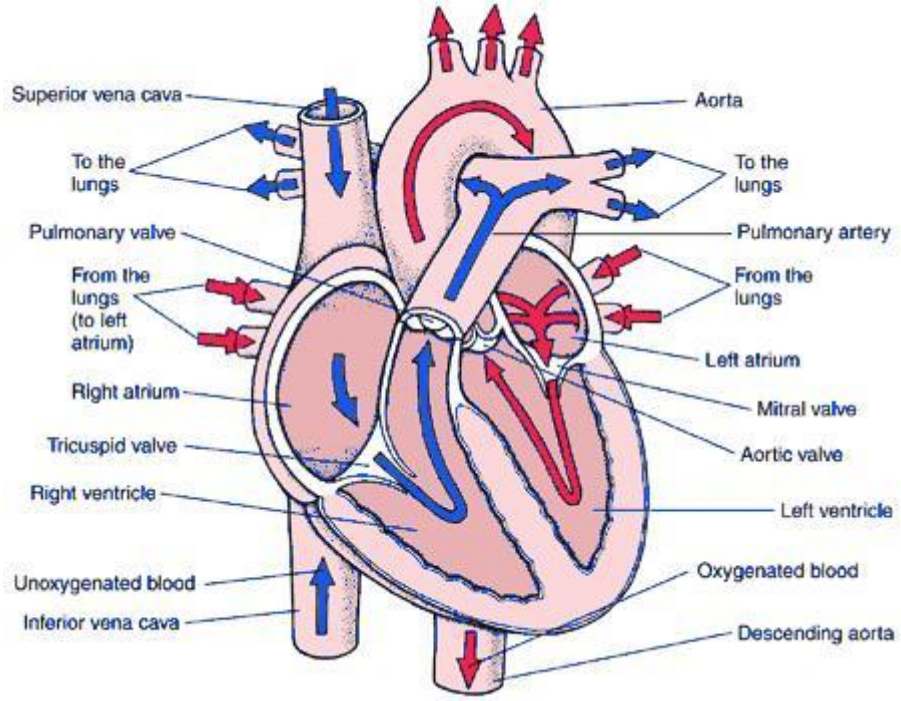

Figure 2.2 Schematic showing the structure of the heart and direction of blood flow through the heart (Webster, 1998).

The heart serves as a pump because of its ability to contract under electrical stimulus. When an electrical triggering signal is received, the heart will contract, starting in the atria, which undergo a shallow, ripple-like contracting motion. A fraction of a second later, the ventricles also begin to contract, from the bottom up, in a motion that resembles wringing out a dishrag or sponge. The ventricular contraction is known as ***systole*** and the ventricular relaxation is known as ***diastole***.

2.1.3 Electroconduction System of the Heart

The conduction system of the heart (Fig. 2.3) consists of the sinoatrial (SA) node, bundle of His, atrioventricular (AV) node, the bundle branches, and Purkinje fibers.

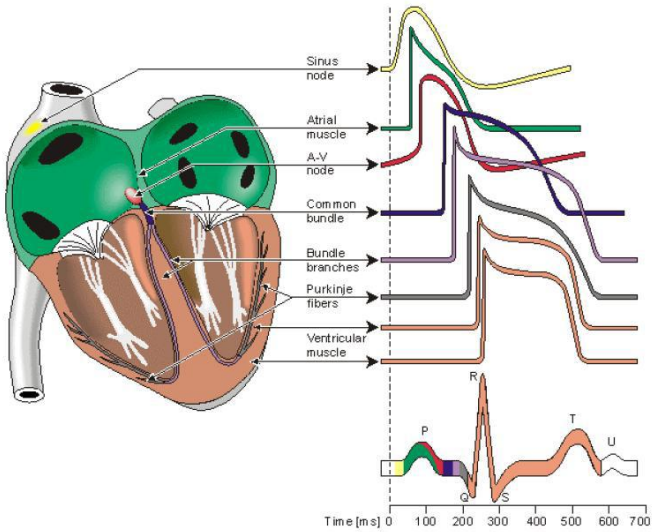

Figure 2.3 Electrophysiology of the heart. The different waveforms for each of the specialized cells found in the heart are shown. The latency shown approximates that normally found in a healthy heart (Webster, 1993).

The SA node serves as a pacemaker for the heart, and it provides the trigger signal. It is a small bundle of cells located on the rear wall of the right atrium, just below the point where superior vena cava is attached. The SA node fires electrical impulses through the bioelectric mechanism. It is capable of ***self-excitation*** (firing on its own).

When the SA node discharges a pulse, the electrical current spreads across the atria, causing them to contract. Blood in the atria is forced by the contraction through the valves to the ventricles.

There is a band of specialized tissue between the SA node and the AV node, however, in which the velocity of propagation is faster than it is in atrial tissue. This internal conduction pathway carries the signal to the ventricles.

It would not be desirable for the ventricles to contract in response to an action potential before the atria are empty of their contents. A delay is needed, therefore, to prevent such an occurrence; this is the function of the AV node. The action potential will reach the AV node 30 to 50 ms after the SA node discharges, but another 110 ms will pass before the pulse is transmitted from the AV node. The AV node operates like a delay line to retard the advance of the action potential along the internal electroconduction system toward the ventricles.

Conduction into the bundle branches is rapid, consuming only another 60 ms to reach the furthest Purkinje fibers. The muscle cells of the ventricles are actually excited by the Purkinje fibers. The action potential travels along these fibers at a much faster rate, on the order of 2 to 4 m/s. The fibers are arranged in two bundles, one branch to the left and one to the right.

2.1.4 Cardiac Regulation

The rate at which the heart beats in the absence of neurohumoral (nerve chemical) influences is referred to as the intrinsic heart rate. In heart transplant patients, the SA node - and hence the heart as a unit - cycles close to an intrinsic rate of 90-95 beats per minute (bpm). However, in a normal healthy individual, the beating of the heart is modulated to a slower rate by the influence of extrinsic nervous influence on the SA and AV nodes by the autonomic nervous system (ANS). Other factors such as temperature change and tissue stretch may also influence the discharge frequency of the SA node although autonomic control is the principal controller (Cooper, Lei, Cheng, & Kohl, 2000). In conscious dogs, variations in conduction time through the AV node occur on a beat-to-beat basis in conjunction with respiration and the oscillatory activity of AV conduction is not dependent on simultaneous changes in heart rate (Webster, 1993). In addition, during atrial pacing autonomic neural activity associated with respiration and blood pressure appears to dynamically modulate AV conduction with respiratory effects predominating at low heart rates and blood pressure effects at high heart rates (Warner & Loeb, 1986). The quantity of blood pumped by the heart (cardiac output) may be considered as the product of heart rate and stroke volume. Therefore, cardiac activity is related to both regulation of pacemaker activity and myocardial performance, with heart

rate being regulated mainly by the ANS. However, baroreceptor, chemoreceptor, pulmonary inflation, atrial receptor (Bainbridge) and ventricular receptor reflexes can also regulate heart rate (Berne & Levy, 1997).

2.1.4.1 Cardiac Autonomic Control

The ANS regulates two processes; firstly, the overall cardiac cycle length and hence heart rate (the chronotropic effect), and secondly the speed of conduction of the electrical activity through the heart including the AV node (termed the dromotropic effect). The ANS comprises two divisions, parasympathetic and sympathetic, both of which innervate the heart (Fig. 2.4). Shortened cycle lengths or reduced conduction times are produced by a diminution of parasympathetic and/or an increase in sympathetic activity; increased cycle lengths or conduction times are produced by opposite changes in neural activity. Typically, parasympathetic tone predominates in healthy, resting individuals.

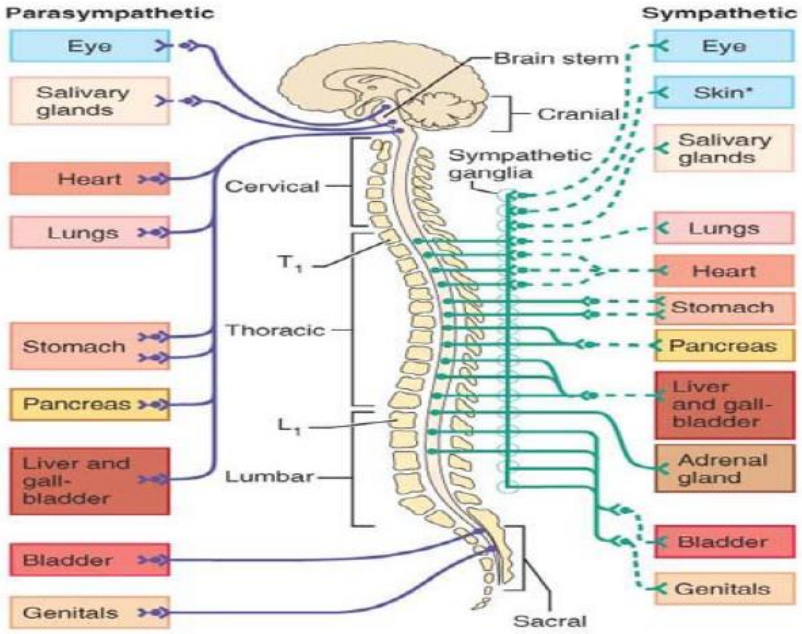

Figure 2.4 Parasympathetic and sympathetic divisions of ANS (Berne & Levy, 1997).

The cardiac parasympathetic fibers originate in the medulla oblongata in cells in the dorsal moto nucleus of the vagus (Fig. 2.5). Efferent vagal fibers pass inferiorly through

the neck as cervical vagus nerves and then through the mediastinum to synapse with postganglionic cells on the epicardial surface or within the walls of the heart. Most cardiac ganglionic cells are located near the SA node (predominately affected by right vagus) and AV conduction tissue (mainly inhibited by the left vagus) (Berne & Levy, 1997). The SA and AV nodes are rich in cholinesterase and thus the effects of a vagal pulse are short lived due to the fact that acetylcholine released at the nerve terminals is rapidly hydrolyzed; in addition, short latency in the order of 50 to 100 ms is exhibited (acetylcholine activates special potassium ion channels in cardiac cells). For instance, if the vagus is stimulated at a constant frequency for several seconds, heart rate decreases sharply and reaches steady state in one or two cardiac cycles. Removal of the stimulus causes a rapid return to the basal level (Berne & Levy, 1997); thus, it can be seen that the parasympathetic nervous system is capable of providing beat by beat control of SA and AV nodal function and hence heart rate.

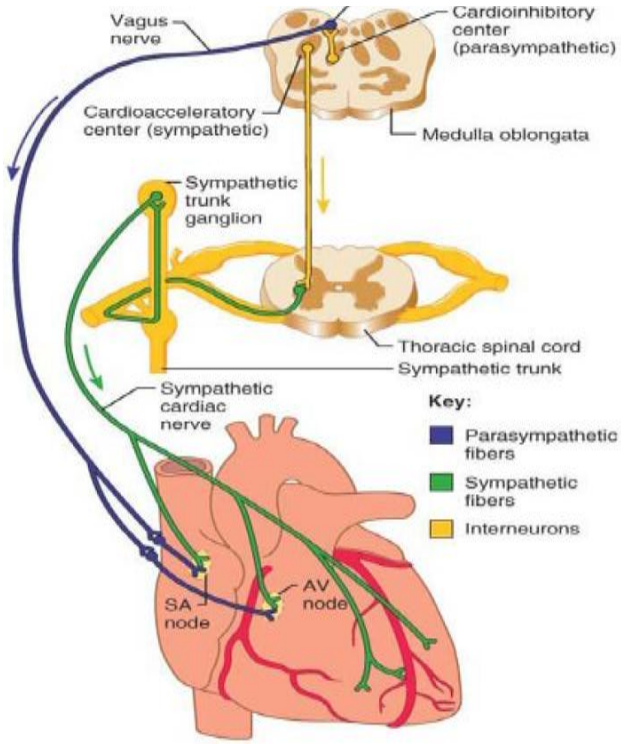

Figure 2.5 The cardiac parasympathetic and sympathetic fibers (Berne & Levy, 1997).

The cardiac sympathetic fibers originate in the inter-mediolateral columns of the upper five or six thoracic and lower one or two cervical segments of the spinal cord and

alter the cardiac cycle through adrenergic neurotransmitters (Fig. 2.5). At the onset of sympathetic stimulation, the facilitator effects on heart rate are much slower than inhibitory vagal influences; the recovery after stimulus removal is also slower than that of the parasympathetic branch. The major part of the norepinephrine (also known as noradrenalin) released during sympathetic stimulation is taken up again by the nerve terminals and most of the remainder carried away in the bloodstream - relatively slow processes.

2.1.4.2 Nervous Influence on Conduction

The cardiac parasympathetic effect on the SA node is primarily via small branches of the tenth cranial nerves (vagal nerves). AV conduction is influenced predominately by changes in parasympathetic activity which is the major determinant of respiratory related AV interval oscillations; sympathetic activity produces fluctuations in both AV conduction and blood pressure. Both divisions of the ANS continually modulate intrinsic rate-dependent properties of the AV node. AV conduction time is not solely determined by the autonomic nervous system - it is also influenced by refractory effects (Warner & Loeb, 1986).

Acute changes in arterial blood pressure can cause inverse changes in heart rate via the baroreceptors located in the aortic arch and carotid sinus; this effect may be termed the baroreflex and is most pronounced over an intermediate range of arterial blood pressures. Some of the feedback mechanisms involved in the regulation of mean arterial blood pressure (MAP) during periods of isotonic exercise is illustrated in Fig. 2.6.

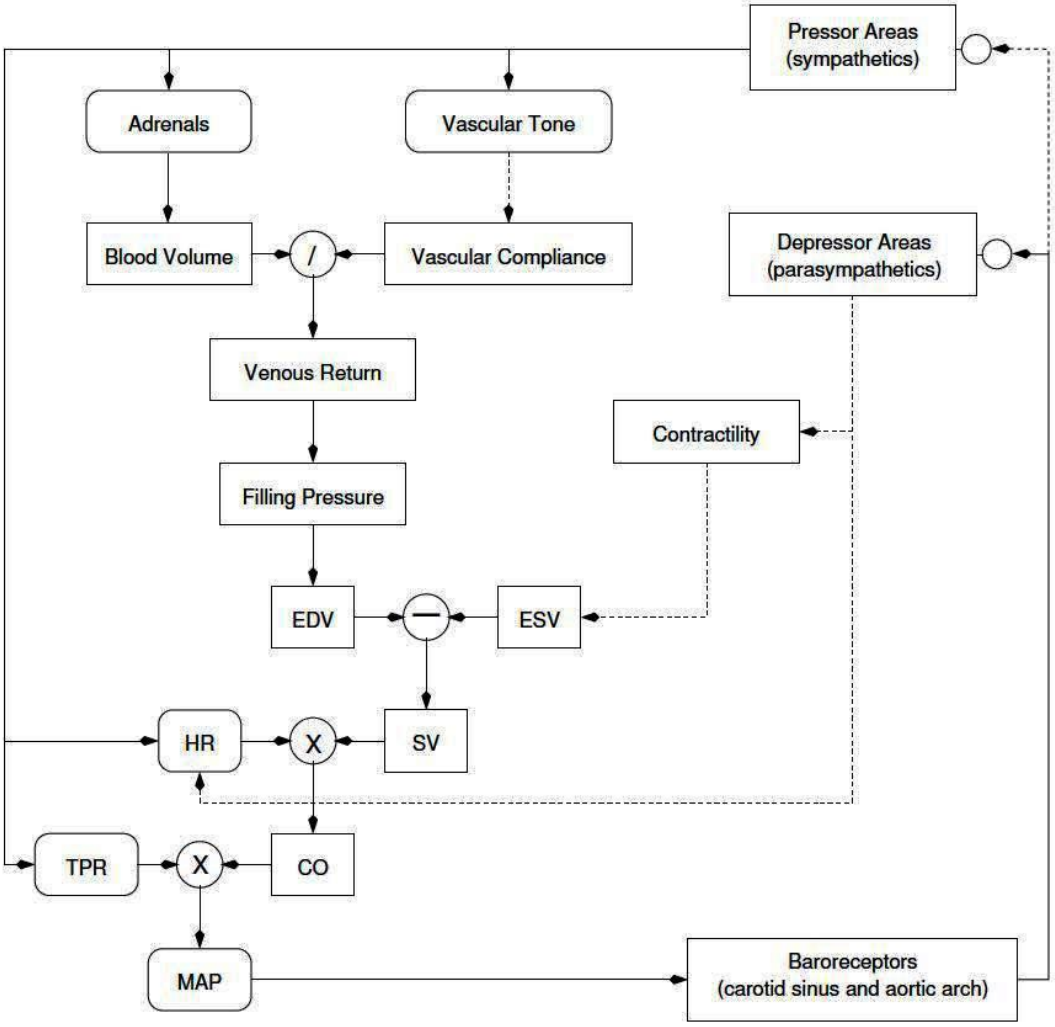

Figure 2.6 Homoeostatic feedback mechanisms involved in the regulation of mean arterial blood pressure (MAP) during periods of isotonic exercise. EDV = end diastolic volume, ESV = end systolic volume, HR = heart rate, SV = stroke volume, TPR = total peripheral resistance, CO = cardiac output. Broken lines indicate inhibitory input.

2.1.4.3 Respiratory Influences on Conduction

Respiratory cardiac arrhythmia - variations in heart rate occurring at the frequency of respiration - is visible in most people and usually pronounced in children. These variations manifest as cardiac acceleration during inspiration and deceleration during expiration. Inspiration is associated with both a reduction in the activity of vagal efferent nerve fibers controlling the heart and an increase in sympathetic activity. The neural activity in the vagal fibers increases during expiration; the rapid removal of acetylcholine at the vagal endings causes the rhythmic changes in heart rate, albeit somewhat damped by the slower removal of norepinephrine at the sympathetic endings.

As a result, vagal activity dominates the respiratory sinus arrhythmia; however, in addition, central and reflex factors can also contribute (Berne & Levy, 1997). According to Berne and Levy: “During inspiration, intrathoracic pressure decreases, and therefore venous return to the right side of the heart is accelerated, which elicits the Bainbridge reflex. After a time delay required for the increased venous return to reach the left side of the heart, left ventricular output increases and raises arterial blood pressure. This in turn reduces heart rate reflexly through baroreceptor stimulation. Fluctuations in sympathetic activity to the arterioles cause peripheral resistance to vary at the respiratory frequency.” Thus, oscillations in arterial blood pressure can affect heart rate via the baroreceptor reflex. The respiratory center in the medulla is also capable of influencing the cardiac autonomic centers (Fig. 2.7).

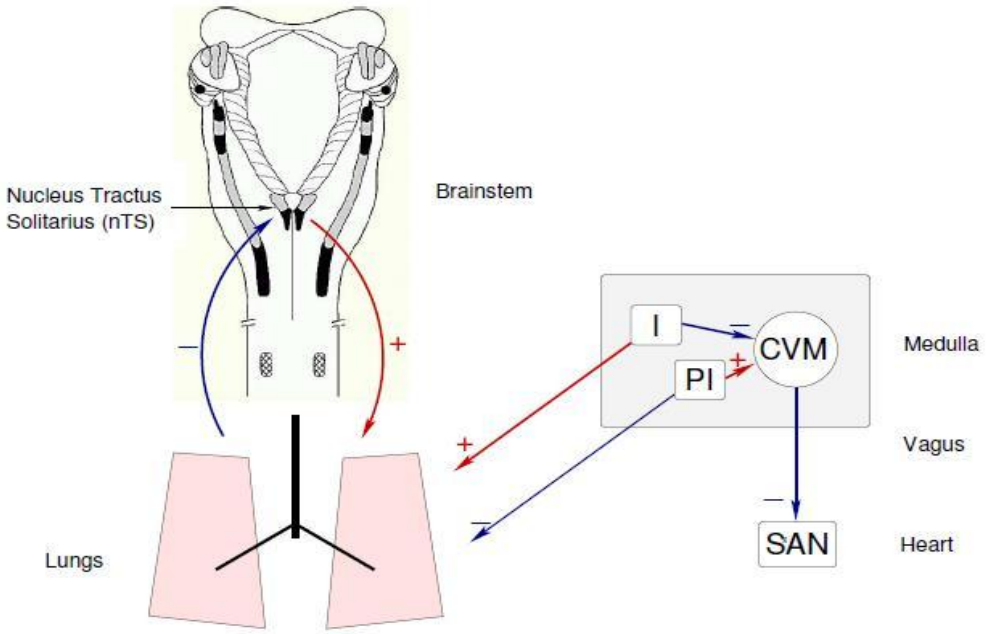

Figure 2.7 Regulation of respiratory activity at the level of the Medulla in the brain stem. The inset shows neural interplay, from which the sinus arrhythmia phenomenon arises. CVM = cardiac vagal moto nucleus; I = inspiratory phase, PI = post inspiration (Berne & Levy, 1997).

Inspiration, while usually resulting in a decrease in cycle length, also tends to shorten AV conduction time. However, the reduction in cycle length, of itself, tends to increase AV conduction time, so that the actual AV conduction delay is dependent upon the balance between these opposing effects; its exact behavior will depend on the

relative contribution of both effects. These considerations suggest that the respiratory AV conduction variability will be small, and complex in nature.

2.2 The Electrocardiogram

The action potential generated in the SA node stimulates the muscle fibers of the myocardium, causing them to contract. When the muscle is in contraction, it is shorter, and the volume of the ventricular chamber is less, so blood is squeezed out. The contraction of so many muscle cells at one time creates a mass electrical signal that can be detected by electrodes placed on the surface of the patient's chest or the patient's extremities. This electrical discharge can be mechanically plotted as a function of time, and the resultant waveform is called an electrocardiogram (ECG).

A typical scalar ECG is shown in Fig. 2.3. It's composed of several waveforms called the P, QRS, and T waves respectively. In the same figure, the action potentials of various cardiac cells and when they are initiated are also shown. The P wave is the result of a summation of atrial muscle action potentials during depolarization, or in other words, it represents the atrial depolarization. The P-R interval represents the delay from the SA node through the AV node and is known as the atrioventricular conduction time. Conduction then occurs through the bundle of His to the myocardial fibres of the ventricles. Ventricular depolarization appears as the QRS complex. In addition, repolarization of the ventricles is shown as the T wave. Some ECG waveforms show an additional waveform after T wave, which is named the U wave. Usually its origin is attributed to slow repolarization of ventricular papillary muscles.

2.2.1 Leads

The ECG is recorded on electrocardiographic leads. The term 'lead' refers to a measurement configuration of electrodes. Three bipolar limb leads of the frontal plane are connected between limbs (Fig. 2.8). Taking lead I as an example, the negative terminal electrode is connected to the right arm (RA) and the positive terminal electrode to the left arm (LA). These three limb leads constitute Einthoven's triangle. If any two

of the three electrocardiographic leads are known, the third one can be determined mathematically from the first two (Einthoven's law). The other three unipolar frontal leads are aVR (on the right arm), aVL (on the left arm) and aVF (on the foot), which are usually called augmented unipolar leads, measuring the potential difference on a limb with respect to a reference point formed by the two resistors between the electrodes on the other two limbs (Fig. 2.9).

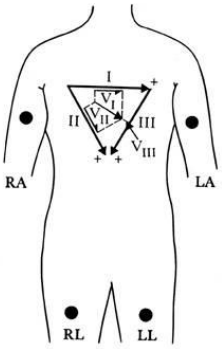

Figure 2.8 Directions of standard limb lead vectors (Webster, 1993).

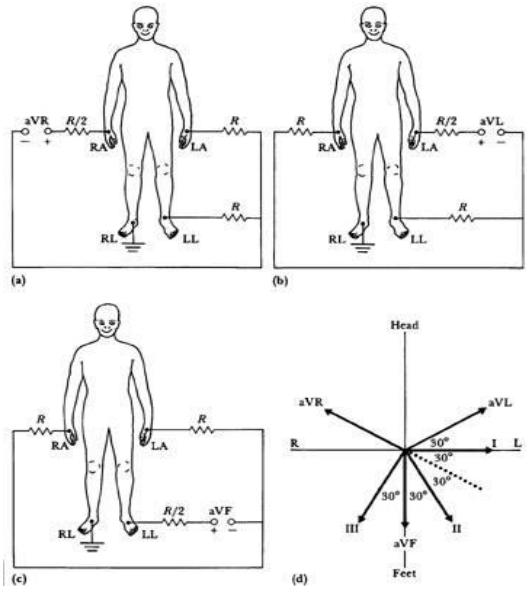

Figure 2.9 (a), (b), (c) Connections of electrodes for the augmented limb leads, (d) Vector diagram showing the directions of limb lead vectors in the frontal plane (Webster, 1998).

The six precordial leads, VI-V6, are unipolar and measure the cardiac vector projection on the horizontal plane (Fig. 2.10). These precordial leads are measured with respect to theWilson's central terminal, which is formed by a three-resistor network in Fig. 2.11, yielding an average of right and left arms and left leg.

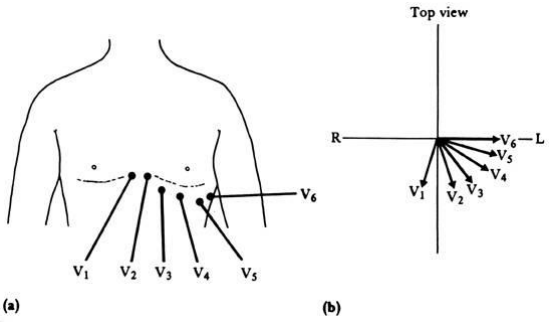

Figure 2.10 (a) Positions of precordial leads on the chest wall, (b) Directions of precordial lead vectors in the transverse plane (Webster, 1998).

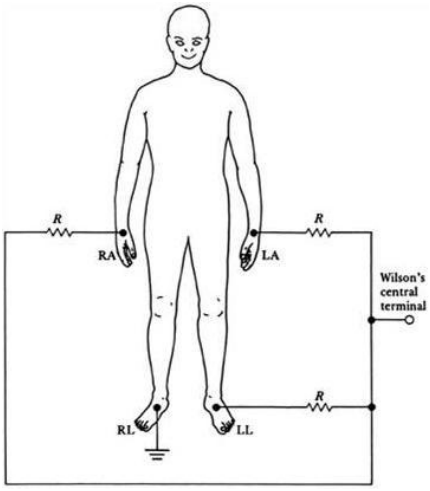

Figure 2.11 Connection of electrodes to the body to obtain Wilsons central terminal (Webster, 1998).

In order to use the surface ECG to diagnose abnormalities, it is important to know the normal characteristics of the ECG. A sample of a normal 12 lead ECG (10 s strip, paper speed 25 mm/s) is demonstrated in Fig. 2.12. For a normal ECG, typical P wave duration is less than 0.11 s (equivalent to 2.75 mm measured on this figure), and the morphology does not include any notches or peaks. The P wave is normally positive in leads I, II, aVF, V4 and V6, and negative in aVR. It can be positive, negative, or

biphasic in all other leads. The QRS complex duration is normally less than 0.12 s, and the morphology differs in different leads. In some leads there exist downward deflections of Q and S waves, and a large upward deflection of R wave in between as shown in Fig. 2.8. The normal morphology of the T wave is rounded and asymmetrical. It is positive in leads I, II, V3 and V6, and negative in aVR. The polarity may vary in leads III, V1 and V2. Typically the P-R interval is 0.18-0.2s, and R-R interval is 0.6-1.0s (Yanowitz, 2006).

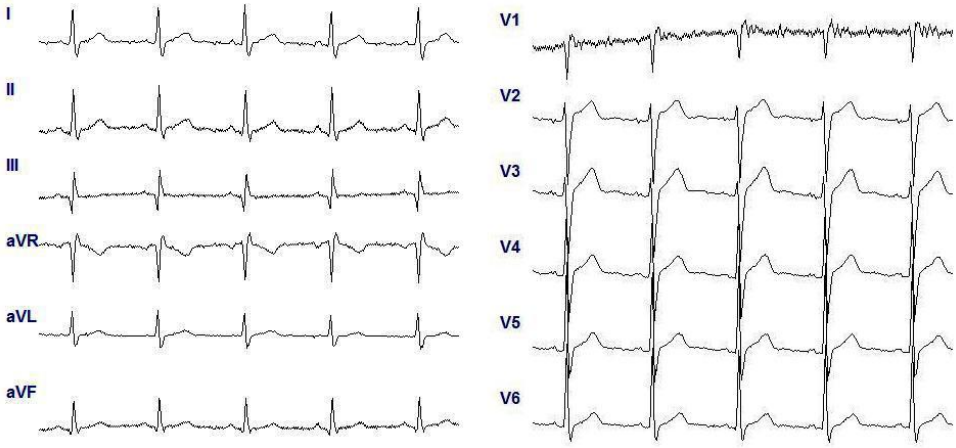

Figure 2.12 An example of a 12-lead ECG record. This ECG was recorded from my son, Ali Atakan İşler, using the BIOPAC MP30 bio-signal recording device.

2.2.2 QRS Detection

The aim in ECG analysis is to examine the sinus rhythm modulated by the autonomic nervous system (ANS). Therefore, one should technically detect the occurrence times of the SA-node action potentials. This is, however, practically impossible and, thus, the fiducial points for the heart beat is usually determined from the ECG recording. The nearest observable activity in the ECG compared to SA-node firing is the Pwave resulting from atrial depolarization (Figure 2.3) and, thus, the heart beat period is generally defined as the time difference between two successive P-waves. The signal- to-noise ratio of the P-wave is, however, clearly lower than that of the strong QRS complex which results primarily from ventricular depolarization. Therefore, the heart beat period is commonly evaluated as the time difference between the easily detectable QRS complexes.

A typical QRS detector consists of a preprocessing part followed by a decision rule. Several different QRS detectors have been proposed in the literature. For an easy to read review of these methods, see Kohler, Henning, & Orglmeister, (2002). The preprocessing of the ECG usually includes at least band-pass filtering to reduce power line noise, baseline wander, muscle noise, and other interference components. The pass band can be set to approximately 5-30 Hz which covers most of the frequency content of QRS complex (İşler, Özyürek, Çobanoğlu, & Kuntalp, 2008; Pahlm & Sornmo, 1984). In addition, preprocessing can include differentiation and/or squaring of the samples. After preprocessing, the decision rules are applied to determine whether or not a QRS complex has occurred. The decision rule usually includes an amplitude threshold which is adjusted adaptively as the detection progresses. In addition, the average heart beat period is often used in the decision. The fiducial point is generally selected to be the R-wave and the corresponding time instants are given as the output of the detector.

2.3 Heart Problems

The physician uses the ECG and other tests to determine the gross condition of the heart. Although a complete discussion of heart problems is beyond the scope of this dissertation, some of the more common problems are discussed below in generalized terms.

The heart is a muscle and must be perfused with blood to keep it healthy. Blood is supplied to the heart through the coronary arteries that branch off from the aorta just before it joins the heart. If an artery bringing blood to the heart becomes partially or totally blocked off, the area of the heart served by that vessel will suffer damage from the loss of the blood flow. That area of the heart is said to be infarcted and is dysfunctional. This type of damage is referred to as a myocardial infarction, another term for heart attack.

Another class of heart problem is cardiac arrhythmias. These are abnormal heartbeat rhythms and may be seen as ECG changes. Conditions under this classification include extremes in heart rate, premature contractions, heart block, and fibrillation.

The human heart rate varies normally over a range of 60 to 110 beats/min (bpm). Rates, faster than this, are called tachycardia. Various authorities list slightly different figures as the threshold for defined tachycardia, but most list 120 bpm, with the range being 110 to 130 bpm.

The opposite condition, too slow a heart rate, is called bradycardia, and again different sources list slightly different thresholds, but all are within the 40- to 60-beats/min range.

Premature contractions occur when an area of the heart becomes irritable enough to produce a spurious action potential at a time between normal beats. The action potential spreads across the myocardium in much the same manner as the regular discharge. Beats occurring at improper times are called ectopic beats. If it results in atrial contraction, then it is an atrial premature contraction (APC), and if in the ventricle, a ventricular premature contraction (VPC).

Detailed information about the other abnormalities in the ECG can be found in an excellent online tutorial web site (Yanowitz, 2006). However, a special heart problem is congestive heart failure (CHF), which is the subject of this dissertation, will be described in the following section in detail.

2.4 Congestive Heart Failure

During the past two decades, a shift in understanding of heart failure has taken place. Traditionally, the pathophysiology of heart failure was described in terms of the structural and functional alterations observed. For most cardiac diseases, heart failure represents the final common pathway. Anything that causes damage to the heart muscle can lead to heart failure and their indications can be quite different.

- The cardiac pump may be defective:

If the heart does not manage to empty, this is systolic heart failure. If the heart does not manage to fill up, on the other hand, this is diastolic heart failure: the heart fills poorly (its walls are rigid) and does not relax to receive the blood during diastole. Often both mechanisms coexist and are revealed by an oedema in the legs or the lungs.

- The defective pump may be predominant:

In the "right heart" (in other words, the right side of the heart, which acts as a reservoir, with a thin wall): which causes a further oedema in the legs and an enlarged liver. In the "left heart" (in other words the left side of the heart, which acts as a pump with a thicker muscular wall) which cause more breathlessness. The pump's deficiency is either due to the deterioration of the cardiac muscle itself, or else to the "exhaustion" of the muscle if it has been asked to do excessive work, because of a defect in a valve (for example, when there is a leak, the heart has to work harder).

- Impairment of the cardiac muscle (cardiomyopathy).

By far the most frequent cases of impairment are the consequences of coronary disease:

1. If there has been an infarction, the scar, which replaces the destroyed muscle, does not contract like the healthy muscle.
2. If the heart as a whole has suffered from ischaemia, it has become rigid all over. This is a so-called ischaemic cardiomyopathy which is a form of systolic heart failure.
3. Hypertension in the long term results in the exhaustion of the cardiac muscle, if it is not properly controlled by treatment. This is mainly diastolic heart failure.
4. The other forms of cardiomyopathy are much rarer and have very varied causes: alcohol, infections, haemochromatosis, AIDS.

- Deterioration of the heart valves.

This used to be the most frequent cause of heart failure, particularly because poorly treated sore throat could be complicated by a disease known as ”acute rheumatic fever” (becoming less prevalent in industrialized countries). This disease damages the heart’s valves. This heart failure as a result of a leak or a constriction of the valves, or both together, is much less frequent, unlike aortic constriction: an illness on the increase due to ageing with a calcium deposit on the aortic valves.

CHF is a complex syndrome, and patients who have this syndrome may present at different ages, having comorbid conditions, having various etiologies of heart failure, and possessing different expectations from the health care team. All management decisions should begin by establishing goals of care, negotiated between the patient and physician. Patient education is essential in this process. Without a firm understanding of the prognosis and natural history of the syndrome, patients will not be able to participate fully in their own care (Wilbur & James, 2005).

Optimal management of CHF relies on risk factor control, life-style modification, and patient self-assessment and self-management. If this nonpharmacologic therapy is not enough, pharmacologic therapy that is using medication is essential. Because the management of the heart failure is out of scope for this study, detailed information on this topic can be found in AHA’a committee report updated in 2006 (American Heart Association, 2006).

Once the diagnosis is established, heart failure can be further staged and classified based on various scoring systems (American Heart Association, 2005). In 2001, the American College of Cardiology (AAC) and the American Heart Association (AHA) published practice guidelines for evaluation of heart failure, which proposed new staging analogous to staging for cancer and is based on clinically measurable findings in the heart. One impetus for this method of staging was to promote recognition of presymptomatic stages of heart failure, so that intervention could occur earlier. This staging system compliments the New York Heart Association (NYHA) functional

classification scheme, and the two can be employed together. Table 2.1 summarizes the both classification schemes with short descriptions.

Table 2.1 Staging and classification schemes for heart failure (Wilbur & James, 2005).

AAC/AHA Staging System	
Stage A	High risk
Stage B	Structural abnormalities without the development of symptoms
Stage C	Current or prior symptoms of heart failure with normal or decreased ejection fraction (blood output)
Stage D	End stage, refractory heart failure
NYHA Functional Classification System	
Class I	No limitation of activities
Class II	Slight, mild limitation of activities
Class III	Marked limitation of activity (shortness of breath, exercise tolerance)
Class IV	Activity severely limited

2.4.1 Electrocardiography in CHF

Structural heart disease, electrical instability, and decreased sympathetic activity can generate a number of specific and non-specific ECG changes and arrhythmias in patients with CHF. This section describes direct alterations of the P–QRS–T complex and ECG-derived parameters in CHF, together with the significance of cardiac arrhythmias, markers of atrial and ventricular electrical instability, and the parameters of sympathetic nervous system activity, especially heart rate variability (HRV).

2.4.1.1 General ECG Alterations in CHF

Patients with CHF may display specific ECG alterations such as Q-waves after MI or persistent ST-segment elevation in MI-related leads consistent with a left ventricular (LV) aneurysm (Hombach, 2006). The conventional ECG may be used as first-line diagnostic tool for CHF (Fonseca et al., 2004). In this investigation, 6300 subjects in a general population were screened for CHF by symptoms or signs, chest X-ray, ECG, and echocardiography. The diagnosis was confirmed in 551 cases. Patients with right atrial enlargement, atrial flutter or fibrillation, first- and second-degree AV-blocks, left

bundle branch block (LBBB), and lung oedema were more likely to be diagnosed with CHF. An abnormal ECG had an estimated sensitivity of 81% and a negative predictive value of 75%, and for an abnormal chest X-ray the numbers were 57% and 83%, respectively. In addition, a recent study provides an overview of the most significant tests and indexes related to disturbed cardiac repolarization and sympathovagal balance, their pathophysiologic role in the initiation of malignant ventricular tachyarrhythmias, and clinical significance for investigating CHF patients (Hombach, 2006).

In addition to these statistical studies related to CHF, there are some studies tried to design classifiers which discriminate the patients with CHF from others. These are presented in a chronological order in the following paragraphs.

Osowski et al. presented the application of support vector machine (SVM) for reliable heartbeat recognition on the basis of the ECG waveform. They applied two different preprocessing methods for generation of features. One method involved the higher order statistics (HOS) while the second the Hermite characterization of QRS complex of the registered ECG waveform. The SVM had the same number of inputs and one output. In learning multiclass recognition problem, they applied the one-against-one strategy leading to many network structures adapted for the recognition between two classes at one time. The classification accuracy of their model was 95.77% for Hermite preprocessing and 94.26% for HOS preprocessing. The recurrent neural networks (RNN) trained on the features extracted by the usage of eigenvector methods indicated significantly higher performance than that of the SVM presented by (Osowski, Hoai, & Markiewicz, 2004).

Acır used six fast least square support vector machines (LSSVMs) for classification of six types of ECG beats obtained from the MIT-BIH database. The classification accuracy was 95.2% by the proposed fast LSSVMs together with discrete cosine transform. The results of the present study indicated that the usage of RNN significantly improve the classification accuracy of ECG beats. The author also tried to classify same beats using multi-layer perceptron (MLP) with the maximum accuracy of 91.8% (Acır, 2005).

A combined and a MLP neural networks were trained, cross validated and tested with the extracted features using discrete wavelet transform of the ECG signals. Four types of ECG beats (normal beat, congestive heart failure beat, ventricular tachyarrhythmia beat, atrial fibrillation beat) obtained from the Physiobank database (Goldberger et al., 2000) were classified with the accuracy of 96.94% by the cellular neural networks (CNN) and the accuracy of 96.88% by the MLP (Güler & Übeyli, 2005a, 2005b).

A multi-class SVM with the error correcting output codes, a RNN and a MLP neural network are used in the classification of ECG beats. Four types of ECG beats (normal beat, congestive heart failure beat, ventricular tachyarrhythmia beat, atrial fibrillation beat) obtained from the Physiobank database (Goldberger et al., 2000) were classified with the accuracy of 98.06% by the RNN (Übeyli, 2009), the accuracy of 98.61% by the SVM (Übeyli, 2007), and the accuracy of 91.39% by the MLP (Übeyli, 2007).

2.4.1.2 Heart Rate Variability Analysis in CHF

Analysis of HRV provides a non-invasive measure of autonomic control of the heart. A healthy heart rapidly adjusts HR and other autonomic parameters in response to internal and external stimuli. A heart that has been compromised is less able to make such adjustments and therefore exhibits lower HRV (Task Force, 1996).

Numerous studies have shown that the altered cardiac autonomic tone associated with CHF is reflected by an increased HR and a decreased HRV. In addition, there are well-prepared review papers that summarize the studies for investigating the development and progression of CHF using HRV indices in the literature such as Chattipakorn, Incharoen, Kanlop, & Chattipakorn, (2007), Richard, Sandercock, & Brodie, (2006), and Sanderson, (1998). These studies are summarized as follows.

Majority of the studies presented the similar results. For example, the altered cardiac autonomic tone associated with CHF is reflected by an increased HR and a decreased

variability in HR (Casolo, Balli, Taddei, Amuhasi, & Gori, 1989; Coumel et al., 1991; Kienzle et al., 1992; Panina, Khot, Nunziata, Cody, & Binkley, 1995; Ponikowski et al., 1996; Saul et al., 1988).

Since time-domain measures are simple statistical methods to calculate from both long- and short-term raw HRV data, these have been investigated in detail. The studies have shown that various combinations of these measures predicted increase risk of cardiac death and death to progressive CHF (see Table 2.2).

Table 2.2 Time-domain HRV measures used in prognosis purpose.

Parameter	**Related Literature**
SDNN	(Bilchick et al., 2002; Boveda et al., 2001; La Rovere et al., 2003; Makikallio et al., 2001)
SDANN	(Binder et al., 1992)
SDNN and SDANN	(Aronson, Mittleman, & Burger, 2004; Jiang et al., 1997; Ponikowski et al., 1997)
SDNN and PNN50	(Szabo et al., 1997)
SDNN, SDANN, and pNN50	(Bonaduce et al., 1999)
SDANN and RMSSD	(Galinier et al., 2000)

On the other hand, frequency-domain measures provide the basic information on how power distributes as a function of frequency. These measures have been calculated using FFT-, AR modeling-, and LS-based PSD estimation techniques. Since the clinical meanings of the power in corresponding frequency bands, these give expressive results (see Table 2.3).

Conventional methods of quantifying HRV using linear methods have shown that decreased variability is associated with increased mortality in heart failure. However, there are some occasions in which raw HRV data is less suitable for analysis with linear methods. Poincare plot measures (Brouwer et al., 1996; Woo, Stevenson, Moser, Trelease, & Harper, 1992; Woo, Stevenson, & Middlekauf, 1994) and DFA (Ho et al., 1997) have also been used in the literature.

In addition, some studies also investigated the relation between the severity of CHF and HRV indices. For example, decreased HRV correlated with NYHA class (Casolo et al., 1995), the absence of LF power indicated with worse prognosis (Mortara et al.,

1994), increased LF power in NYHA class II and the absence of LF power in NYHA class IV (Guzzetti et al., 1995) have been reported. In contradiction, HRV is also reported as no association with all-cause mortality and the severity in CHF (Anastasiou-Nana et al., 2005; Kienzle et al., 1992).

Table 2.3 Frequency-domain HRV measures used in prognosis purpose.

Parameter	**Related Literature**
reduced HF (vagal activity)	(Anastasiou-Nana et al., 2005; Binkley, Nunziata, Haas, Nelson, & Cody, 1991; Casolo et al., 1989; Fei et al., 1994; Kienzle et al., 1992; Kingwell et al., 1994; Makikallio et al., 2001; Saul et al., 1988),
increased or absence of LF (both sympathetic and vagal activities)	(Mortara et al., 1994), reduced LF (Anastasiou-Nana et al., 2005; Bonaduce et al., 1999; Fei et al., 1994; Ho et al., 1997; La Rovere et al., 2003; Lucreziotti et al., 2000; Ponikowski et al., 1997; Sanderson et al., 1996; Van de Borne, Montano, Pagani, Oren, & Somers, 1997)
increased LF/HF	(Binkley et al., 1991; Bonaduce et al., 1999; La Rovere et al., 2003; Lucreziotti et al., 2000)
reduced TP	(Aronson, Mittleman, & Burger, 2004; Butler, Ando, & Floras, 1997; Fei et al., 1994; Hadase et al., 2004; Ho et al., 1997; Lucreziotti et al., 2000)
reduced VLF	(Hadase et al., 2004; Ho et al., 1997; Ponikowski et al., 1996)
lnVLF	(Hadase et al., 2004; Makikallio et al., 2001)
LFday/LFnight	(Galinier et al., 2000)
LFnight < LFday	(Tanabe, Iwamoto, Fusegawa, Yoshioka, & Shina, 1995)
LFnight and HFnight	(Guzzetti et al., 2005)

CHF has been the subject of many studies using HRV analysis. Majority of the CHF studies, summarized above, use HRV measures as predictors of the risk of mortality (prognosis). However, only a few studies have been focused on using HRV measures for diagnosis purpose. These studies are summarized in the following paragraphs.

Asyalı studied on discriminating CHF patients from normals using linear discriminant analysis and Bayesian classifier (Asyalı, 2003). In his study, only 9 common long-term (24-hour) time-domain and classical FFT-based frequency-domain HRV measures were used and sensitivity and specificity rates of 81.8% and 98.1% are obtained, respectively.

Some researchers tried to discriminate the loss of complexity due to whether aging or CHF (Costa & Healey, 2003). They used Fisher's linear discriminant to evaluate the use of multi scale entropy (MSE) features for classification. In discriminant tests on the training data, they found that MSE features could separate CHF subjects' data from healthy subjects with a positive predictivity of 76% and a specificity of 83%.

In another interesting study, researchers tried to discriminate patients from the clinical notes written by human experts (Pakhomov, Buntrock, & Chute, 2003). This can be classified as a character recognition study. They used two different classifiers: Naive Bayes and Perceptron. In Naive Bayes classifier case, they achieved a positive predictivity of 100% and accuracy 69.2%. In the other classifier model, test results became 95% and 76.92%, respectively.

CHAPTER THREE
HEART RATE VARIABILITY

3.1 Introduction

Over the last three decades there has been a widespread interest in the study of variations in the beat-to-beat timing of the heart, known as heart rate variability (HRV). In certain circumstances, the evaluation of HRV has been shown to provide an indication of cardiovascular health (Malik & Camm, 1995). However, often contradictory results have left clinical researchers skeptical about the efficacy of HRV assessment and there exists no clear consensus on how to estimate HRV in clinical practice.

Heart rate variability (HRV) is an important aspect of this thesis because all experiments start with these calculations. HRV makes up what is called the feature space that is used as inputs into our classification models.

HRV is a complex and often ambiguous variable. Lack of standardized quantification procedures for HRV is the most significant barrier for further diagnostic and clinical use of it. Different or even conflicting results of their studies might be because of using different HRV measurements and standards for HRV calculation. Such problems include: lack of rules for artifact rejection and correction, choosing re-sampling frequency, choosing length of segment for HRV evaluation, considering sleep states, stationarity of data within a time period as well as standardized methods to interpret different HRV measures. Determination of the affected factors for HRV measures, and further study into exposing the relationship between these measures is important for proper use of HRV.

The aim of this chapter is to give a short introduction to the analysis of cardiovascular signals. The origin and derivation of HRV signal was given. One problematic feature of this signal that has to be considered prior to analysis is that they are nonequidistantly sampled. In this thesis, a cubic spline interpolation was used to

overcome this problem. Prior to analysis, cardiovascular variability signals should also always be checked for artifacts. The most common artifact types of this signal were discussed. The optimal case would be to include only artifact-free regions in the analysis. This is not, however, always possible in which case artifacts need to be corrected in some way before analysis.

3.2 Background

The sinoatrial node (SAN) is the pacemaker of the heart and is responsible for the HRV. The cells of the SAN slowly but automatically depolarize; when reaching a threshold, they rapidly depolarize, followed by a repolarization, and the process repeats itself again and again as explained in the previous chapter in detail. The depolarization quickly propagates to the surrounding cardiac muscle cells and the contraction of the heart begins. In healthy subjects, the SAN cells generate depolarization or action potentials at a frequency that is regulated through direct innervations of both branches of ANS: sympathetic and parasympathetic (or vagal). The parasympathetic branch releases acetylcholine (ACh) that slows the rate of SAN depolarization, while the sympathetic branch releases norepineprine that increases the rate of SAN depolarization. The SAN effectively integrates both inputs from ANS, both temporally and spatially, and this pacemaker activity is often modeled as an integrate pulse frequency modulation (Chang, Monahan, Griffin, Lake, & Moorman, 2001). This is the source of HRV (Cao, 2004).

3.3 Clinical Relevance of HRV

The clinical relevance of HRV was first appreciated in 1965 when Hon and Lee noted that fetal distress was preceded by alterations in inter-beat intervals before any appreciable change occurred in heart rate (HR) itself (Hon & Lee, 1965). About thirty years ago, Sayers (Sayers, 1973) and others (Hirsh & Bishop, 1981; Luczak & Lauring, 1973; Penaz, Roukenz, & Van der Vaal, 1968) focused attention on the existence of physiological rhythms embedded in the beat-to-beat HR signal. During the 1970s, Ewing and colleagues devised a number of simple bedside tests of short-term RR differences to detect autonomic neuropathy in diabetic patients (Braune & Geisenorfer, 1995; Ewing, Martin, Young, & Clarke, 1985). The association of higher risk of post-

infarction mortality with reduced HRV was first shown in 1977 (Wolf, Varigos, Hunt, & Sloman, 1978). In 1981, it has been introduced power spectral analysis of HR fluctuations to quantitatively evaluate beat-to-beat cardiovascular control (Akselrod et al., 1981).

These frequency domain analyses contributed to the understanding of autonomic background of RR interval fluctuations in the HR record (Pagani, 2000; Pagani et al., 1986; Pomeranz et al., 1985). The clinical importance of HRV became appreciated in the late 1980s, when it was confirmed that HRV was a strong and independent predictor of mortality after an acute myocardial infarction (Bigger et al., 1992; Huikuri et al., 2003; Kleiger, Miller, Bigger, & Moss, 1987; Lombardi, Makikallio, Myerburg, & Huikuri, 2001; Malik, Cripps, Farrel, & Camm, 1989; Malik, Farrel, Cripps, & Camm, 1989). With the availability of new, digital, high-frequency, 24-hour, multichannel ECG recorders, HRV has the potential to provide additional valuable insight into physiological and pathological conditions and to enhance risk stratification. Since then, people have recognized consistently the significant association between HRV and ANS (Task Force, 1996).

As a result, even though HRV has been studied extensively during the last decades within which numerous research articles have been published, the practical use of HRV have reached general consensus only in two clinical applications (Task Force, 1996). That is, it can be used as a predictor of risk after myocardial infarction (Huikuri et al., 2003; Lombardi et al., 2001) and as an early warning sign of diabetic neuropathy (Braune & Geisenorfer, 1995; Pagani, 2000). In addition, HRV has been found to correlate with, gender, age, mental and physical stress, and attention (Berntson et al., 1997).

3.4 Considerations

Determination of the standard for HRV calculation is also an important step to ensure more comparable results. Different standards for HRV calculation might result in different or even conflicting results in HRV analysis. Therefore, the same standard for the HRV calculation of all subjects were used during the thesis.

3.4.1 Appropriate Analytical Epochs

HRV in both time and frequency domain are greatly influenced by the length of epochs being analyzed. It tends to increase with the length of the epochs analyzed. Comparison of HRV measures must be done for a fixed length of data for all subjects. It is necessary to define criteria for choosing the duration. Shorter epochs are recommended, because RR intervals over longer periods of time are more likely to be nonstationary, and HRV calculated from them are influenced by slower trends. Moreover, the slower HR activity is not clearly vagal and reflects interactions with the sympathetic nervous system. Its removal reduces the non-vagal influences on these HRV measures. Shorter epochs function as filtering the slow HR activity, and make the HRV measures more focused on the vagal influences (Izard, Simons, Haynes, Porges, & Cohen, 1991).

Stationarity of the data is an important issue to be considered when choosing the length of epochs, especially for the spectral analysis of HRV. Most biomedical signals are not stationary. Physical activity and posture changes can be the cause of nonstationarity. Since many signal analysis techniques require stationarity from the signal, there is no ideal solution to this problem. Choosing shorter segments may somewhat solve this problem, because during short duration, the subject's posture, activity and respiratory frequency can be considered as constant. The use of short segments and a Hanning window in the time domain (which further shortens the 'effective' length of a segment) also tend to minimize the effects of nonstationarity (Myers et al., 1986). However, the epochs cannot be too short, because biological rhythms generally vary from cycle to cycle. Recordings should be sufficiently long to evaluate the slow variance of interest. The recording duration should be at least 10 times the wavelength of the lower frequency component that was investigated. For the HRV analysis, a recording of approximately one minute is needed to address the HF component, and approximately two minutes is needed to assess LF component. Five minutes segments are highly recommended for clinical studies of HF and LF variability.

A variety of epochs were used in the study of HRV, such as 30-sec (Izard et al., 1991), 60-sec (Harper, Hoppenbrouwers, Sterman, McGinty, & Hodgman, 1976;

Rosenstock, Cassuto, & Zmora, 1999; Schechtman, Henslee, & Harper, 1998), 120-sec (Antila et al., 1990; Liao, Barnes, Chambless, & Heiss, 1996; Myers et al., 1986; Spicer & Lawrence, 1987), and 100-sec (Stevens, Wilson, Franks, & Southall, 1988). Stevens and colleagues support 100-second segments, because it is sufficiently long to get a reliable estimate of parameters, while it is also sufficiently short to allow short-term pattern changes to become apparent. Some researchers use the whole length of the data, 24-hour recording (Leistner et al., 1980; Pikkujamsa et al., 1999). A 5-minute segment is the most popular (Berntson et al., 1997; Bigger et al., 1992; Edlinger, Litscher, & Pfurtscheller, 1994; Kleiger et al., 1991; Rottman et al., 1990; Task Force, 1996).

Another issue, the reproducibility and reliability of HRV metrics were discussed in the literature. Although there were contradictory results, the most of 5-min HRV metrics were reported as reliable and reproducible (Dionne, White, & Tremblay, 2002; Hamilton, Mckenchnie, & Macfarlane, 2004; McNames & Aboy, 2006). Therefore, it is decided to use 5-minute segments for the HRV analysis during the thesis, as the best balance between stationarity issues and enough data to be representative.

3.4.2 Overlapped or Non-Overlapped Segments

Most of the analyses of HRV have been performed for non-overlapping consecutive segments of the RR interval time series. However overlapped segments were also used in some studies (Costa et al., 1994; Myers et al., 1986). Myers and colleagues used overlapped segments of RR interval data in the frequency analysis of HRV. Up to 20 segments of 2-min epochs of RR intervals were selected in each hour, beginning on the hour. Succeeding segments began at the midpoint of the previous segment. Twenty consecutive segments were used if the data in these segments was acceptable. Most of the time, they used the first 21 minutes of data each hour. Noisy segments or segments with premature beats were excluded. In such an instance, the segment began three beats after the last premature or noisy beat. When doing frequency analysis, each 2-min epoch of RR intervals were evenly sampled to 1024 points, the mean of the RR interval was subtracted, and a Hanning window was applied in the time domain. Lastly, an FFT was performed to estimate the power spectrum (Myers et al., 1986).

3.4.3 Effect of Sleep State

HR and HRV are sleep-state dependent variables. It is assumed that the awake-state has the highest HR and HRV, and quiet sleep has the lowest value of HR and HRV. The value for REM is in between. In addition, HR is the slowest and contains the highest frequencies in quiet sleep (Landes, Scher, Sun, & Sclabassi, 1996). Next, sleep-state differences are also shown in the frequency analysis of HRV. The HF component of HRV dominates during quiet sleep, while LF component of HRV dominates in REM (Medigue et al., 1997). Therefore, in order to perform all the HRV analysis and group comparisons in the same awake states, all the data segments used in the study were selected from the same time intervals as possible.

3.5 Derivation of Cardiovascular Time Series

After the QRS complex occurrence times have been estimated, the HRV time series can be derived. The inter-beat intervals or RR intervals are obtained as differences between successive R-wave occurrence times, i.e. $T_n = t_n - t_{n-1}$ (Figure 3.1(a)). The time series constructed from all available RR intervals can be represented as a tachogram, i.e.(n, T_n) (Figure 3.1(b)) or a function, i.e.(t_n, T_n), (Figure 3.1(c)). Majority of studies related to analysis of HRV signal in the literature are preferred to use the latter approach (Task Force, 1996).

In some context, normal-to-normal (NN) may also be used when referring to these intervals indicating strictly intervals between successive QRS complexes resulting from SA-node depolarization (Task Force, 1996). In practice, the NN and RR intervals appear to be the same and throughout this thesis the term RR is preferred.

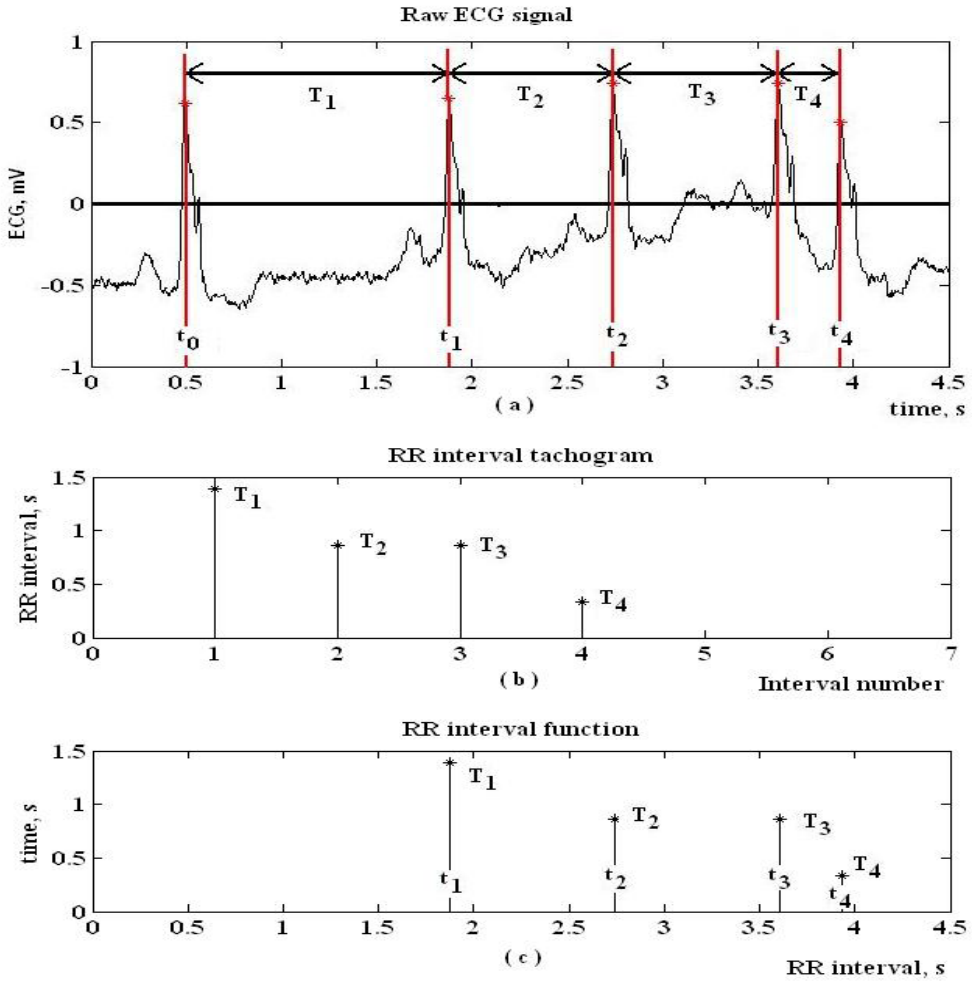

Figure 3.1 Derivation of two HRV signals from ECG: (a) raw ECG signal, (b) the interval tachogram and (c) the interval function of the signal.

3.6 Preprocessing of Cardiovascular Time Series

Any artifact in the RR interval time series may interfere the analysis of these signals. The artifacts within cardiovascular signals can be divided into technical and physiological artifacts. The technical artifacts can include missing or additional QRS complex detections, errors in R-wave occurrence times. These artifacts may be due to measurement artifacts or the computational algorithm. The physiological artifacts, on the other hand, include ectopic beats and arrhythmic events. In order to avoid the interference of such artifacts, the ECG recordings and the corresponding event series should always be manually checked for artifacts and only artifact-free sections should be included in the analysis (Task Force, 1996). Alternatively, if the amount of artifact-free data is insufficient, proper interpolation methods can be used to reduce these artifacts

(Clifford & Tarassenko, 2005; Lippman, Stein, & Lerman, 1993, 1994; Mateo & Laguna, 2003).

Another common feature that can alter the analysis significantly is the slow linear or more complex trends within the analyzed time series. Such slow nonstationarities are characteristic for cardiovascular variability signals and should be considered before the analysis. The origins of nonstationarities in HRV are discussed (Berntson et al., 1997). Two kinds of methods have been used to get around the nonstationarity problem. In (Weber, Molenaar, & Van der Molan, 1992), it was suggested that HRV data should be systematically tested for nonstationarities and that only stationary segments should be analyzed. Representativeness of these segments in comparison with the whole HRV signal was, however, questioned in (Grossman, 1992). Other methods try to remove the slow nonstationary trends from the HRV signal before analysis. The detrending is usually based on first order (Litvack, Oberlander, Carney, & Saul, 1995; Mitov, 1998) or higher order polynomial (Mitov, 1998) models. Recently, an advanced detrending procedure based on smoothness priors' regularization was presented (Tarvainen, Ranta-aho, & Karjalainen, 2002).

3.6.1 Artifact Removal

The first aim is to detect ectopic beats, which are QRS complexes not resulting from SAN depolarization (Clifford, Azuaje, & McSharry, 2006). Atrial and ventricular premature complexes (APCs and VPCs) can easily be identified through an analysis of the temporal series of the RR tachogram. When an APC occurs, a sudden reduction in the tachogram is present. The following sinus beat, however, has a normal distance from the ectopic one. A comparison of the RR intervals with respect to the mean of the preceding RR interval can be implemented to automatically detect APC. A VPC, instead, is characterized by a prolonged RR interval immediately following the ectopic beat (so-called compensatory pause) (Fig. 3.2).

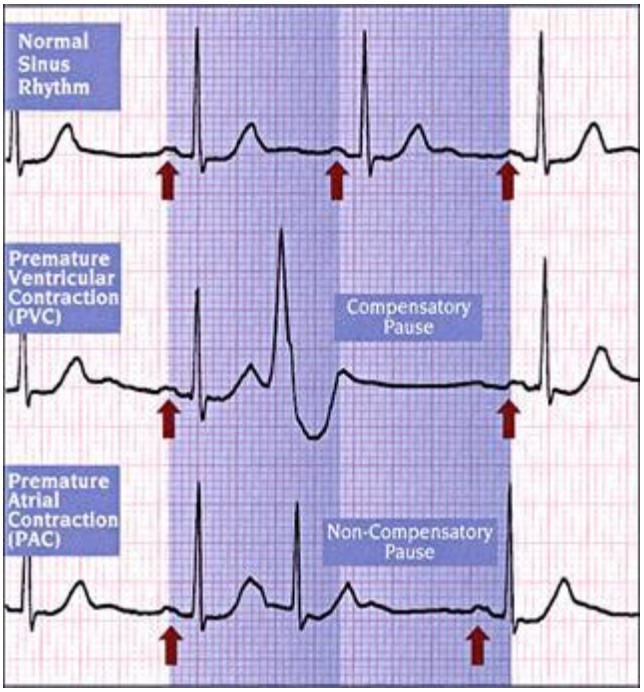

Figure 3.2 Examples of normal, APC, and VPC beats by means of compensatory and non-compensatory pauses (Clifford, Azuaje, & McSharry, 2006).

The effects of calculating the HRV indices on an artificial tachogram for varying level of ectopy have been illustrated as significant (Clifford & Tarassenko, 2005). Therefore, it is obvious that ectopic beats must be removed from the RR tachogram. In general, FFT-based techniques require the replacement of the removed beat at a location where one would have been expected the beat to have occurred if it was a sinus beat. Methods for performing beat replacement range from linear and cubic spline interpolation, AR model prediction, segment removal, and segment replacement (Clifford, Azuaje, & McSharry, 2006). The same procedure is also necessary for missing beats (Clifford & Tarassenko, 2005). Clifford & Tarassenko offer using Lomb-Scargle Periodogram method, which allows the removal of up to 20% of the data points in an RR tachogram without introducing a significant resampling error in an HRV metric.

3.6.2 Interpolation

Since the RR interval time series signal is sampled unevenly (according to the duration of each beat), the data must be evenly re-sampled. Selecting the optimal

sampling frequency is an important step. To avoid aliasing, the required sampling frequency must be at least twice the highest resolvable frequency, and a sampling frequency of 4 times the target frequency is more appropriate. So, for the HRV studies of humans, a sampling rate of 4 Hz is sufficient to capture the HF components. That sampling frequency is also appropriate for infants, who have high respiratory rates, and for adults during exercise (Berntson et al., 1997). Nonetheless, Clifford studied the effect of resampling and offered a sampling rate of at least 7 Hz in his studies (Clifford & Tarassenko, 2005). In this study, the cubic spline interpolation method with 7-Hz sampling frequency was chosen.

3.6.3 Detrending

Any estimation that attempts to characterize the specific periodicities over time may be distorted by slow linear or irregular trends, and might lead to misinterpretations of the results. As a result, 5-minute segments were chosen in this study for HRV analysis as offered in (Task Force, 1996). Then, remove the trends from these HRV data segments using smoothness priors detrending method were applied (Tarvainen, Ranta-aho, & Karjalainen, 2002).

Special attention was appointed to the slow trend components that are characteristic of cardiovascular signals. For removing such trend components, an advanced detrending method should be preferred. The method is based on smoothness priors formulation and was originally presented with an application to HRV analysis (Tarvainen, Ranta-aho, & Karjalainen, 2002). The main advantage of this method is its simplicity compared to methods presented in (Litvack et al., 1995). The frequency response of the method is adjusted with a single parameter. This smoothing parameter λ should be selected in such a way that the spectral components of interest are not significantly affected by detrending. Another advantage of this method is that the filtering effect is attenuated in the beginning and end of the data and thus the distortion of data end points is avoided.

3.7 Analysis Methods of HRV

In this section, a short review of measures used in the analysis of short-term HRV recordings is given. The selection of the presented measures is based on the guidelines given in (Task Force, 1996). The analysis methods of HRV can be roughly divided into time-domain, frequency-domain, and nonlinear methods. In addition, time-varying methods such as time-frequency representations have been utilized. The presented HRV measures are explained below in detail.

3.7.1 Time - Domain Measures

Time domain analysis, which is the statistical analysis of the fluctuations in RR intervals, is the most commonly used method in the study of HRV. Generally speaking, time domain measures are simple and inexpensive to compute. However, simple descriptive statistics only provide global estimates of HRV. They cannot differentiate frequency components and attribute different components to different physiological activities precisely. The parameters of short-term time-domain HRV measures are listed in Table 3.1.

In the analysis of HRV, there are two different approximations that emphasize short-term (fast) and long-term (slow) variability. Short-term HRV is assumed to be associated with parasympathetic (vagal) activity. Long-term HRV is assumed to reflect both sympathetic and vagal influences. There is more disagreement on interpreting long-term variability. It has not been demonstrated whether they are related mainly to sympathetic influences, or to the sympathetic and vagal balance (Izard et al., 1991; Malik & Camm, 1995; Porges & Byrne, 1992).

Table 3.1 The most commonly used time domain HRV measures

MEAN	Arithmetic mean of all RR values. (4.2 $$MEAN = \overline{RR} = \frac{1}{N}\sum_{i=1}^{N} RR_i$$
SDNN	Standard deviation of normal-to-normal RR intervals over a period of time is a broad-band measure, containing both high and low frequency components of RR interval fluctuations (Berntson et al., 1997). In many studies, SDNN is calculated over a 24-hour period and thus it measures all sources of HRV, short-term high frequency variations as well as the lowest frequency components seen in the 24-hour period, such as circadian rhythms. $$SDNN = \sqrt{\frac{1}{N-1}\sum_{i=1}^{N}(RR_i - \overline{RR})^2}$$
SDSD	Standard deviation of successive differences between normal-to-normal RR intervals is defined as: $$SDSD = \sqrt{\frac{1}{N-2}\sum_{i=2}^{N}\left(RR_i - RR_{i-1} - \frac{1}{N-1}\sum_{k=2}^{N}(RR_k - RR_{k-1})\right)^2}$$
RMSSD	Root mean square of successive differences between normal-to-normal RR intervals (Antila et al., 1990; Berntson et al., 1997; Bigger et al., 1989) is defined as: $$RMSSD = \sqrt{\frac{1}{N-1}\sum_{i=2}^{N}(RR_i - RR_{i-1})^2}$$
NN_{dd}	The absolute number of differences between successive normal RR intervals that are greater than *dd* ms. Although *dd* value accepted as *50* in common (Bigger et al., 1989), recent researches show that the value of *20* is more effective for discriminating the patients from normals (Mietus, Peng, Henry, Goldsmith, & Goldberger, 2002).
pNN_{dd}	The percent of absolute differences between successive normal RR intervals that are greater than *dd* ms.

3.7.2 Frequency - Domain Measures

Compared with time domain measures, frequency domain measures of HRV have the advantage of better separation of parasympathetic and sympathetic influences. Frequency domain methods decompose the total variation of the RR interval time series into many different frequency components, which can be attributed to different physiologic effects. There are three major frequency bands for HRV in adults. The

definition of these three frequency bands is not exactly the same throughout the literature (Bigger et al., 1992; Costa et al., 1994; Kleiger et al., 1991; Mazursky, Birkett, Bedell, Ben-Haim, & Segar, 1998; Mrowka, Schluter, Gerhardt, & Patzak, 1996; Myers et al., 1986; Ori, Monir, Weiss, Sayhouni, & Singer, 1992; Task Force, 1996). After the task force published in 1996, these main spectral components are standardized for short-term HRV recordings: very low frequency (VLF), low frequency (LF), and high frequency (HF) components. These frequency bands are limited bounded with the limits 0-0.04 Hz, 0.04-0.15 Hz, and 0.15-0.40 Hz, respectively. In addition, researchers also show that the regulators of these frequency bands are circadian rhythm (Barrett, Navakatikyan, & Malpas, 2001; Braga, Da Silva, Da Silva, Fontes, & dos Santos, 2002), temperature & humoral systems (Braga et al., 2002; Porter & Rivkees, 2004; Vornanen, Ryukkynen, & Nurmi, 2002; Williams, Chambers, Henderson, Rashotte, & Overton, 2002) for VLF, ANS (Sympathetic and Parasympathetic systems) (Goldstein et al., 1998; Lanfranchi & Somers, 2002; Malpas, 2002) for LF, and Vagal innervations & RSA (Barbieri, Triedman, & Saul, 2002; Rentero et al., 2002) for HF.

In order to calculate these measures, there exist several power spectral density (PSD) estimation methods such as FFT-, Autoregressive-modeling, Lomb-Scargle-, and Wavelet-based periodogram techniques in the literature. The most commonly used frequency domain parameters are summarized in Table 3.2.

3.7.3 Nonlinear Parameters

Nonlinear characteristics are certainly involved in HRV. Some investigators emphasize the importance of using nonlinear techniques to quantify HRV. It has been suggested that through nonlinear analysis of HRV, it might be possible to obtain precious information for physiological interpretation of HRV and to obtain (diagnosis) / to predict (prognosis) patients for various cardiac and non-cardiac diseases. However, these nonlinear methods have not been used systematically to investigate large patient populations. At present, they are just potential tools for HRV assessment (Task Force, 1996).

Table 3.2 The most commonly used frequency domain HRV measures

TP	Total power is defined as the area under the power spectral curve (Bigger et al., 1989, 1992; Ori et al., 1992), or the sum of HF and LF (Kleiger et al., 1991).
PVLF	Absolute very low frequency power is the area under the power spectral curve related to VLF band.
PLF	Absolute low frequency power is the area under the power spectral curve related to low frequency band. Some studies suggest that LF is a quantitative marker of sympathetic modulations, while others view LF as reflecting both sympathetic activity and vagal activity (Rottman et al., 1990; Yeragani et al., 1998).
PHF	Absolute high frequency power is the area under the power spectral curve related to high frequency band. Most researchers agree that vagal activity is the major contributor to the HF component.
NLF	Normalized LF is defined as $LF/(LF + HF)$.
NHF	Normalized HF is defined as $HF/(LF + HF)$.
LFHF	The ratio of LF over HF (LF/HF), which is considered by some investigators to reflect the balance between sympathetic and vagal or to reflect the sympathetic modulation (Task Force, 1996).

There are several nonlinear methods such as Detrended Fluctuation Analysis (Hu, Ivanov, Chen, Carpena, & Stanley, 2001; Kantelhardt, Koscielny-Bunde, Rego, Havlin, & Bunde, 2001; Peng et al., 1994; Taqqu, Teverovsky, & Willinger, 1995), Approximate Entropy (Pincus, 1991; Yeragani et al., 1998), Sample Entropy (Goldberger et al., 2000), Multiscale entropy analysis (Costa, Goldberger, & Peng, 2002, 2005), Poincare plot (Kamen, Krum, & Tonkin, 1996; Kamen & Tonkin, 1995), Symbolic Dynamic (Mokikallio et al., 1997) in the literature, which are used in HRV analyses. In a recent study, minimum 10000 samples are required for the reliability of the validity for all nonlinear measures except the Poincare plots' measures (Şeker, Saliu, Birand, & Kudaiberdieva, 2000). Because this thesis is focused on only 5-min HRV analysis, there are approximately 300 samples for each data. Therefore, only Poincare plots' measures were used in the thesis.

CHAPTER FOUR
METHODS

The act of taking raw data and making an action based on the category of the pattern is so-called ***Pattern Recognition*** (Duda, Hart, & Stork, 2001). The primary goal of pattern recognition is supervised or unsupervised classification of some patterns (data). Among the various frameworks in which pattern recognition has been traditionally formulated, the statistical approach most intensively studied and used in practice (Jain, Duin, & Mao, 2000). A general pattern recognition system consists of six stages: data acquisition, preprocessing, feature extraction, feature selection, classification, and evaluating the model.

4.1 Data Acquisition Stage

In the data acquisition stage, the data is collected from the human using an electrocardiography or a Holter device. In the former one, the patient is in the resting position while ECG is being recorded. This is preferred if the record is processed in a short-term (5- or 6-second and maximum 10-minute) duration. In the latter one, the patient is equipped with the Holter device which is taken back after 24- or 48-hour duration. Alternatively, the already recorded data can be used in the research.

4.2 Preprocessing Stage

This stage is the most problem-dependent part of the system. The data preprocessing step includes noise removal, data transformation (from ECG data to HRV data), artifact removal (bad data rejection), interpolation (resampling), and detrending (Lynn & Chiang, 2001). These steps are explained in the following subsections.

4.2.1 Noise Removal

In general, the aim of the preprocessing steps is to improve the signal-to-noise ratio (SNR) of the ECG for more accurate analysis and measurement. Noises may disturb the

ECG to such an extent that measurements from the original signals are unreliable. The main categories of noise are low-frequency baseline wander caused by respiration and body movements, high-frequency random noises by mains interference (50 Hz or 60 Hz), and muscular activity, and random shifts of the ECG signal amplitude caused by poor electrode contact and body movements. Robust classical deterministic digital filtering techniques are mostly used in the field of arrhythmia detection. On the other hand, in the domain of ST segment analysis where accurate wave measurements are the main features of interest, filtering must not disturb the fine structure of the useful signal. In such cases, it is not possible to improve the SNR solely by using deterministic digital filtering techniques, and advanced nonlinear techniques are required (Clifford, Azuaje, & McSharry, 2006).

Since low-frequency baseline wander among these noises cause the ST segment elevation in ECG (Sornmo, 1993), elimination of this makes the clinical information more valuable (Mozaffary & Tinati, 2005). This noise has been investigated using various methods in the literature. In a study, baseline is estimated using the function approximation method of ***Cubic Spline*** and it is removed from the original ECG signal (Meyer & Kelser, 1977). In another study, baseline wander is estimated from PR segments in ECG using linear interpolation technique (MacFarlane, Peden, Lennox, Watts, & Lawrie, 1977). This method is a nonlinear one and it does not give correct results in lower heart rates. In addition to these methods, filtering is very common method with the cut-off frequencies of 0.8 Hz (Van Aleste & Schilder, 1985) or 0.64 Hz (Christov, Dotsinsky, & Daskalov, 1992). Nonetheless, there are some problems in using filters: First, the number of coefficients to implement filter and the response time delay are extremely high when FIR structure is used. Next, since the frequency ranges of baseline wander and those of ECG signal are overlapped, removal of baseline wander using filtering causes the information losses in ECG components. In addition, these cut-off frequencies do not satisfy the lowest ECG frequency (0.05 Hz) offered by American Heart Association (AHA), which causes the distortion on the ST segment and the QRS complexes (American Heart Association, 1975). Therefore, alternative filtering techniques such as time-varying filter (Sornmo, 1993), wavelet packets transformation

(Mozaffary & Tinati, 2005) and adaptive bionic wavelet transform (Soyadi & Shamsollahi, 2008) have been used in the literature.

4.2.2 Data Transformation

This subsection is the QRS detection. Fig. 4.1 shows the various processes involved in the analysis of the ECG signal. In order to isolate the portion of the wave, of which QRS energy dominant, the signal is passed through a band-pass filter that is composed of cascaded low- and high-pass filters. Then the signal is subjected to differentiation, squaring, time averaging, and finally peak is detected by applying threshold logic (Pan & Tompkins, 1985).

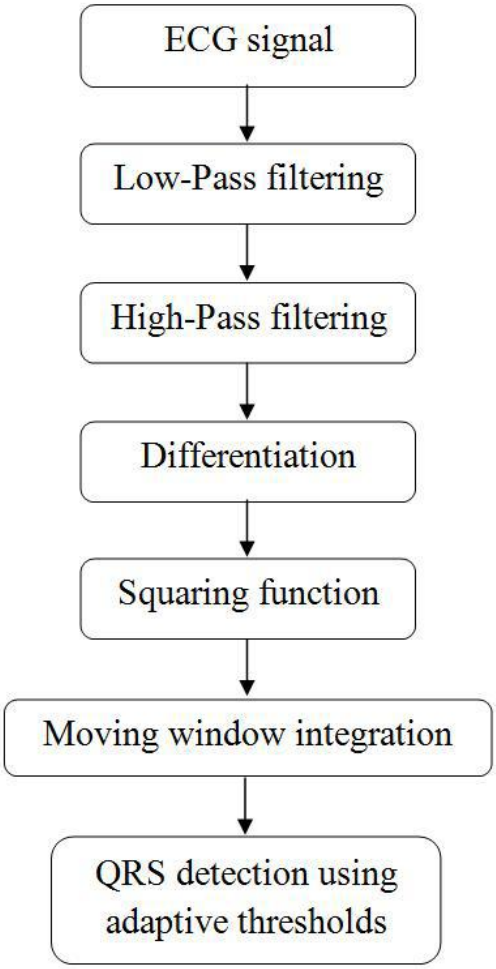

Figure 4.1 Block diagram of the QRS detector used in the study.

4.2.2.1 Low-Pass Filtering

The transfer function of the second-order low-pass filter is

$$H(z) = \frac{(1 - z^{-6})^2}{(1 - z^{-1})^2} \tag{4.1}$$

and the difference equation of this filter is

$$y(nT) = 2y(nT - T) - y(nT - 2T) + x(nT) - 2x(nT - 6T) + x(nT - 12T) \tag{4.2}$$

The cutoff frequency is about 11 Hz, the delay is five samples (or 25 ms for a sampling rate of 200 sps), and the gain is 36.

4.2.2.2 High-Pass Filtering

A high-pass filter is implemented by subtracting a first-order low-pass filter from an all-pass filter with delay. The high-pass filter is obtained by dividing the output of the low-pass filter by its DC gain and then subtracting from the original signal. The transfer function of the high-pass filter is

$$H(z) = z^{-16} - \frac{\frac{1 - z^{-32^2}}{1 - z^{-1}}}{32} \tag{4.3}$$

and the difference equation of this filter is

$$y(nT) = x(nT - 16T) - \frac{y(nT - T) + x(nT) - x(nT - 32T)}{32} \tag{4.4}$$

The low cut-off frequency of this filter is about 5 Hz, the delay is about 16T (or 80 ms), and the gain is 1.

Fig. 4.2 shows the amplitude-response of the band-pass filter which is composed of the cascade of the low-pass and high-pass filters. The center frequency of the pass-band is at 10 Hz. The amplitude response of this filter is designed to approximate the spectrum of the average QRS complex. Thus this filter optimally passes the frequencies characteristic of a QRS complex while attenuating lower and higher frequency signals.

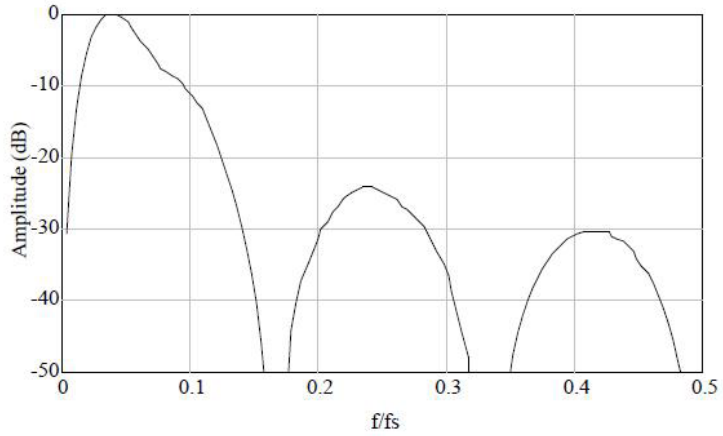

Figure 4.2 Amplitude response of band-pass filter composed of low-pass and high-pass filters (Tompkins, 2000).

4.2.2.3 Differentiation

After the signal has been filtered, it is then differentiated to provide information about the slope of the QRS complex. A five-point derivative has the transfer function

$$H(z) = 0.1(2 + z^{-1} - z^{-3} - 2z^{-4}) \tag{4.5}$$

This derivative is implemented with the difference equation

$$y(nT) = \frac{2x(nT) + x(nT - T) - x(nT - 3T) - 2x(nT - 4T)}{8} \tag{4.6}$$

The fraction 1/8 is an approximation of the actual gain of 0.1. Throughout these filter designs; we approximate parameters with power-of-two values to facilitate real-

time operation. Note that P and T waves are further attenuated while the peak-to-peak signal corresponding to the QRS complex is further enhanced (Tompkins, 2000).

4.2.2.4 Squaring Function

The previous processes and the moving-window integration, which is explained in the next subsection, are linear processing parts of the QRS detector. The squaring function that the signal now passes through is a nonlinear operation. The equation that implements this operation is

$$y(nT) = [x(nT)]^2 \tag{4.7}$$

This operation makes all data points in the processed signal positive, and it amplifies the output of the derivative process nonlinearly. It emphasizes the higher frequencies in the signal, which are mainly due to the QRS complex. A fact to note in this operation is that the output of this stage should be hard-limited to a certain maximum level corresponding to the number of bits used to represent the data type of the signal.

4.2.2.5 Moving Window Averaging

The slope of the R wave alone is not a guaranteed way to detect a QRS event. Many abnormal QRS complexes that have large amplitudes and long durations (not very steep slopes) might not be detected using information about slope of the R wave only. Thus, we need to extract more information from the signal to detect a QRS event. Moving window integration extracts features in addition to the slope of the R wave. It is implemented with the following difference equation:

$$y(nT) = \frac{1}{N}\sum_{k=0}^{N-1} x((n-k)T) \tag{4.8}$$

where N is the number of samples in the width of the moving window. The value of this parameter should be chosen carefully. For a sample rate of 200 sps, the window chosen for this algorithm was 30 samples wide (which correspond to 150 ms).

Fig. 4.3 shows the appearance of some of the filter outputs of this algorithm. Note the processing delay between the original ECG complexes and corresponding waves in the moving window integral signal.

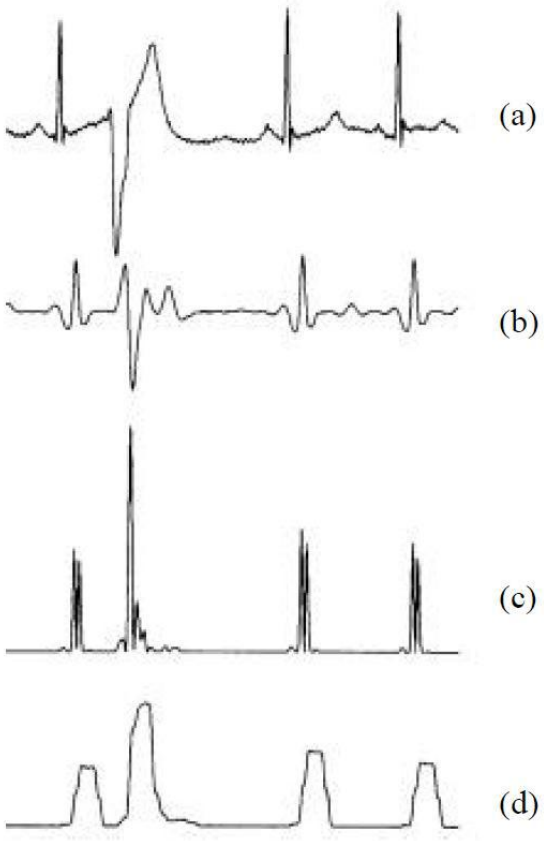

Figure 4.3 QRS detector signals: (a) Unfiltered ECG, (b) Output of band-pass filter, (c) Output after differentiation, and squaring processes, and (d) Final moving-window integral (Tompkins, 2000).

4.2.2.6 Adaptive Threshold Logic

The set of thresholds detection algorithm were set such that signal peaks (i.e., valid QRS complexes) were detected (Pan & Tompkins, 1985). Signal peaks are defined as

those of the QRS complex, while noise peaks are those of the T waves, muscle noise, etc. After the ECG signal has passed through the band-pass filter stages, its signal-to-noise ratio increases. This permits the use of thresholds that are just above the noise peak levels. Thus, the overall sensitivity of the detector improves.

Two sets of thresholds are used, each of which has two threshold levels. The set of thresholds that is applied to the waveform from the moving window integrator is

$$SPKI = 0.125(PEAKI) + 0.875(SPKI) \tag{4.9}$$

if PEAKI is the signal peak,

$$NPKI = 0.125(PEAKI) + 0.875(NPKI) \tag{4.10}$$

if PEAKI is the noise peak, and

$$THRESHOLD1 = (NPKI) + 0.25(SPKI - NPKI) \tag{4.11}$$

$$THRESHOLD2 = 0.5(THRESHOLD1) \tag{4.12}$$

where PEAKI is the overall peak, SPKI is the running estimate of the signal peak, NPKI is the running estimate of the noise peak, THRESHOLD1 is the first threshold applied, and THRESHOLD2 is the second threshold applied.

A peak is determined when the signal changes direction within a certain time interval. Thus, SPKI is the peak that the algorithm has learned to be that of the QRS complex, while NPKI peak is any peak that is not related to the signal of interest.

As can be seen from the equations, new values of thresholds are calculated from previous ones, and thus the algorithm adapts to changes in the ECG signal from a particular person.

Whenever a new peak is detected, it must be categorized as a noise peak or a signal peak. If the peak level exceeds THRESHOLD1 during the first analysis of the signal, then it is a QRS peak. If search-back technique is used, then the signal peak should exceed THRESHOLD2 to be classified as a QRS peak. If the QRS complex is found using this second threshold level, then the peak value adjustment is twice as fast as usual.

The output of the final filtering stages, after the moving window integrator, must be detected for peaks. A peak detector algorithm finds peaks and a detection algorithm stores the maximum levels at this stage of the filtered signal since the last peak detection. A new peak is defined only when a level that is less than half the height of the peak level is reached. Fig. 4.4 illustrates that this occurs halfway down the falling edge of the peak (Pan & Tompkins, 1985).

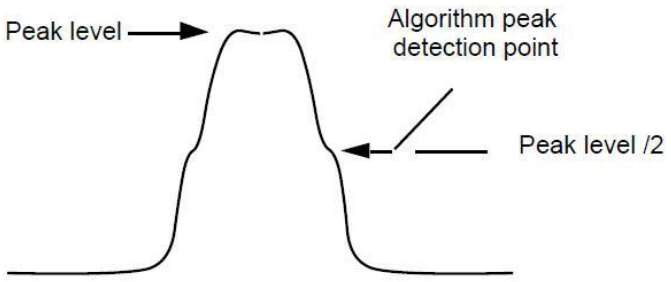

Figure 4.4 Output after the moving window integrator, with peak detection point (Tompkins, 2000).

The accuracy of the R-wave occurrence time estimates is often required to be 1-2 ms and, thus, the sampling frequency of the ECG should be at least 500-1000 Hz (Task Force, 1996). If the sampling frequency of the ECG is less than 500 Hz, the errors in R-wave occurrence times can cause critical distortion to HRV analysis results, especially to spectrum estimates (Merri, Farden, Mottley, & Titlebaum, 1990). The distortion of the spectrum is even bigger if the overall variability in HR is small (Pinna, Maestri, di Cesare, Colombo, & Minuco, 1994). The estimation accuracy can, however, be improved by interpolating the QRS complex, e.g., by using a cubic spline interpolation (Daskalov & Christov, 1997). It should be, however, noted that when the SA-node

impulses are of interest there is an unavoidable estimation error of approximately 3 ms due to fluctuations in the AV-nodal conduction time (Rompelman, 1993).

4.2.3 Artifact Removal

In ECG analysis, it is desirable to use only those heartbeats which are expected not to be disturbed by waves of the previous or following heartbeats. Therefore, abnormal beats like ventricular premature and atrial premature beats, and their neighbors, should be excluded from the beat sequence. These beats are also called as bad data or outliers in the literature (Clifford, Azuaje, & McSharry, 2006). Langley and colleague's algorithm identifies as possible ectopic those beats whose RR interval falls below the moving average of RR less 20% (Langley et al., 2001). Among these, the beats followed by beat introducing a ±10% variation from the mean RR classified as atrial; those followed by RR value exceeding the moving RR average of ±30% as ventricular (Fig. 4.5).

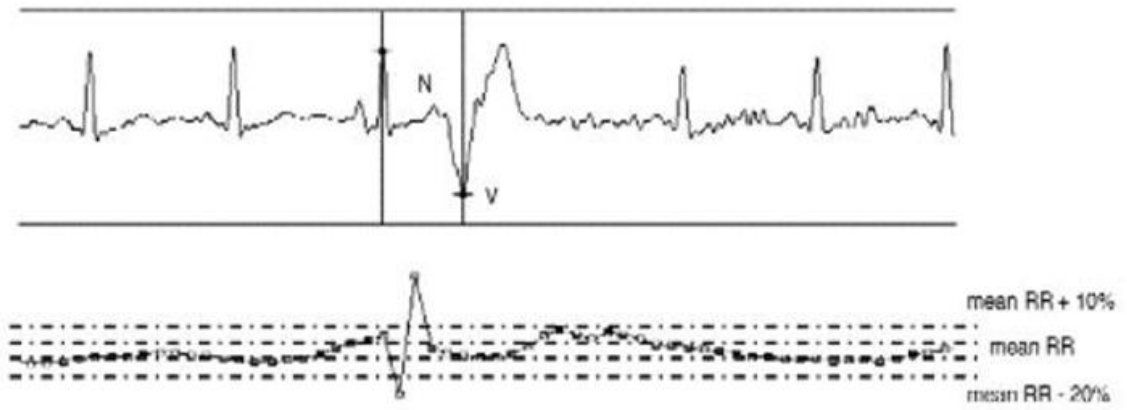

Figure 4.5 Example of an RR series where a ventricular ectopic beat can easily be identified (Langley et al., 2001).

4.2.4 Interpolation

The idea is that the points are in some sense correct and lie on an underlying but unknown curve, the problem is to be able to estimate the values of the curve at any position between the known points. Cubic spline method is possibly the most preferred method among interpolation techniques because it is a smoother function and offers true

continuity between the segments (Kreyzig, 1993). Fig. 4.6 shows the principle with an example application of both linear and cubic spline interpolation techniques.

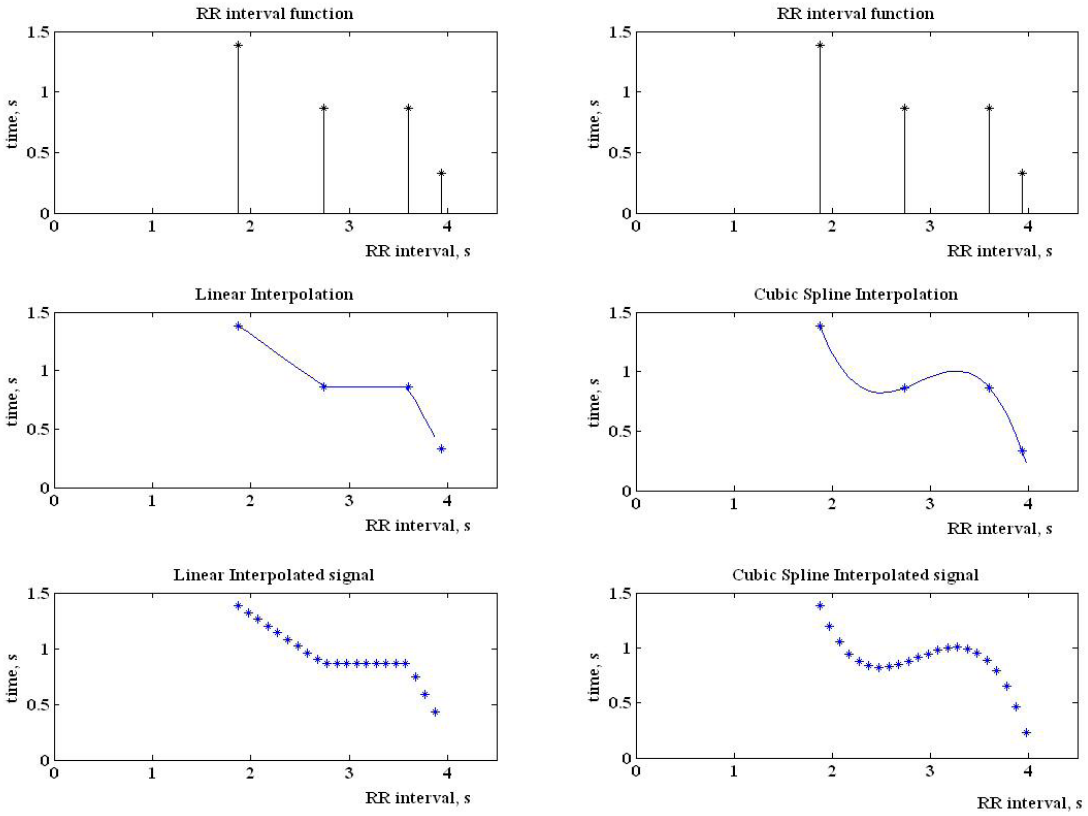

Figure 4.6 Interpolation methods with an example application. Linear interpolation is on the left and cubic spline interpolation is on the right. The first row is the real values of the data, the second row illustrates the fitted functions for the data, and the bottom row gives the interpolated values with 10-Hz resampling rate.

4.2.4.1 Cubic Spline Interpolation

Given $N+1$ distinct ***knots*** x_i such that $a = x_0 < x_1 < \cdots < x_{N-1} < x_N = b$ with $N+1$ ***knot values*** $y_i = f(x_i)$, we are trying to find a spline function of degree N

$$S(x) = \begin{Bmatrix} S_0(x) & x \in [x_0 \quad x_1] \\ S_1(x) & x \in [x_1 \quad x_2] \\ \vdots & \vdots \\ S_{N-1}(x) & x \in [x_{N-1} \quad x_N] \end{Bmatrix} \tag{4.13}$$

where each

$$S_i(x) = \sum_{k=0}^{3} \left(\beta_{i,k}(x - x_i)^k\right) \tag{4.14}$$

For a data set x_i of $N + 1$ points, we can construct a cubic spline with N piecewise cubic polynomials between the data points (Fig. 4.7). If $S(x)$ represents the spline function interpolating the function$f$, we require:

- the interpolating property, $S_i(x_i) = f(x_i)$, $i = 0,1, \dots, N$,
- the spline to join up, $S_{i-1}(x_i) = S_i(x_i)$, $i = 1,2, \dots, N-1$, and
- twice continuous differentiable, $S'_{i-1}(x_i) = S'_i(x_i)$ and $S''_{i-1}(x_i) = S''_i(x_i)$, $i=1, i = 1,2, \dots, N-1$.

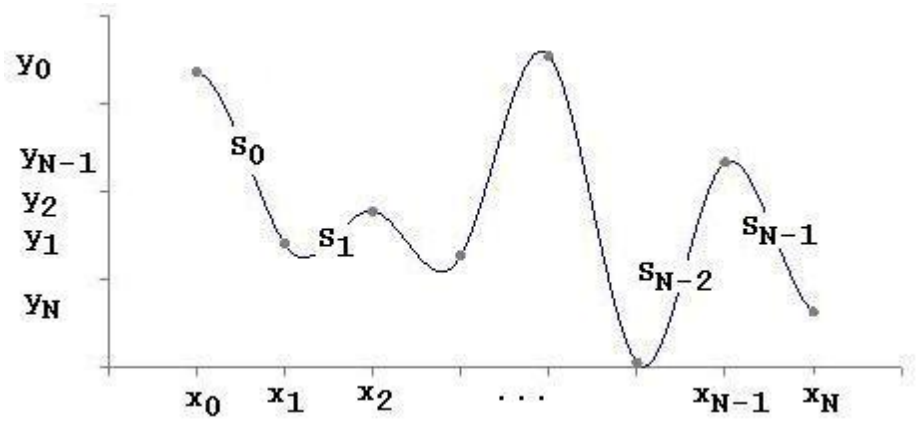

Figure 4.7 Cubic Spline interpolation method.

For the N cubic polynomials comprising S, this means to determine these polynomials, we need to determine $4N$ conditions (since for one polynomial of degree three, there are four conditions on choosing the curve). However, the interpolating property gives us $N + 1$ conditions, and the conditions on the interior data points give us $N - 1$ data points each, summing to $4N - 2$ conditions. We require two other conditions, and these can be imposed upon the problem for different reasons.

One such choice results in the so-called clamped cubic spline, with $S'(x_0) = u$ and $S'(x_n) = v$ for given values u and v. Alternately, we can set $S''(x_0)$ and $S''(x_n)$ to 0 resulting in the natural cubic spline.

Amongst all twice continuously differentiable functions, clamped and natural cubic spline yield the least oscillation about the function f which is interpolated.

After solving these equations (Schilling & Sandra, 1999), the interpolation using natural cubic spline can be defined as

$$S_i(x) = \frac{z_{i+1}(x - x_i)^3 + z_i(x_{i+1} - x)^3}{6h_i} + \left(\frac{y_{i+1}}{h_i} - \frac{h_i}{6} z_{i+1}\right)(x - x_i) + \left(\frac{y_i}{h_i} - \frac{h_i}{6} z_i\right)(x_i - x) \tag{4.15}$$

where

$$h_i = x_{i+1} - x_i \tag{4.16}$$

The coefficients can be found by solving this system of equations:

$$z_o = 0$$

$$h_{i-1} z_{i-1} + 2(h_{i-1} + h_i) z_i + h_i z_{i+1} = 6\left(\frac{y_{i+1} - y_i}{h_i} - \frac{y_i - y_{i-1}}{h_{i-1}}\right) \tag{4.17}$$

$$z_n = 0$$

4.2.5 Detrending

Any estimation that attempts to characterize the specific periodicities over time may be distorted by slow linear or irregular trends, and might lead to misinterpretations of the results. Spectral analysis requires that the data series is at least weakly stationary. Actually, in the study of HRV, this is a difficult issue because the actual heart period data are commonly nonstationary. Several methods have been suggested to deal with

this problem: (a) choosing shorter analytical epochs, because nonstationarity increases with the length of the sample epoch; (b) removing slow nonstationary trends before analysis; (c) applying band-pass filters to isolate the frequency component of the interest (Berntson et al., 1997). Alternatively, techniques designed for evaluating nonstationary signals, such as wavelets, should be used. Recently, a robust and ease-to-use detrending method was published (Tarvainen, Ranta-aho, & Karjalainen, 2002) of which principles are explained below in detail.

4.2.5.1 Smoothness Priors Method

Let $x \in R^N$ denote the RR interval time series which can be considered to consist of two components

$$x = x_{stat} + x_{trend} \tag{4.18}$$

where x_{stat} is the nearly stationary RR interval series of interest and x_{trend} is the low frequency aperiodic trend component. Suppose that the trend component can be modeled with a linear observation model as

$$x_{trend} = H\theta + e \tag{4.19}$$

where $H \in R^{Nxp}$ is the observation matrix, $\theta \in R^p$ are the regression parameters, and e is the observation error. The task is then to estimate the parameters by some fitting procedure so that $\hat{x}_{trend} = H\hat{\theta}$ can be used as the estimate of the trend. The properties of the estimate depend strongly on the properties of the basis vectors (columns of the matrix H) in the fitting. A widely used method for the solution of the estimate $\hat{\theta}$ is the least squares method. However, a more general approach for the estimation of $\hat{\theta}$ is used here. That is, the so-called regularized least squares solution

$$\hat{\theta}_\lambda = argmin_\theta\{\|x - H\theta\|^2 + \lambda\|D_d(H\theta)\|^2\} \tag{4.20}$$

where λ is the regularization parameter and D_d indicates the discrete approximation of the d-th derivative operator. This is clearly a modification of the ordinary least squares solution to the direction in which the side norm $\|D_d(H\theta)\|$ gets smaller. In this way, prior information about the predicted trend $H\theta$ can be implemented to the estimation. The solution of (4.20) can be written in the form (Tarvainen, Ranta-aho, & Karjalainen, 2002)

$$\hat{\theta}_\lambda = (H^T H + \lambda H^T D_d^T D_d H)^{-1} H^T x \tag{4.21}$$

and the estimate for the trend which is to be removed as

$$\hat{x}_{trend} = H\hat{\theta}_\lambda \tag{4.22}$$

The selection of the observation matrix H can be implemented according to some known properties of the data x. For example, a generic set of Gaussian shaped functions or sigmoids can be used. Here, however, the trivial choice of identity matrix $H = I \in R^{NxN}$ is used. In this case, the regularization part of (4.20) can be understood to draw the solution toward the null space of the regularization matrix D_d. The null space of the second order difference matrix contains all first order curves and, thus, D_2 is a good choice for estimating the aperiodic trend of RR series. With these specific choices, the detrended nearly stationary RR series can be written as

$$x_{stat} = x - H\hat{\theta}_\lambda = (I - (I + \lambda D_2^T D_2)^{-1})x \tag{4.23}$$

Fig. 4.8 illustrates the all above processes.

4.3 Feature Extraction Stage

Useful information that best represent characteristics of data must be extracted and rearranged into proper format. Feature extraction is the linear or non-linear transformation of the original feature space. The extracted features will then be fed into a classifier for classification (Lynn & Chiang, 2001). The most widely used feature extraction techniques can be roughly divided into time-domain, frequency-domain and

nonlinear methods. In addition, time-varying methods such as time-frequency representations have been utilized. In the following subsections, these methods (except time-domain HRV measures which was given in Table 3.1) used in the analysis of HRV are explained in detail.

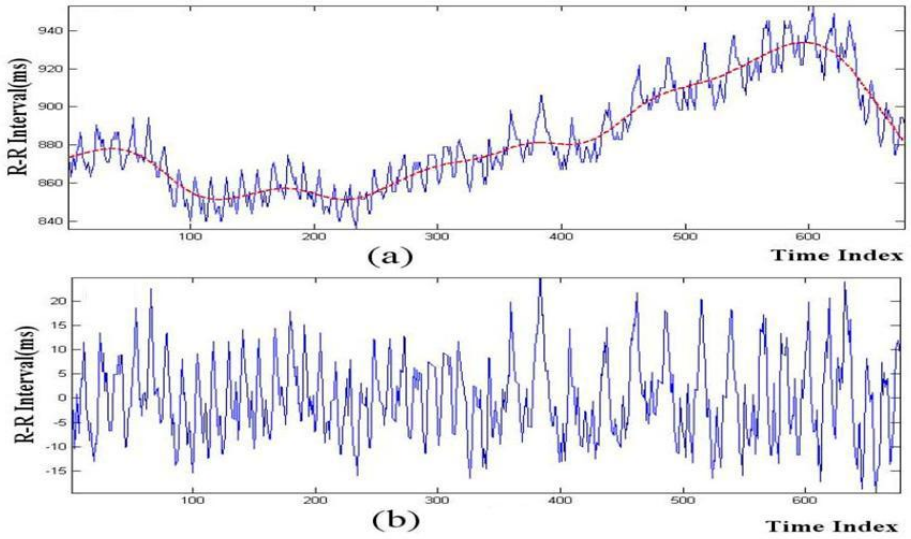

Figure 4.8 Smoothness priors detrending method: (a) interpolated RR interval function with trend and (b) detrended RR interval function.

4.3.1 Frequency - Domain Measures

In order to calculate these measures, there exist several methods in the literature. FFT-, Auto Regressive-, and Lomb-Scargle-based periodograms are the most popular ones due to their several advantages. In the following subsections, detailed information can be found.

4.3.1.1 FFT-based Periodogram

The Discrete Fourier Transform (DFT) of an N-point evenly-spaced sequence is given by

$$X(k) = \sum_{n=0}^{N-1} \left(x(n) e^{-j2\pi kn/N} \right) \tag{4.28}$$

where $k = 0, \mp 1, \mp 2, \ldots, \mp(N-1)$.

Although the DFT is a computable transform, the implementation of (4.28) is very inefficient, especially when the sequence length *N* is large. In 1965, Cooley and Tukey showed a procedure to substantially reduce the amount of computations involved in DFT (Cooley & Tukey, 1965). This and other similar efficient algorithms are collectively known as fast Fourier transform (FFT) algorithms. Implementation of these algorithms can be found in popular digital signal processing books such as (Ingle & Proakis, 2000).

Parseval's relation computes the energy in the frequency domain as

$$E_x = \sum_{n=0}^{N-1} |x(n)|^2 = \frac{1}{N} \sum_{k=0}^{N-1} |X(k)|^2 \tag{4.29}$$

The quantity $|X(k)|^2/N$ is called the energy spectrum of finite-duration sequences. Similarly, for periodic sequences, the quantity $|X(k)|^2/N$ is called power spectral density (PSD).

4.3.1.2 Autoregressive Model-Based Periodogram

Parametric methods can yield higher resolutions than nonparametric methods in cases when the signal length is short. These methods use a different approach to spectral estimation; instead of trying to estimate the PSD directly from the data, they model the data as the output of a linear system driven by white noise, and then attempt to estimate the parameters of that linear system.

The AR methods tend to adequately describe spectra of data that is "peaky," that is, data whose PSD is large at certain frequencies. The data in many practical applications (such as speech) tends to have "peaky spectra" so that AR models are often useful. In addition, the AR models lead to a system of linear equations which is relatively simple to solve (Wang & Paliwal, 2003). An AR process model is defined as

$$x(t) = n(t) + \sum_{k=1}^{p} a_k x(t-k) \tag{4.30}$$

where *p* is model order and *n(t)* is white noise.

Selection of the model order, *p*, of the parametric process is an important issue. If it is chosen too high or low, it may come with failing to represent data properly. There are a number of criteria to optimize the AR model order. Akaike's final prediction error (FPE) is probably the most common used criterion among them. FPE, which selects *p* minimizing the function *FPE(p)*, defined as:

$$FPE(p) = \sigma_p^2 \left(\frac{N+p+1}{N-p-1}\right) \tag{4.31}$$

where *N* is the number of samples and σ_p^2 is the variance of the AR model with the order *p*. It is seen that whereas σ_p^2 decreases with *p*, the term $\frac{N+p+1}{N-p-1}$ increases with *p*. The *FPE* is an estimate of the prediction error power when the prediction coefficients must be estimated from the data. The term $\frac{N+p+1}{N-p-1}$ accounts for the increase in variance of the prediction error power estimator due to the inaccuracies in the prediction coefficient estimates (Proakis & Manolakis, 1996).

An AR method yields a PSD estimate given by

$$P(f) = \frac{1}{f_s} \frac{\sigma_p^2}{\left|1 + \sum_{k=1}^{p} a_k e^{-j2\pi k f / f_s}\right|^2} \tag{4.32}$$

4.3.1.3 Lomb-Scargle Periodogram

In addition to classical methods used in the calculation of PSD, a more appropriate PSD estimation for unevenly sampled data is the Lomb-Scargle (LS) periodogram

(Clifford & Tarassenko, 2005; Laguna, Moody, & Mark, 1998; Lomb, 1976; Scargle, 1982). LS method is able to be used without the need to resample and detrend the RR data (Laguna, Moody, & Mark, 1998). The detailed explanation of this periodogram method is introduced in the following paragraphs.

Consider a physical variable *X* measured at a set of times t_j where the sampling is at equal times ($\Delta t = t_{j+1} - t_j = constant$) from a stochastic process. The resulting time series data, $x(t_j)$ where (j=1,2,…,N), are assumed to be the sum of a signal x_s and random observational errors, *R*;

$$x_j = x(t_j) = x_s(t_j) + R(t_j) \tag{4.33}$$

Furthermore, it is assumed that the signal is periodic, that the errors at different times are independent ($R(t_j) \neq f(R(t_k))$ where $j \neq k$) and that $R(t_j)$ is normally distributed with zero mean and constant variance, σ^2.

The *N*-point discrete Fourier transform (DFT) of this sequence is

$$FT_X(w_n) = \sum_{j=0}^{N-1} \left(x(t_j)e^{-iw_n t_j}\right) \tag{4.34}$$

where $w_n = 2\pi f_n,\ n = 1,2,\dots,N$, and the power spectral density (PSD) estimate is therefore given by the standard method for calculating a periodogram:

$$P_X(w_n) = \frac{1}{N}\sum_{j=0}^{N-1} \left|x(t_j e^{-iw_n t_j})\right|^2 \tag{4.35}$$

Now consider arbitrary t_j's or uneven sampling ($\Delta t = t_{j+1} - t_j \neq constant$) and a generalization of the *N*-point DFT (Scargle, 1982):

$$FT_X(w_n) = \sqrt{\frac{N}{2}} \sum_{j=0}^{N-1} x(t_j)\left(A\cos\left(w_n t_j\right) - iB\sin\left(w_n t_j\right)\right) \tag{4.36}$$

where $i = \sqrt{-1}$, j is the summation index, and A and B are as yet unspecified functions of the angular frequency w_n. This angular frequency may depend on the vector sample times, $\{t_j\}$, but not on the data, $\{x(t_j)\}$, nor on the summation index j. The corresponding periodogram is then

$$\begin{aligned} P_X(w_n) &= \frac{1}{N}|FT_x(w_n)|^2 \\ &= \frac{A^2}{2}\left[\sum_{j=0}^{N-1} x(t_j)\cos\left(w_n t_j\right)\right]^2 + \frac{B^2}{2}\left[\sum_{j=0}^{N-1} x(t_j)\sin\left(w_n t_j\right)\right]^2 \end{aligned} \tag{4.37}$$

If $A = B = \sqrt{\frac{2}{N}}$, Equations 4.36 and 4.37 reduce the classical definitions [Equations 4.34 and 4.35]. For even sampling FT_X reduces to the DFT and in the limit $\Delta t \to 0$ and $N \to \infty$, it is proportional to the Fourier transform. Scargle shows how Equation 4.37 is not unique and further conditions must be imposed in order to derive the corrected expression for the LSP:

$$\begin{aligned} P(w_n) = \frac{1}{2\sigma^2}\Bigg\{ &\frac{\left[\sum_{j=0}^{N-1}\left(x\left(t_j\right) - \bar{x}\right)\cos\left(w_n\left(t_j - \tau\right)\right)\right]^2}{\sum_{j=0}^{N-1}\cos^2\left(w_n\left(t_j - \tau\right)\right)} \\ &+ \frac{\left[\sum_{j=0}^{N-1}\left(x\left(t_j\right) - \bar{x}\right)\sin\left(w_n\left(t_j - \tau\right)\right)\right]^2}{\sum_{j=0}^{N-1}\sin^2\left(w_n\left(t_j - \tau\right)\right)}\Bigg\} \end{aligned} \tag{4.38}$$

where

$$\tau \equiv \frac{1}{2w}\tan^{-1}\left(\frac{\sum_{j=1}^{N}\sin\left(wt_j\right)}{\sum_{j=1}^{N}\cos\left(wt_j\right)}\right) \tag{4.39}$$

τ is an offset that makes $P_N(w)$ completely independent of shifting all the t_j's by any constant (Clifford & Tarassenko, 2005; Laguna et al., 1998). C and MATLAB codes for this calculation are available from PhysioNet (Goldberger et al., 2000).

4.3.2 Time - Frequency - Domain Measures

Power spectral density (PSD) estimation allows quantitative analysis of the frequency components of the RR interval time series, and it is an important method to understand tonic cardiovascular activities. The power spectrum is often assessed by FFT and LSP as described above. However, these traditional methods have their own limitation when used in the analysis of HRV. They assume that the signal is at least quasi-stationarity, which is not always true in physiological signals. This obscures the accuracy of PSD estimation of nonstationary signals. Furthermore, traditional spectral analysis methods have an excellent frequency resolution, but their time resolution is insufficient. The wavelet transform, popular time - frequency domain method, is a better alternative. Compared with traditional frequency analysis methods, the wavelet transform has many advantages (Pichot et al., 1999):

- It has no prerequisite over the stationarity of the analyzed signal. The time - frequency localization property of the wavelet transform makes it more suitable for the analysis of nonstationary signals, such as the RR interval. It provides the status of HRV at any time, and can capture any sudden changes in autonomic tone.
- It exhibits good frequency resolution as well as time resolution.
- It offers a flexible multi-resolution signal representation and variable scale. Long windows can be used to analyze low frequency components, while short windows can be used for high frequency components.
- It provides different shapes of mother wavelets to fit the analyzed signal better than the fixed sinusoidal shape of the Fourier transform.

Wavelets have challenged the traditional Fourier transforms for analyzing and processing signals. Instead of relying on fixed sinusoidal functions in Fourier transform, wavelets use a 'mother' wavelet with various shapes. It is a mathematical function that breaks down the signals into a number of scales related to frequency components and

analysis each scale with a certain resolution. This breaking down process is called a wavelet transform. It offers a flexible multi-resolution signal representation which is useful in many applications.

4.3.2.1 Continuous Wavelet Transform

In mathematical terms, the continuous wavelet transform (CWT) decomposes a signal *x(t)* by performing scalar product with a family of $\psi(a,b)$ functions, which are built by dilation and trans-location of the mother wavelet ψ. The transform is defined as (Aldroubi & Unser, 1996):

$$C(a,b) = \int_R x(t) \frac{1}{\sqrt{a}} \psi\left(\frac{t-b}{a}\right) dt \tag{4.40}$$

The resultant *C(a,b)* are called wavelet coefficients, which represent the correlation between the signal and the chosen wavelet at different scales. The amplitude of the coefficients therefore tends to be maximum at those scales and locations where the signal most resembles the chosen wavelet. The wavelet transform is a tool for time-frequency signal analysis since each wavelet function $\psi(a,b)$ is predominantly localized in a certain region of the time-frequency plane. The wavelet function $\psi(a,b)$ depends on two parameters, scale *a* and trans-location parameter *b*, which vary continuously over the real numbers. For smaller values of scale *a*, the wavelet is contracted in the time domain and the wavelet transform gives information about the detail of the signal, which is also called high frequency component. For larger values of *a*, the wavelet expands to give a global view of the signal, which is the low frequency component of the signal.

4.3.2.2 Discrete Wavelet Transform

To reduce the redundancy of the continuous wavelet transform, the discrete wavelet transform (DWT) has been introduced. It can be understood as a CWT sampled on a discrete plane (Fig. 4.9). The most popularly used algorithm in HRV study is the orthogonal multi-resolution pyramidal DWT algorithm (Malik, Cripps et al., 1989),

because of its non-redundancy and computational efficiency. The principle of the dyadic pyramid algorithm is depicted in Fig. 4.10.

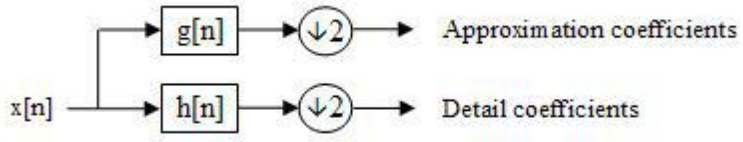

Figure 4.9 Block diagram of filter analysis.

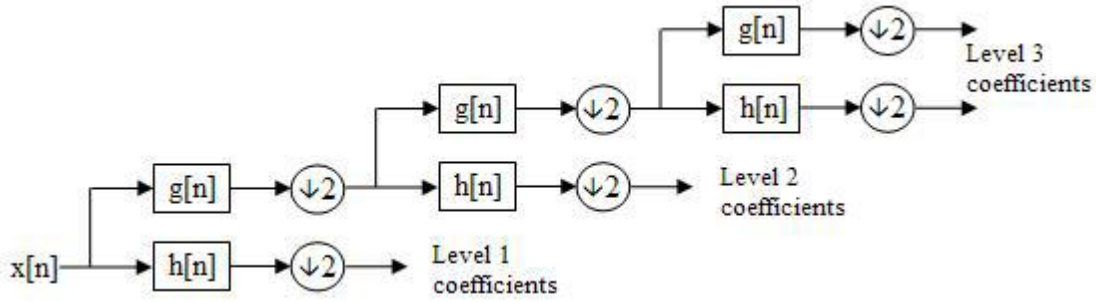

Figure 4.10 A 3-level filter bank.

One other important issue is to find out the relationship between wavelet scale (level) and the Fourier frequency, so as to make the results from both frequency and time-frequency analysis of HRV comparable. The frequency interpretation was given in Fig. 4.11 as following (Medigue et al., 1997): for a given signal sampled at f_s Hz, the wavelet decomposition at scale m acts as a band-passfilter between $\frac{f_s}{2^{-m-1}}$ Hz and $\frac{f_s}{2^{-m}}$ Hz. Previously, this equation has been used to interpret HRV with wavelet in adults (Shimazu, Ojima, Takasugi, Nejime, & Kamishima, 1999). For example a signal with 32 samples, frequency range 0 to $\frac{f_s}{2}$ and 3 levels of decomposition, 4 output scales are produced:

Table 4.1 Frequency bands for each level in a 3-level DWT where d_i's are detail coefficients and a_3 is the approximation coefficients of the last level.

Level	***Frequencies***		***Number of Samples***
a_3	0	$\frac{f_s}{16}$	4
d_3	$\frac{f_s}{16}$	$\frac{f_s}{8}$	4
d_2	$\frac{f_s}{8}$	$\frac{f_s}{4}$	8
d_1	$\frac{f_s}{4}$	$\frac{f_s}{2}$	16

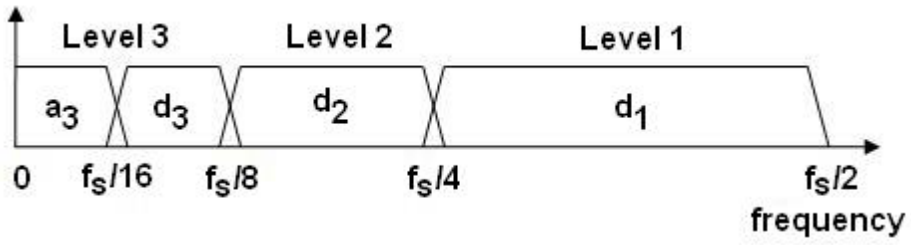

Figure 4.11 Frequency domain representation of the DWT.

4.3.2.3 Wavelet Packet Decomposition

Wavelet packet decomposition (WPD) (sometimes known as just wavelet packets) is a wavelet transform where the signal is passed though more filters than the DWT. In the DWT, each level is calculated by passing the previous approximation coefficients though a high and low pass filters. However in the WPD, both the detail and approximation coefficients are decomposed (Fig. 4.12).

For *n* levels of decomposition the WPD produces 2^n different sets of coefficients (or nodes) as opposed to *n+1* sets for the DWT (Fig. 4.13). However, due to the down-sampling process the overall number of coefficients is still the same and there is no redundancy.

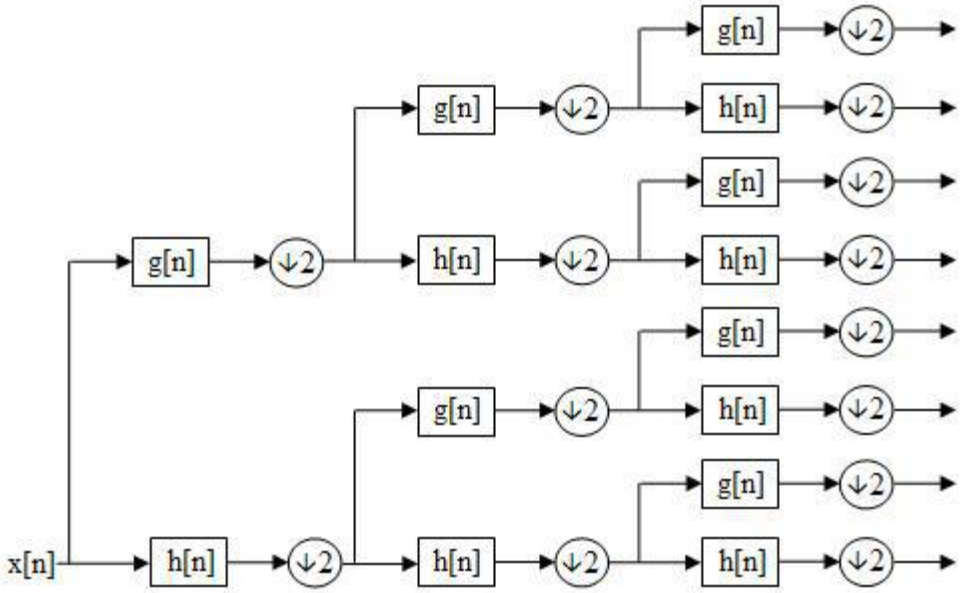

Figure 4.12 Wavelet Packet decomposition over 3 levels.

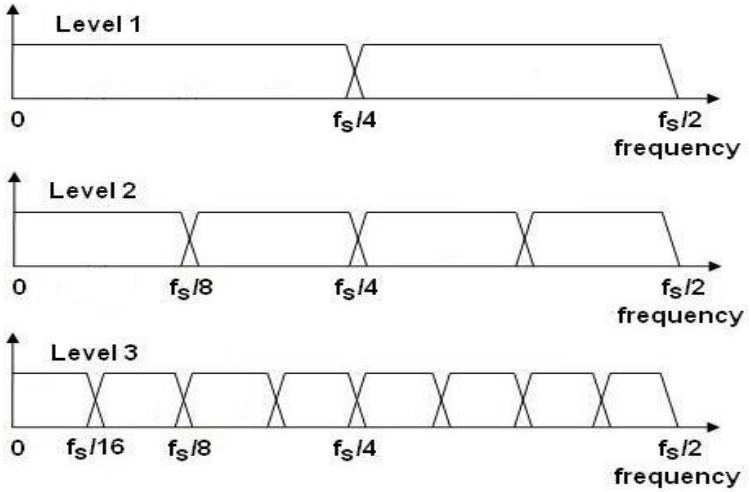

Figure 4.13 Frequency domain representation of the WPT.

4.3.2.4 Mother Wavelet

Choosing an appropriate mother wavelet is another important issue in all wavelet applications. In the literature, many studies related to the analysis of ECG and HRV preferred Daubechies 4 wavelet as mother wavelet (Fig. 4.14) (Asyalı, 2003; Bakardjian & Yamamoto, 1995; Pichot et al., 1999; Shimazu et al., 1999; Torrence & Compo, 1998; Wiklund, Akay, & Niklasson, 1997).

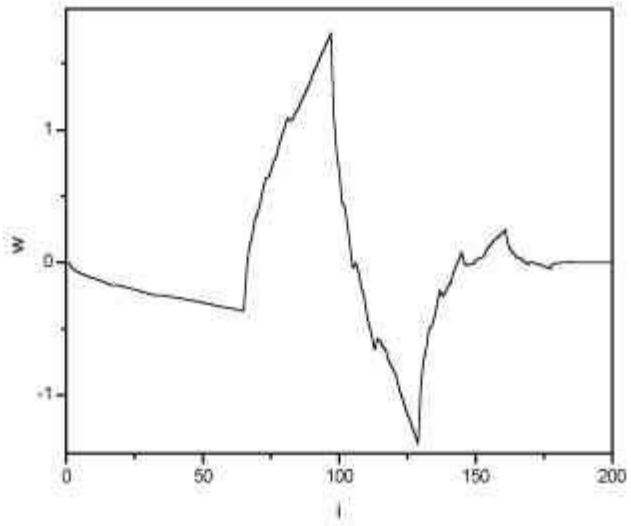

Figure 4.14 Daubechies 4 wavelet mother function.

4.3.2.5 Wavelet-Based Measures

Like frequency domain measures, similar parameters are defined here to quantify different frequency components, which are calculated from the wavelet transform (Medigue et al., 1997; Shimazu et al., 1999). These measurements are called ***Wavelet Variance***, ***Wavelet Energy***, and ***Wavelet Entropy*** measures. In order to calculate these measures, there is a three-step procedure defined in the literature (Rosso, Quian, Blanco, Figliola, & Başar, 1998; Rosso et al., 2001): i) obtaining the coefficients for wavelet packet analysis, ii) calculating the wavelet energy and variance, and iii) calculating the wavelet entropy. The last two steps are described below in detail.

4.3.2.5.1 Wavelet Variance. Once the wavelet coefficients are known, the variance for each wavelet scale level can be calculated as

$$D_m = \sum_{k=1}^{N_m} (C_k - \bar{C}_k)^2 \tag{4.41}$$

where N_m is the number of wavelet coefficients and $\bar{C}_k$ is the mean value of all wavelet coefficients for wavelet level *m* (Engin, 2007).

4.3.2.5.2 Wavelet Energy. In addition to the wavelet variance, the energy for each wavelet coefficient can be calculated using wavelet coefficients as

$$E_j = C_j^2 \tag{4.42}$$

where C_j is the j-th coefficient of the last level of wavelet packets (Rosso et al., 1998, 2001).

The total energy can be evaluated as

$$E_{total}(m) = \sum_{j=1}^{N} E_j \tag{4.43}$$

where N is the number of wavelet coefficients at the last level of wavelet packets.

4.3.2.5.3 Wavelet Entropy. The normalized values, which represent the relative wavelet energy (or the probability distribution), can be defined as

$$p_j = \frac{E_j}{E_{total}} \tag{4.44}$$

Clearly, $\sum_j p_j = 1$ and, then, following the definition of entropy given by Shannon (Shannon, 1948), the wavelet entropy can be defined as

$$WS_f = -\sum_{j \in f} \left(p_j \log_2(p_j)\right) \tag{4.45}$$

where all p_j values are in the frequency band, f, of interest (Rosso et al., 2001).

4.3.3 Nonlinear Parameters

Nonlinear characteristics are certainly involved in biomedical signals. It has been suggested that through nonlinear analysis, it might be possible to obtain precious information for physiological interpretation and to obtain (diagnosis) / to predict (prognosis) patients for various cardiac and non-cardiac diseases. However, these nonlinear methods have not been used systematically to investigate large patient populations. At present, they are just potential tools for ECG and HRV assessments (Task Force, 1996).

4.3.3.1 Poincare Plot Measures

The Poincare plot, a technique taken from nonlinear dynamics, portrays the nature of the signal. It is a graph of each data on x axis plotted against the next data on y axis (Fig. 4.15). The plot provides summary information as well as detailed information on the behavior of the heart (Kamen, Krun, & Tonkin, 1996; Kamen & Tonkin, 1995; Woo et al., 1992). The overall shape of the distribution is used to characterize the dynamics of the time series (Berntson et al., 1997). The Poincare plot is becoming a popular technique due to its simple visual interpretation and proved clinical ability as a predictor of disease and cardiac dysfunction (Kamen, 1996). Poincare plot is drawn using the raw dataset.

Fitting an ellipse to the Poincare plot's shape is becoming increasingly popular technique (Marciano, Migaux, Acanfora, Furgi, & Rengo, 1994). The standard deviation of the distance of the points on the plot determines the width (SD1) and length (SD2) of the ellipse (Brennan, Palaniswami, & Kamen, 2001). These measures can be calculated as follows (Landes et al., 1996):

$$SD_1 = \sqrt{\frac{1}{2}(SDSD)^2} \tag{4.46}$$

$$SD_2 = \sqrt{2(SD)^2 - \frac{1}{2}(SDSD)^2} \tag{4.47}$$

where *SDSD* is standard deviation of successive differences and *SD* is the standard deviation of the data where *lag=1* instead of the equations of

$$SD_1 = std\left(\frac{x_{i+lag} - x_i}{\sqrt{2}}\right) \tag{4.48}$$

$$SD_2 = std\left(\frac{x_{i+lag} + x_i}{\sqrt{2}}\right) \tag{4.49}$$

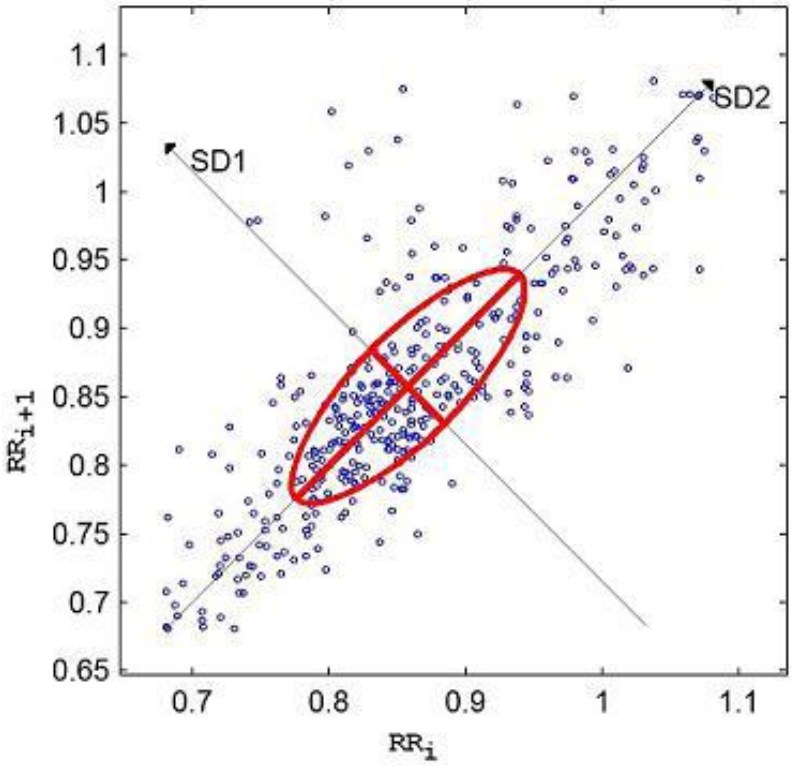

Figure 4.15 An example Poincare plot and the measures of SD1 and SD2.

In addition, the product (SD_1SD_2) and the ratio ($\frac{SD_1}{SD_2}$) may also be computed to describe the relationships between these components. The ratio is assumed to be indicator of the balance between the sympathetic and vagal activities (Kamen & Tonkin, 1995). In the literature, the conventional value of lag is 1 (Smith, Reynolds, & Owen, 2007; Stein, Le, & Domitrovich, 2008), but some studies used different values from 1 to 10 (Contreras, Canetti, & Migliaro, 2007; Thakre & Smith, 2006). The results for lagged Poincare plots carry over to higher-dimensional Poincare plots (Brennan, Palaniswami, & Kamen, 2001).

4.3.4 Feature Normalization

In order to prevent any initial bias due to the natural ranges of values for the original features, input feature values should be normalized. The performance of the classifiers can be improved by using the normalization (Kotsiantis, Kanellopoulos, & Pintelas, 2006). In this scope, the ***Min-Max normalization***, ***Rank normalization***, or ***Z-score standardization*** techniques may be used.

In the min-max normalization, all the samples are normalized into the range of [0,1] as

$$f_{i,N} = \frac{f_i - \min(f_i)}{\max(f_i) - \min(f_i)} \tag{4.50}$$

where $i=1,2,\ldots,d$, d is the number of features, $f_{i,N}$ is the normalized i-th feature, f_i is the i-th feature, $min(f_i)$ and $max(f_i)$ are the minimum and the maximum values of the i-th feature, respectively.

In the rank normalization, all the samples are ordered and numbered with an integer number. After this ordering, the corresponding numbers can be divided by the maximum order number to fit the normalized values into the range of [0,1].

In the z-score standardization, all the samples are normalized into the zero mean and unity variance values as

$$f_{i,N} = \frac{f_i - \bar{f}_i}{\mathrm{std}(f_i)} \tag{4.51}$$

where $i=1,2,\ldots,d$, d is the number of features, $f_{i,N}$ is the normalized i-th feature, f_i is the i-th feature, $\bar{f}_i$ and $std(f_i)$ are the mean and the standard deviation values of the i-th feature, respectively.

4.4 Feature Selection Stage

Feature selection, also known as variable selection, feature reduction, attribute selection or variable subset selection, is the technique, commonly used in machine learning, of selecting a subset of relevant features for building robust learning models (Duda, Hart, & Stork, 2001). By removing most irrelevant and redundant features from the data, feature selection helps improve the performance of learning models by:

- alleviating the effect of the curse of dimensionality,
- enhancing generalization capability,
- speeding up learning process, and
- improving model understandability.

Feature selection also helps people to acquire better understanding about their data by telling them that which are the important features and how they are related with each other.

The feature selection algorithms can be divided into two major groups (Fig. 4.16), the filter approach and the wrapper approach (John, Kohavi, & Pfleger, 1994). The filter approach assesses the relevance of the features from the data set and the selection is mainly based on statistical measures. The effects of the selected features on the performance of a particular classifier are neglected. In contrast, the wrapper approach uses the classification performance of the classifier itself as part of the search for evaluating the feature subsets. Since the selection of a feature subset which takes the classification algorithm into account achieves a high predictive accuracy on unknown test data, the wrapper approach is more appropriate. However, this approach is associated with high computational costs, although advances in computer technology make the wrapper method feasible. The filter approach is mostly used in data mining applications where huge data sets are considered.

In addition, the feature selection algorithms can also be split up into methods which guarantee finding the optimal solution and algorithms which may result in suboptimal feature sets (Jain & Zongker, 1997; Zongker & Jain, 1996).

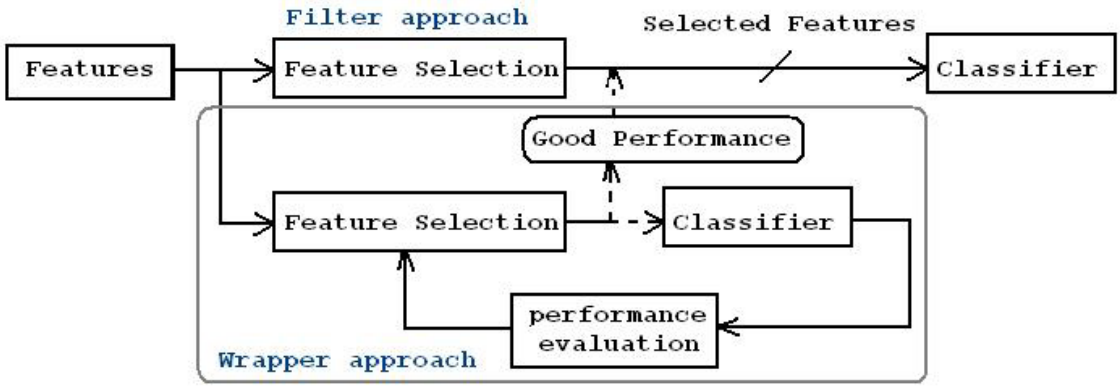

Figure 4.16 The feature selection algorithms: the filter approach (upper) and the wrapper approach (bottom).

4.4.1 Optimal methods

Exhaustive search for feature selection is too time-consuming even for a moderate-number of features. The total number of competing subsets is given by $2^n - 1$. Even if the size of the final feature subset d is given, the total number of subsets $\binom{n}{d} = \frac{n!}{d!(n-d)!}$ is too high for performing an exhaustive search (Jain, Duin, & Mao, 2000), where n is the number of extracted features and $d \leq n$ denotes the size of the final feature subset.

4.4.2 Suboptimal methods

These feature selection algorithms may result in suboptimal feature subsets using a deterministic or stochastic approach for the search. Sequential feature selection algorithms search in a sequential deterministic manner for the suboptimal best feature subset. Basically, forward and backward algorithms are available. The forward methods start with an empty set and add features until a stopping criterion concludes the search. The backward algorithms begin with all features and remove features iteratively. The detailed list can be found in the literature (Jain, Duin, & Mao, 2000; Pernkopf, 2005). In stochastic approach, genetic algorithms (GA) are probably the most widely used methods in the literature.

4.4.2.1 Genetic algorithms

GA is optimization algorithms founded upon the principles of natural evolution discovered by Darwin. In nature, individuals have to adapt to their environment in order to survive in a process of further development. GA turns out to be competitive for certain problems, e.g. large-scale search and optimization tasks. It uses a stochastic, directed and highly parallel search based on principles of population genetics that artificially evolve solutions to a given problem (Goldberg, 1989, Holland, 1975). GA work well even if the space to be searched is large, not smooth or not well understood, or if the fitness function is noisy and, in addition, when finding a good solution (not necessarily the exact global optimum) is sufficient (Koza, 1992).

GA is stochastic optimization procedures which have been successfully applied in many feature selection tasks. The problem of dimensionality reduction is well suited to formulation as an optimization problem. Given a set of *d*-dimensional input patterns, the task of the GA is to find a transformed set of patterns in an *m*-dimensional space ($m < d$) that maximizes a set of optimization criteria (Raymer, Punch, Goodman, Kuhn, & Jain, 2000). Typically, the transformed patterns are evaluated based upon their dimensionality, and their class separation or the classification accuracy that can be obtained on the patterns with a given classifier.

The main factors that make GA different from traditional methods of search and optimization are (Koza, 1992):

- GA work with a coding of the design variables as opposed to the design variables themselves;
- GA work with a population of points as opposed to a single point, thus reducing the risk of getting stuck at local minimum;
- GA requires only the objective function value, not the derivatives. This aspect makes GA application problem-independent; and
- GA is a family of probabilistic search methods, not deterministic, making the search highly exploitative.

Main elements of a GA mechanism, used in the feature selection, will be given in the following.

4.4.2.1.1 The representation scheme. A direct approach to using GA for feature selection was introduced by (Siedlecki & Sklansky, 1989). In their work, a GA is used to find an optimal binary vector, where each bit is associated with a feature (Fig. 4.17). If the *i*-th bit of this vector equals 1, then the *i*-th feature is allowed to participate in classification; otherwise, the corresponding feature does not participate.

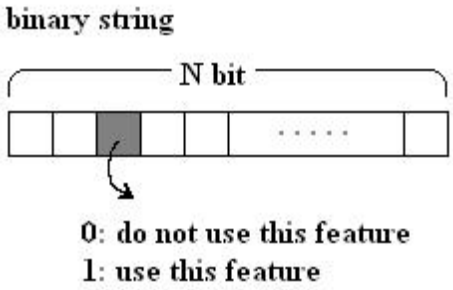

Figure 4.17 N-bit binary representation of whole feature space (Siedlecki & Sklansky, 1989).

4.4.2.1.2 Fitness. The evolutionary process is driven by the fitness measure. The fitness assigns a value to each resulting subset of features is evaluated according to its classification accuracy on the testing data set. Because the implementation of GA in MATLAB is designed to find the minimum values, the fitness value is calculated as

$$fitness = \frac{N_F}{N} = 1 - \frac{N_C}{N} \tag{4.52}$$

where N is the size of the dataset, N_F and N_C are the number of failed and correctly classified samples, respectively.

4.4.2.1.3 The Selection Scheme. The selection operator improves the average quality of the population by giving individuals with higher fitness a higher probability to undertake any genetic operation. An important feature of the selection mechanism is its

independence of the representation scheme, as only the fitness is taken into account. The probabilistic feature allocates to every individual a chance of being selected occasionally.

The most popular of the stochastic selection strategies is fitness proportionate selection, also called biased roulette wheel selection. It can be regarded as allocating pie slices on a roulette wheel, with each slice proportional to a string's fitness. Selection of a string to be a parent can then be viewed as a spin of the wheel, with the winning slice being the one where the spin ends up. Although this is a random procedure, the chance of a string to be selected is directly proportional to its fitness and the least fit individuals will gradually be driven out of a population. For example, if we generate a random number *C* between *0* and *1* and we get the value *0.61*, string *3* in Fig. 4.18 would be selected.

A second common strategy is called tournament selection (Goldberg & Deb, 1991). A subpopulation of individuals is chosen at random. The individual from this subpopulation with the highest fitness wins the tournament. Generally, tournaments are held between two individuals (binary tournament). However, this can be generalized to an arbitrary group whose size is called the tournament size. This algorithm can be implemented efficiently as no sorting of the population is required. More important, it guarantees diversity of the population. The most important feature of this selection scheme is that it does not use the value the fitness function. It is only necessary to determine whether an individual is fitter than any other or not. Other selection schemes and their comparative analysis have been reviewed by (Goldberg & Deb, 1991).

4.4.2.1.4 Crossover. The crossover operator is responsible for combining good information from two strings and for testing new points in the search space. The two off-springs are composed entirely of the genetic material from their two parents. By recombining randomly certain effective parts of a character string, there is a good chance of obtaining an even more fit string and making progress toward solving the optimization problem.

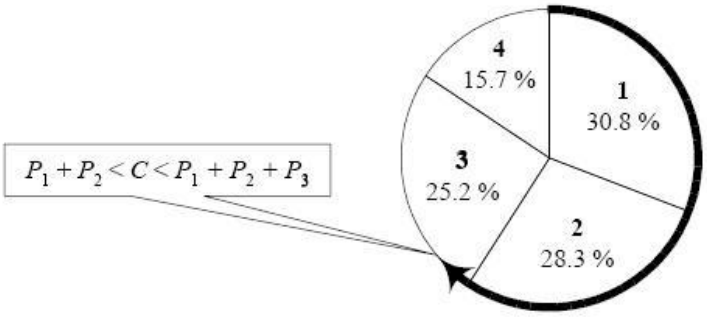

	F_i	$P_i = F_i / \sum F_i$
1	9.8	0.308
2	9	0.283
3	8	0.252
4	5	0.157
$C = 0.61$ ($0 \le C < 1$ at random)		

Figure 4.18 Fitness proportionate method (Goldberg & Deb, 1991).

Several ways of performing crossover can be used. The simplest but very effective is the one-point crossover (Goldberg, 1989). Two individual strings are selected at random from the population. Next, a crossover point is selected at random along the string length, and two new strings are generated by exchanging the substrings that come after the crossover point in both parents. The mechanism is illustrated in Fig. 4.19.

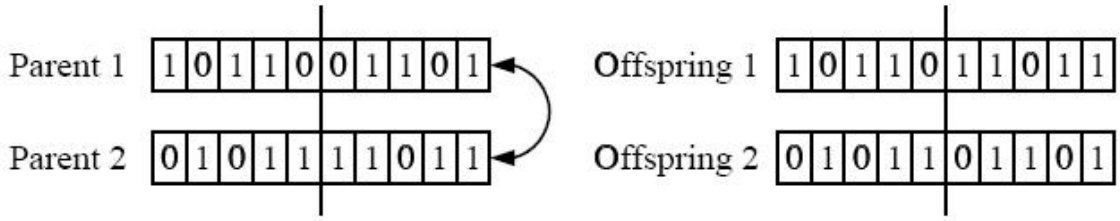

Figure 4.19 GA One-point crossover.

A more general case is the multi-point crossover in which parts of the information from the two parents are swapped among more string segments (de Jong, 1975). An example is the two-point crossover, where two crossover points are selected at random and the substring lying in between the points are swapped.

In uniform crossover, each bit of the offspring is created by copying the corresponding bit from one or the other parent selected at random with equal probability (Syswerda, 1989). Uniform crossover has the advantage that the ordering of bits is entirely irrelevant because there is no linkage between adjacent bits. Multi-point crossover takes half of the material from each parent in alternation, while uniform crossover decides independently which parent to choose. When the population has largely converged, the exchange between two similar parents leads to a very similar offspring. This is less likely to happen with uniform crossover particularly with small population size, and so, gives more robust performance.

4.4.2.1.5 Mutation. Mutation prevents the population from premature convergence or from having multiple copies of the same string. This feature refers to the phenomenon in which the GA loses population diversity because an individual that does not represent the global optimum becomes dominant. In such cases the algorithm would be unable to explore the possibility of a better solution.

Mutation consists of the random alteration of a string with low probability. It is implemented by randomly selecting a string location and changing its value from 0 to 1 or vice versa, as shown in Fig. 4.20.

Figure 4.20 GA mutation.

4.4.2.1.6 Simple Genetic Algorithm. For feature selection, each individual is represented by binary values. The advantage of this representation is that the classical GA operators (binary mutation and crossover) can easily be applied without any modification. This assures that the basic GA implementation can be used (Vafaie & De Jong, 1995).

Assuming we have *n* tuning parameters encoded with binary values, GA works as follows:

- Start with a randomly generated population of individuals of length *n*-bits.
- Iteratively perform the following steps on the population:
    - calculate the fitness of each chromosome by least-squares,
    - sort the population,
    - create a new population:
        - Calculate the *elite* according to input parameter P_e, which is an additional operator that transfers unchanged a relatively small number of the fittest individuals to the next generation. Such individuals can be lost if they are destroyed by crossover or mutation (de Jong, 1975).
        - Fill up the population with the surviving strings according to tournament selection of size 2.
        - With the probability P_c, select a pair of individuals from the current population. The same string can be selected more than once to become a parent. Recombine sub-strings using the *single-point crossover*. Two new offspring are inserted into the new population instead of their parents.
        - With the probability P_m, *mutate* a randomly selected string at a randomly selected point.
    - Check the termination criteria (the maximum number of iteration exceeded, the fittest value found …). If not satisfied, go to the iteration.

Each iteration of this process is called a ***generation***. The entire set of generations is called a ***run***. At the end of the run, there are one or more highly fit strings in the population. Generally, it is necessary to make multiple independent runs of a GA obtain a result that can be considered successful for a given problem.

4.5 Classification Stage

The last stage of the pattern recognition system, the classification stage, gives a decision usually based on the availability of a set of patterns that have already been classified. This set of patterns is termed the training set and the resulting learning

strategy is characterized as supervised. Learning can also be unsupervised, in the sense that the system is not given an a priori labeling of patterns. In this case, it establishes the classes based on the statistical properties of the patterns (Vatanabe, 1985).

The classifier usually uses one of the several types of classification approaches. Nonetheless, the rapidly growing and available computing power, while enabling faster processing of huge data sets, has also facilitated the use of elaborate and diverse methods for data analysis and classification. In more recently, demands on automatic pattern recognition systems have raised enormously due to the availability of large databases and high performance of computers. In many of recognition applications, it is clear that no single approach is optimal. Therefore, multiple methods and approaches are needed to be used. Thus, combining several methods and classifiers is now commonly used in pattern recognition (Jain, Duin, & Mao, 2000).

A learning rule is defined as a procedure for modifying the parameters of a network, which can also be referred to as a training algorithm. The learning rule is applied to train the network to perform some particular task. Learning rules fall into two broad categories: supervised learning, and unsupervised learning.

In supervised learning, the learning rule is provided with a set of examples (the training set) of proper network behavior $\{(p_1,t_1), (p_2, t_2), \ldots, (p_N, t_N)\}$ where p_i is an input to the network, and t_i is the corresponding correct (target) output. As the inputs are applied to the network, the network outputs are compared to the targets. The learning rule is then used to adjust the parameters of the network in order to force the network outputs closer to the targets.

In unsupervised learning, on the other hand, the parameters are modified in response to network inputs only. There are no target outputs available. Most of these algorithms perform clustering operations. They categorize the input patterns into a finite number of classes. This is especially useful in such applications as vector quantization.

Although there are many classification schemes, the Bayes and the k-Nearest Neighbors classifiers were used in this study due to their simplicity and understandability.

4.5.1 Bayes Classifier

In Bayesian decision theory, tradeoffs between probabilities and decision costs from the basis of a classification decision (Duda, Hart, & Stork, 2001). It is desirable to minimize the cost of making an incorrect classification, given certain theoretical knowledge of the classification task. Bayes's rule provides a method of classifying an object optimally into one of *c* mutually exclusive classes, using

- the prior (***a priori***) probabilities $P(C_k)$, where $k=1,\ldots,c$, and $\sum_{k=1}^{c} P(C_k)$
- the conditional densities $p(x|C_k)$, where $P(.)$ denotes a probability mass function and a lowercase $p(.)$ to denote a probability density function. The class conditional probability density function determines how the feature values are distributed for each class. Feature vector x, where $x = \{x_1, \ldots, x_d\}$, will have a distribution described by the probability density function $p(x)$. The probability $P(x)$ of a feature vector x lying in a region R is

$$P(x \in R) = \int_{x=R} p(x)dx \tag{4.53}$$

$p(x)$ is normalized s.t. $P(x \in R) = 1$ if R spans all possible values of x. The class densities are the separate probability density functions formed for each class: $p(x|C_k)$. The unconditional probability density function is the sum of class conditional probability density functions weighted by prior probabilities and is independent of class (Duda, Hart, & Stork, 2001):

$$p(x) = \sum_{k=1}^{c} (p(x|C_k)P(C_k)) \tag{4.54}$$

The posterior probabilities may be calculated from

$$posterior = \frac{likelihood \times prior}{evidence}$$

$$P(C_k|x) = \frac{p(x|C_k) \times P(C_k)}{p(x)} \tag{4.55}$$

where $P(C_k|x)$ is the posterior probability for class C_k, $p(x|C_k)$ is the class conditional probability density function for class C_k, $P(C_k)$ is the prior probability of class C_k, $p(x)$ is the unconditional probability density function (from Equation 4.54). Assuming that the feature vectors can provide actual classifying information, the posterior probability can increase confidence in the final decision relative to the prior probabilities (Duda, Hart, & Stork, 2001).

To classify x, the class C_k with the highest posterior probability is chosen (or a random choice in the case of equal posterior probabilities) using

$$P(C_k|x) \geq P(C_j|x) \qquad \forall j \neq k \tag{4.56}$$

With Bayes's rule, a classifier is a means of partitioning the input space into c decision regions R_k so that feature values in each decision region are associated with a particular class. The probability density of a correct classification at point x, for a class C_k, in a region is $p(x|C_k)P(C_k)$. Therefore, the overall probability of an accurate decision is obtained (Duda, Hart, & Stork, 2001) by integration of the probability density over all regions is

$$P_{correct} = \sum_{k=1}^{c} \int_{R_k} p(x|C_k)P(C_k)dx \tag{4.57}$$

$P_{correct}$ is maximized by the choice of regions to maximize each of c integrands, i.e. by assigning a pattern to class C_k that maximizes $p(x|C_k)P(C_k)$. Since $p(x|C_k)P(C_k) \propto P(C_k|x)$, it may be seen that the maximum $P_{correct}$ value is achieved by maximizing $P(C_k|x)$, the posterior probability.

If *p(x|Ck)* for different classes overlap, e.g. for the cases of two curves with overlapping joint probability density functions, the best classification choice is to minimize the overlap area (to maximize Equation 4.57); however, in this case, a perfect classifier cannot be realized.

4.5.2 k-Nearest Neighbors Classifier

k-nearest neighbors (KNN) is amongst the simplest of all machine learning algorithms. KNN is one of the instance-based classifiers. In instance-based methods, system parameters or classifying system units simply consist of the samples that are presented to the system. This algorithm assumes that all instances correspond to points in the *d*-dimensional space R^d (Mitchell, 1997). An object is classified by a majority vote of its neighbors, with the object being assigned to the class most common amongst its *k* nearest neighbors (Fig. 4.21). *k* is a positive integer, typically small. If *k = 1*, then the object is simply assigned the class of its nearest neighbor. In binary (two class) classification problems, it is helpful to choose *k* to be an odd number as this avoids difficulties with tied votes (Nixon & Aguado, 2002).

The neighbors are taken from a set of objects for which the correct classification is known. This can be thought of as the training set for the algorithm, though no explicit training step is required. In order to identify neighbors, the objects are represented by position vectors in a multidimensional feature space. It is usual to use the Euclidean distance, though other distance measures, such as the Mahalanobis distance could be used instead.

The training phase of the algorithm consists only of storing the feature vectors and class labels of the training samples. In the actual classification phase, the test sample (whose class is not known) is represented as a vector in the feature space. Distances from the new vector to all stored vectors are computed and k closest samples are selected. A major drawback to use this technique to classify a new vector to a class is that the classes with the more frequent examples tend to dominate the prediction of the new vector, as they tend to come up in the KNN when the neighbors are computed due to their large number. One of the ways to overcome this problem is to take into account

the distance of each KNN with the new vector that is to be classified and predict the class of the new vector based on these distances (Vatanabe, 1985).

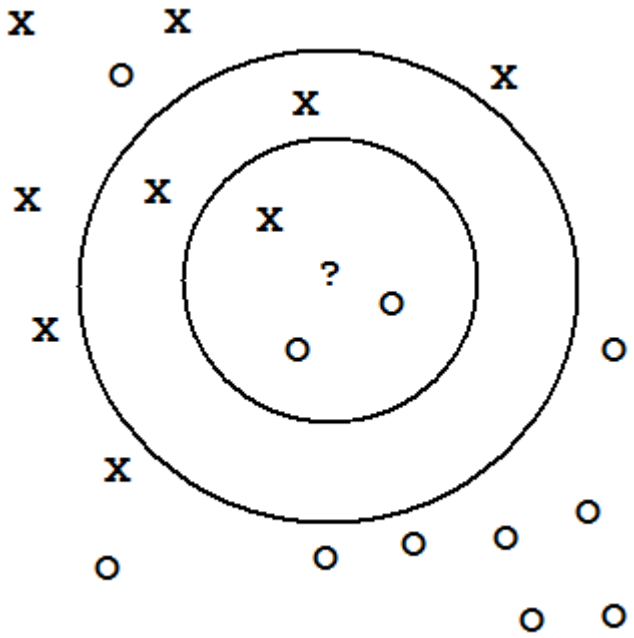

Figure 4.21 An example of KNN classification. The test sample (**?**) should be classified either to the first class of **X**'s or to the second class of **O**'s. If k = 3, it is classified to the second class because there are 2 **O**'s and only 1 **X** inside the inner circle. If k = 5, it is classified to first class (3 **X**'s vs. 2 **O**'s inside the outer circle).

A KNN classifier allows a great deal of generality in the classification because, unlike many other classifiers which assume a multivariate Gaussian distribution of the feature values, the KNN classification method does not depend on the data following any particular distribution (Duda, Hart, & Stork, 2001). They have also advantages in that the information in training data is never lost (Şahan, Polat, Kodaz, & Güneş, 2007). But, there are some problems with this algorithm. First of all, for large data sets, this algorithm is very time-consuming because each sample in the training set is processed while classifying a new data and this requires a longer classification time. This cannot be a problem for some application areas but when it comes to a field like medical diagnosis, time is very important as well as classification accuracy. Nonetheless, the accuracy of the KNN algorithm can be severely degraded by the presence of noisy or

irrelevant features, or if the feature scales are not consistent with their importance. Much research effort has been put into selecting or scaling features to improve classification.

4.6 Model Evaluation Stage

To discuss applications and accomplishments of various classifiers, we will first introduce a few standard measures that will be used throughout this thesis to compare or report various results. These measures have been recommended and used to evaluate physicians and health-care workers by various organizations, and therefore are good measures for evaluating the performance of any automated system that is designed to assist these health-care professionals (Valafar, 2001).

There are at least two reasons for calculating the generalization rate of a classifier on a given problem. One is to see if the classifier performs well enough to be useful; another is to compare its performance with that of a competing design. Estimating the final generalization performance can be calculated using various performance measures in the validation methods. Such techniques can be applied to virtually every classification method, where the specific form of learning or parameter adjustment depends upon general training method (Duda, Hart, & Stork, 2001).

4.6.1 Performance Assessment

The American Heart Association (AHA) recommends the use of four measures to evaluate the procedures for diagnosing CAD (Gibbons et al., 1997). Since these measures are useful in other areas of diagnosis as well, they are used in evaluating most diagnostic systems (Valafar, 2001). In this performance measurement system, the recognition system discriminates the decisions only between two alternatives which are "***positive***" and "***negative***". In each alternative, there are two kinds of responses which are "***true***" and "***false***".

By considering the two-class case, there are four possible outcomes. If the instance is positive and it is classified as positive, it is counted as ***true positive (TP)***; if it is classified as negative, it is counted as ***false negative (FN)***. If the instance is negative

and it is classified as negative, it is counted as ***true negative (TN)***; if it is classified as positive, it is counted as ***false positive (FP)***. Given a classifier and a set of instances (the test set), a two-by-two ***confusion matrix*** (also called a contingency table or decision matrix) can be constructed representing the dispositions of the instances. This matrix forms the basis for many common metrics (Eberhart & Dobbins, 1990). Fig. 4.22 shows this matrix.

		Classification Output	
		Normal	*Heart Failure*
Training Input	*Normal*	True Negative (TN)	False Positive (FP)
	Heart Failure	False Negative (FN)	True Positive (TP)

Figure 4.22 Two-by-two decision matrix.

4.6.1.1 Classical Performance Measures

There are several ways of computing the performance of a recognition system using the decision matrix. They are often considered to be the most informative for characterizing the performance of the classifier and easy to calculate (Eberhart & Dobbins, 1990).

Sensitivity (True Positive Rate) is the ratio of the number of positive decisions correctly made by the recognition system to the total number of positive decisions made by the expert. ***Selectivity*** (Precision) is the ratio of the number of positive decisions correctly made by the recognition system to the total number of positive decisions made by the recognition system. ***Specificity*** (True Negative Rate) is the ratio of the number of negative decisions correctly made by the recognition system to the total number of negative decisions made by the expert. ***Accuracy*** is the ratio of the total number of positive decisions and negative decisions correctly made by the recognition system to the total number of positive decisions and negative decisions made by the recognition system.

$$SEN = \ Sensitivity = \frac{TP}{TP + FN} \times 100\% \tag{4.58}$$

$$SEL = \ Selectivity = \frac{TP}{TP + FP} \times 100\% \tag{4.59}$$

$$SPE = \ Specificity = \frac{TN}{TN + FP} \times 100\% \tag{4.60}$$

$$ACC = Accuracy = \frac{TP + TN}{TP + TN + FP + FN} \times 100\% \tag{4.61}$$

In addition to these calculations, there exist a few performance measures such as positive and negative predictive accuracies. Positive predictive accuracy measure is the same with selectivity measure defined above. Latter accuracy measure can be determined by calculating (Cao, 2004)

$$NEG = \ Negative\ Predictive\ Accuracy = \frac{TN}{TN + FN} \times 100\% \tag{4.62}$$

4.6.2 Cross-Validation

In simple validation, the set of labeled training samples are randomly split into two parts: one is used as the traditional training set for adjusting the model parameters in the classifier; the other set (validation set) is used to estimate the generalization error. Since the ultimate goal of the designer is low generalization error, the classifier is trained until reaching a minimum of this validation error (Fig. 4.23). It is essential that the validation (or the test) set does not include points used in the training process (Duda, Hart, & Stork, 2001).

A simple generalization of above method is ***m-fold cross-validation***. Here the training set is randomly divided into *m* disjoint sets of equal size $\frac{n}{m}$, where *n* is again the total number of patterns in *D*. The classifier is trained *m* times, each time with a different set held out as a validation set. The estimated performance is the mean of these *m* errors. In the limit where *m=n*, the method is in effect the ***leave-one-out*** approach. In this approach, the classifier is trained using the whole dataset except one and then tested on this single excluded data. This process is repeated for all the samples in the dataset.

Here the computational complexity may be very high, especially for large number of samples (*n*). However, it gives the advantage of using the whole dataset in training of the classifier and is especially preferred when the available dataset is small.

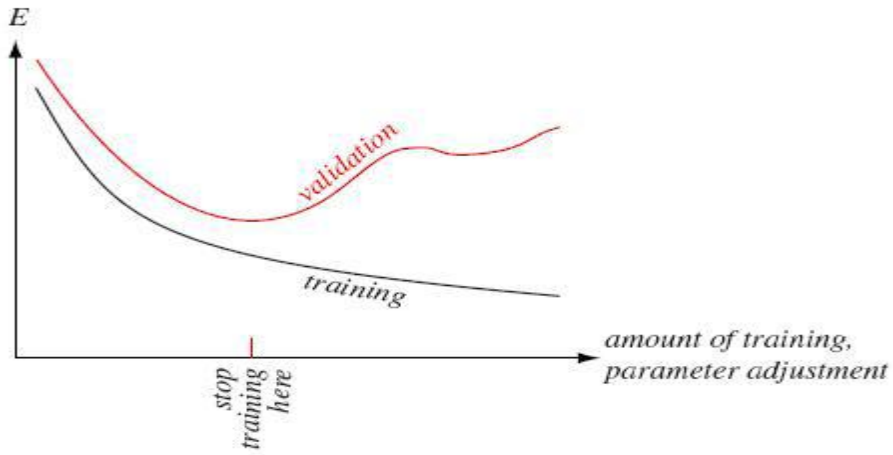

Figure 4.23 In validation, the data set *D* is split into two parts. The first is used as a standard training set for setting free parameters in the classifier model; the other is the validation set and is meant to represent the full generalization task. For most problems, the training error decreases monotonically during training. Typically, the error on the validation set decreases, but then increases, an indication that the classifier may be over-fitting the training data. In validation, training or parameter adjustment is stopped at the first minimum of the validation error. In the more general method of cross-validation, the performance is based on multiple independently formed validation sets (Duda, Hart, & Stork, 2001).

In this study, the leave-one-out method is used in evaluating the goodness of the classifier. The classifier is trained using the whole dataset except one and tested on the single excluded data. This process is repeated for all samples in the dataset.

4.7 Statistical Analysis

Throughout the thesis, all values in the tables are given as mean ± standard deviation unless otherwise noted. In addition, values of the features given in all tables were examined using unpaired t-test (see Appendix One). The p-value < 0.05 was regarded as statistical evidence to conclude that there was significant difference between two groups.

CHAPTER FIVE
RESULTS AND DISCUSSION

In the CHF diagnosis, there are two stages: (i) discriminating the patients from the normal subjects and (ii) determining the type of dysfunctionality. The achieved results related to these stages using the HRV analysis are given in this chapter. All the methods mentioned in chapter 4, entitled Methods, were combined together and visualized as a flowchart in Fig. 5.1. The optional steps can be seen easily in this figure with dashed lines.

The software environment of MATLAB version 2008b was used to implement all the methods given. All the study had been conducted using a Pentium IV-3.0 GHz computer with 3 GB DDR2 memory.

5.1 Discriminating CHF Patients from Normal Subjects

5.1.1 Data Acquisition Stage

The databases from the MIT/BIH, an open-source and freely available dataset via the Web, were used in order to evaluate the results obtained by comparing other studies. The data for the normal control group were obtained from 24 hour Holter monitor recordings of 54 healthy subjects and 29 patients with CHF. The detailed information about the databases (Goldberger et al., 2000; Moody, Goldberger, McClennen, & Swiryn, 2001) used in the study were summarized as follows.

- ***Congestive Heart Failure RR Interval Database (CHF2DB)*** includes beat annotation files for 29 long-term ECG recordings of subjects aged 34 to 79, with congestive heart failure (NYHA classes I, II, and III). Subjects included 8 men and 2 women; gender is not known for the remaining 19 subjects. The original ECG recordings (not available) were digitized at 128 samples per second, and the beat annotations were obtained by automated analysis with manual review and correction.

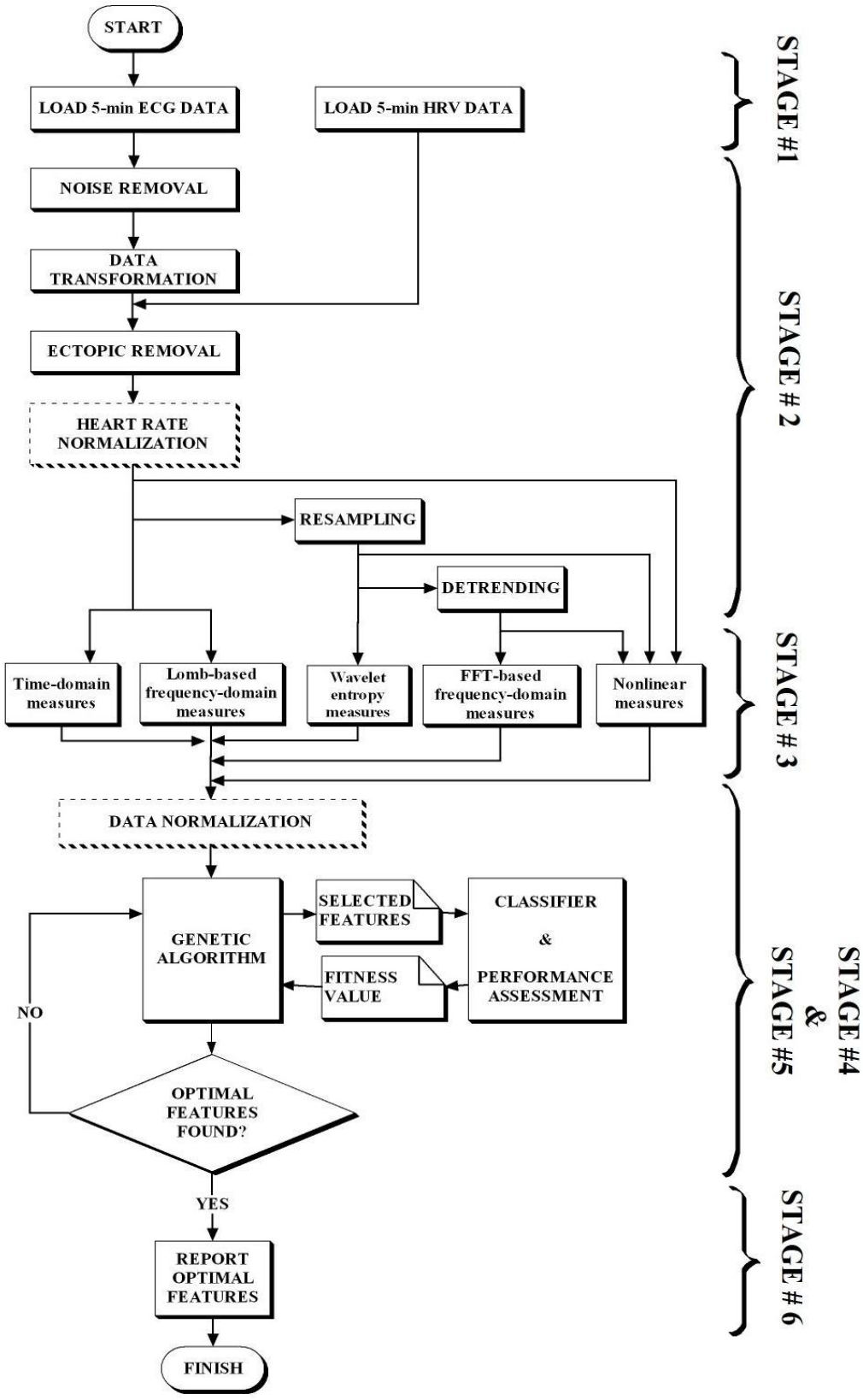

Figure 5.1 The flowchart of the whole study.

- ***Normal Sinus Rhythm RR Interval Database (NSR2DB)*** includes beat annotation files for 54 long-term ECG recordings of subjects in normal sinus rhythm (30 men, aged 28.5 to 76, and 24 women, aged 58 to 73). The original ECG recordings (not available) were digitized at 128 samples per second, and the beat annotations were obtained by automated analysis with manual review and correction.

Although the databases included 24-h HRV data, only 5-min (300-s) ECG data were used to achieve the results quickly. Two example 300-s HRV data for a normal subject and a patient with CHF are shown in Fig. 5.2.

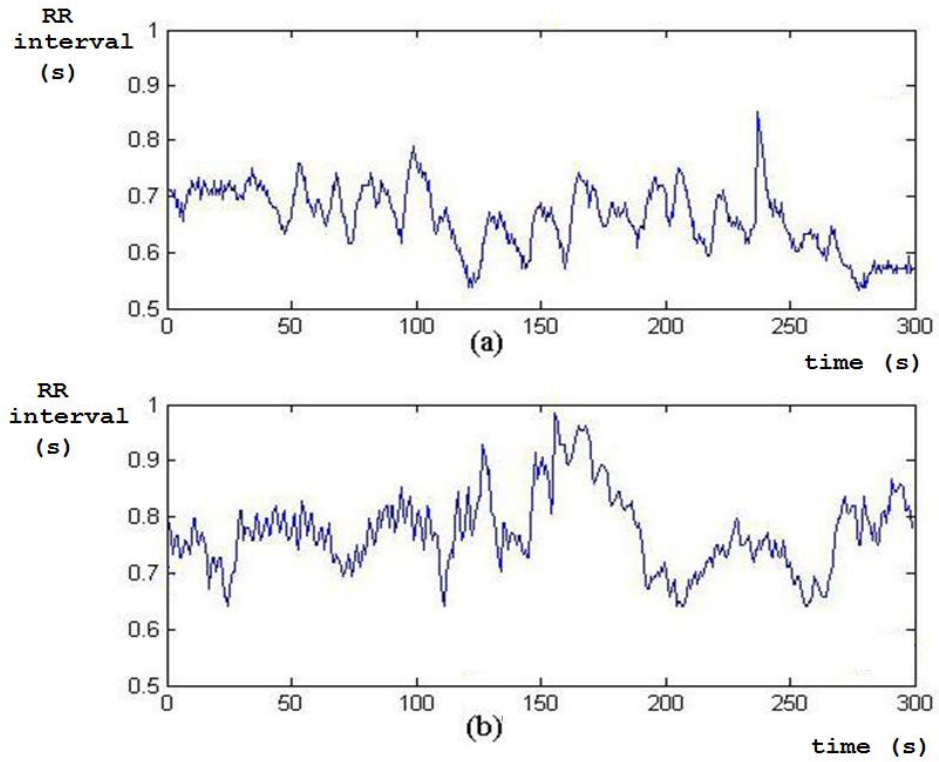

Figure 5.2 HRV data of (a) a normal subject and (b) a patient with CHF.

5.1.2 Preprocessing Stage

In the second stage of the study, because RR databases were used, the first two steps (noise removal and data transformation) would be unnecessary (the second path of the first stage in the flowchart, Fig. 5.1). Therefore, the other steps of removing ectopic beats, heart rate normalization, resampling, and detrending were applied sequentially.

In HRV analysis, it is desirable to use only those heartbeats which are expected not to be disturbed by waves of the previous or following heartbeats. Therefore, abnormal beats like ventricular premature and atrial premature beats, and their following neighbors, should be excluded from the beat sequence (Clifford, Azuaje, & McSharry, 2006). Hence, the algorithm developed by Langley and colleagues (Langley et al., 2001) were used to detect these artifacts.

After removing the artifacts from the data, the heart rate normalization step was applied optionally. The rest of the study was conducted using both HRV data and heart rate normalized HRV data separately in order to find out the effect of the heart rate normalization process. In this optional step, the mean heart rates of all RR datasets were fixed to 75 bpm as offered in Hallstrom et al. (2004).

The cubic spline interpolation method with a rate of 4 Hz (Task Force, 1996) to achieve evenly-sampled RR data and the smoothness priors based detrending method with a parameter of $\lambda=1000$ (Tarvainen, Ranta-aho, & Karjalainen, 2002) to remove trends from the RR data were used. An example of interpolated and detrended HRV data for the normal subject and the patient with CHF was shown in Fig. 5.3 (İşler, Selver, & Kuntalp, 2005).

5.1.3 Feature Extraction Stage

Time-domain, Lomb-Scargle algorithm-based frequency-domain, and Poincare plot measures were calculated directly from the raw HRV data. The wavelet entropy measures, on the other hand, were calculated using DB4 wavelet packet transform method with a scale of 7 from the resampled data. FFT-based frequency-domain measures were calculated from resampled and detrended data. Poincare plot measures were calculated using the method of ellipse fitting. At the end of this stage, the HRV dataset were constructed with 71 features (1 for gender, 12 time-domain measures, 6 FFT-based PSD measures, 6 wavelet entropy measures, 6 LS-based PSD measures, and 4 Poincare plot measures with 10 different lags).

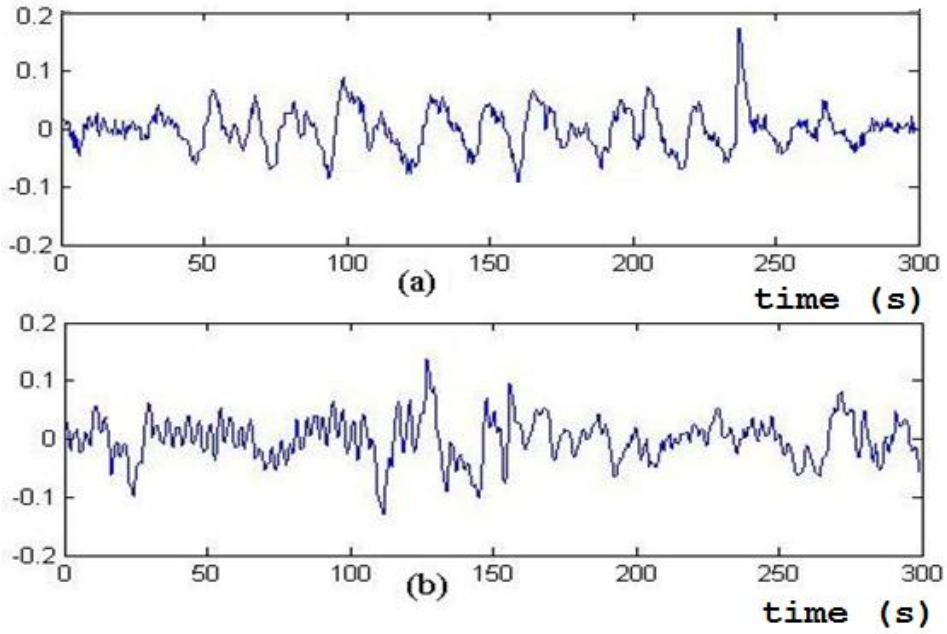

Figure 5.3 Interpolated and detrended HRV data of (a) the normal subject and (b) the patient with CHF.

After being calculated, all features were presented in the form of their mean ± standard deviations in tables. Hence, these were compared statistically using the method of unpaired t-test with unequal variances. In addition, classification performances of each feature were evaluated using Bayes classifier and included into these tables.

Patient information of age for all records in the databases included into the study was summarized in Table 5.1.

Table 5.1 Patient information for normals and patients with CHF from the databases. All values are presented as mean ± standard deviation.

Feature	***NORMAL***	***CHF***	***P***	***SEN***	***SPE***	***POS***	***NEG***	***ACC***
age	61±12	55±12	0.026	83	55	78	65	73

Time domain statistical measures have been found common use because of their simplicity. These measures used in the study were summarized in Table 5.2. MEAN, RMSSD, NN20_2, NN20, PNN20, and SDSD values showed statistically significant differences for HRV data. After heart rate normalization process was applied, the features of SDNN, RMSSD, and SDSD showed statistically significant differences.

Table 5.2 Nominal 5-min time-domain metric values for normals and patients with CHF from the databases. All values are presented as mean ± standard deviation.

Feature	***NORMAL***	***CHF***	***P***	***SEN***	***SPE***	***POS***	***NEG***	***ACC***
BEFORE HEART RATE NORMALIZATION								
MEAN	0.740±0.11	0.670±0.09	0.007	54	66	74	43	58
SDNN	0.061±0.02	0.078±0.07	0.162	67	34	65	36	55
RMSSD	0.035±0.03	0.089±0.11	0.001	85	38	72	58	69
NN20_1	58±28	46±27	0.060	63	66	77	49	64
NN20_2	57±26	44±27	0.033	67	62	77	50	65
NN20	115±54	90±54	0.044	61	66	77	47	63
PNN20	0.297±0.16	0.202±0.12	0.008	56	62	73	43	58
NN50_1	9.888±15.92	13.793±18.28	0.315	69	34	66	37	57
NN50_2	9.833±13.75	14.137±18.16	0.229	69	38	67	39	58
NN50	20±29	28±36	0.268	70	34	67	38	58
PNN50	0.054±0.08	0.062±0.07	0.714	70	34	67	38	58
SDSD	0.059±0.03	0.096±0.10	0.023	80	38	70	50	65
AFTER HEART RATE NORMALIZATION								
MEAN	0.800±0.00	0.800±0.00	0.820	52	52	67	37	52
SDNN	0.064±0.02	0.093±0.09	0.036	72	34	67	40	59
RMSSD	0.038±0.03	0.107±0.13	0.000	89	41	74	67	72
NN20_1	66±28	64±37	0.819	48	55	67	36	51
NN20_2	64±25	62±38	0.820	48	55	67	36	51
NN20	130±52	126±75	0.819	46	55	66	36	49
PNN20	0.320±0.13	0.272±0.14	0.144	56	55	70	40	55
NN50_1	11±14	16±19	0.213	72	34	67	40	59
NN50_2	11±13	16±20	0.168	74	41	70	46	63
NN50	22±27	32±39	0.185	74	38	69	44	61
PNN50	0.058±0.08	0.069±0.08	0.536	70	34	67	38	58
SDSD	0.063±0.03	0.114±0.12	0.005	81	38	71	52	66

Frequency domain measures have also been found common use in all the forms of signal processing field. These measures were calculated using the FFT-based PSD, Lomb-Scargle PSD, and Wavelet entropies (Table 5.3). The former two were processed over 512 equally-spaced frequency points. Among these methods, LS-based frequency-domain measures were noticed as their accuracies were a few higher than those of others (İşler, Avcu, Kocaoğlu, & Kuntalp, 2008). Because heart rate normalization process changed only the mean value of the data, the frequency domain measures were not significantly affected from this process. LS_LF and FFT_VLF were not found statistically different between two groups.

Table 5.3 Nominal 5-min frequency-domain metric values for normals and patients with CHF from the databases. All values are presented as mean ± standard deviation.

Feature	*NORMAL*	*CHF*	*P*	*SEN*	*SPE*	*POS*	*NEG*	*ACC*
BEFORE HEART RATE NORMALIZATION								
LS_LFHF	4.592±3.48	1.692±2.31	0.000	63	83	87	55	70
LS_VLF	0.435±0.18	0.281±0.21	0.001	69	66	79	53	67
LS_LF	0.155±0.10	0.118±0.06	0.089	50	83	84	47	61
LS_HF	0.059±0.05	0.147±0.08	0.000	83	69	83	69	78
LS_NLF	0.744±0.15	0.482±0.20	0.000	80	76	86	67	78
LS_NHF	0.256±0.15	0.517±0.20	0.000	80	76	86	67	78
FFT_LFHF	4.444±3.57	1.841±1.68	0.000	52	86	88	49	64
FFT_VLF	0.000±0.00	0.000±0.00	0.092	87	24	68	50	65
FFT_LF	0.000±0.00	0.005±0.01	0.026	94	14	67	57	66
FFT_HF	0.000±0.00	0.004±0.01	0.020	96	14	68	67	67
FFT_NLF	0.743±0.13	0.558±0.17	0.000	80	76	86	67	78
FFT_NHF	0.256±0.13	0.441±0.17	0.000	80	76	86	67	78
WS_LFHF	4.944±4.34	2.255±1.73	0.002	57	79	84	50	65
WS_VLF	0.000±0.00	0.000±0.00	0.003	85	31	70	53	66
WS_LF	0.000±0.00	0.000±0.00	0.001	91	31	71	64	70
WS_HF	0.000±0.00	0.000±0.00	0.001	91	38	73	69	72
WS_NLF	0.758±0.13	0.622±0.15	0.000	74	66	80	58	71
WS_NHF	0.241±0.13	0.377±0.15	0.000	74	66	80	58	71
AFTER HEART RATE NORMALIZATION								
LS_LFHF	4.592±3.48	1.692±2.31	0.000	63	83	87	55	70
LS_VLF	0.435±0.18	0.282±0.21	0.001	69	66	79	53	67
LS_LF	0.155±0.10	0.118±0.06	0.089	50	83	84	47	61
LS_HF	0.059±0.05	0.147±0.08	0.000	83	69	83	69	78
LS_NLF	0.744±0.15	0.482±0.20	0.000	80	76	86	67	78
LS_NHF	0.256±0.15	0.517±0.20	0.000	80	76	86	67	78
FFT_LFHF	3.974±3.21	1.667±1.49	0.000	48	86	87	47	61
FFT_VLF	0.000±0.00	0.001±0.00	0.031	93	21	68	60	67
FFT_LF	0.001±0.00	0.011±0.02	0.022	96	14	68	67	67
FFT_HF	0.001±0.00	0.010±0.03	0.030	96	14	68	67	67
FFT_NLF	0.721±0.14	0.540±0.17	0.000	74	76	85	61	75
FFT_NHF	0.278±0.14	0.459±0.17	0.000	74	76	85	61	75
WS_LFHF	4.462±3.92	2.269±1.82	0.006	54	79	83	48	63
WS_VLF	0.000±0.00	0.001±0.00	0.001	89	31	71	60	69
WS_LF	0.000±0.00	0.001±0.00	0.001	93	31	71	69	71
WS_HF	0.000±0.00	0.000±0.00	0.002	93	31	71	69	71
WS_NLF	0.745±0.13	0.619±0.16	0.000	65	62	76	49	64
WS_NHF	0.254±0.13	0.381±0.16	0.000	65	62	76	49	64

Poincare Plot is probably the mostly used nonlinear technique in the analysis of HRV. Additional embedded information, which cannot be obtained in the time- and frequency-domain measures, can be obtained. These measures were calculated using the ellipse-fitting method with ten different lag values from 1 to 10 for HRV data (Table

5.4) and heart rate normalized HRV data (Table 5.5). In both tables, statistically significant differences are shown in only SD2 measures although there were improvements in these measures of heart rate normalized HRV analysis. It should be noted that all classifier performances were also increased after the heart rate normalization was applied. Nonetheless, all classifier performances were decreased while the lag values used in Poincare measures were increased.

5.1.4 Feature Selection Stage

In this study, best combination of short-term heart rate variability (HRV) measures were sought for to distinguish 29 patients with congestive heart failure (CHF) from 54 healthy subjects in the control group. In the analysis performed, in addition to the standard HRV measures, wavelet entropy based frequency domain measures and Poincare plot parameters with 10 different lags were also used. A genetic algorithm was used to select the best ones from among all possible combinations of these measures. Using the leave-one-out method and KNN classifier, the fitness values were calculated. New population was constructed until the maximum number of generations was reached as a stopping criterion. The following standard GA parameters were chosen: ***Maximum generations of 250, Population size of 300, Elite count of 4, and Population type of bit string***.

Table 5.4 Poincare plots' measures with 10 different lags for normals and patients with CHF from the databases using HRV data. All values are presented as mean ± standard deviation.

Feature	***NORMAL***	***CHF***	***P***	***SEN***	***SPE***	***POS***	***NEG***	***ACC***
SD1_1	0.025±0.02	0.063±0.07	0.001	85	38	72	58	69
SD2_1	0.081±0.03	0.088±0.08	0.591	63	38	65	35	54
SD1SD2_1	0.002±0.00	0.011±0.02	0.009	91	28	70	62	69
RATIO_1	0.317±0.20	0.645±0.30	0.000	83	66	82	68	77
SD1_2	0.029±0.02	0.064±0.07	0.003	85	38	72	58	69
SD2_2	0.080±0.03	0.087±0.08	0.549	63	38	65	35	54
SD1SD2_2	0.002±0.00	0.011±0.02	0.012	91	28	70	62	75
RATIO_2	0.369±0.20	0.656±0.29	0.000	80	66	81	63	75
SD1_3	0.033±0.02	0.065±0.07	0.006	83	38	71	55	67
SD2_3	0.078±0.03	0.086±0.08	0.539	63	38	65	35	54
SD1SD2_3	0.003±0.00	0.011±0.02	0.015	91	28	70	62	69
RATIO_3	0.427±0.20	0.677±0.26	0.000	80	66	81	63	75
SD1_4	0.035±0.02	0.065±0.07	0.010	80	38	70	50	65
SD2_4	0.077±0.03	0.086±0.08	0.477	65	38	66	37	55
SD1SD2_4	0.003±0.00	0.011±0.02	0.017	89	28	70	57	67
RATIO_4	0.473±0.20	0.677±0.24	0.000	72	66	80	56	70
SD1_5	0.037±0.02	0.067±0.07	0.012	80	38	70	50	65
SD2_5	0.076±0.03	0.085±0.08	0.463	65	38	66	37	55
SD1SD2_5	0.003±0.00	0.011±0.02	0.018	89	28	70	57	67
RATIO_5	0.514±0.21	0.710±0.24	0.000	70	69	81	56	70
SD1_6	0.039±0.02	0.067±0.07	0.016	80	38	70	50	65
SD2_6	0.075±0.03	0.085±0.08	0.438	65	38	66	37	55
SD1SD2_6	0.003±0.00	0.011±0.02	0.019	89	28	70	57	67
RATIO_6	0.546±0.22	0.733±0.24	0.001	69	69	80	54	69
SD1_7	0.040±0.02	0.068±0.07	0.019	80	38	70	50	65
SD2_7	0.074±0.03	0.084±0.07	0.421	65	38	66	37	55
SD1SD2_7	0.003±0.00	0.011±0.02	0.020	87	28	69	53	66
RATIO_7	0.572±0.22	0.739±0.23	0.002	69	66	79	53	67
SD1_8	0.041±0.02	0.067±0.07	0.023	80	38	70	50	65
SD2_8	0.074±0.03	0.085±0.08	0.364	65	38	66	37	55
SD1SD2_8	0.003±0.00	0.011±0.02	0.020	87	28	69	53	66
RATIO_8	0.591±0.23	0.730±0.21	0.010	69	69	80	54	69
SD1_9	0.041±0.02	0.066±0.07	0.023	78	38	70	48	64
SD2_9	0.073±0.03	0.086±0.08	0.346	65	38	66	37	55
SD1SD2_9	0.003±0.00	0.011±0.02	0.020	87	28	69	53	66
RATIO_9	0.602±0.23	0.743±0.22	0.009	69	69	80	54	69
SD1_10	0.042±0.02	0.068±0.07	0.023	80	38	70	50	65
SD2_10	0.073±0.03	0.085±0.08	0.362	65	38	66	37	55
SD1SD2_10	0.003±0.00	0.011±0.02	0.021	87	28	69	53	66
RATIO_10	0.610±0.23	0.752±0.20	0.007	69	69	80	54	69

Table 5.5 Poincare plots' measures with 10 different lags for normals and patients with CHF from the databases using heart rate normalized HRV data. All values are presented as mean ± standard deviation.

Feature	***NORMAL***	***CHF***	***P***	***SEN***	***SPE***	***POS***	***NEG***	***ACC***
SD1_1	0.026±0.02	0.076±0.09	0.000	89	41	74	67	72
SD2_1	0.085±0.03	0.104±0.09	0.186	67	38	67	38	57
SD1SD2_1	0.002±0.00	0.016±0.03	0.004	96	34	73	83	75
RATIO_1	0.317±0.20	0.645±0.30	0.000	83	66	82	68	77
SD1_2	0.030±0.02	0.076±0.09	0.001	89	41	74	67	72
SD2_2	0.084±0.03	0.104±0.09	0.167	67	38	67	38	57
SD1SD2_2	0.002±0.00	0.016±0.03	0.005	96	34	73	83	75
RATIO_2	0.369±0.20	0.656±0.29	0.000	80	66	81	63	75
SD1_3	0.034±0.02	0.078±0.09	0.001	85	38	72	58	69
SD2_3	0.083±0.03	0.102±0.09	0.163	67	38	67	38	57
SD1SD2_3	0.003±0.00	0.016±0.03	0.006	96	34	73	83	75
RATIO_3	0.427±0.20	0.677±0.26	0.000	80	66	81	63	75
SD1_4	0.037±0.02	0.078±0.09	0.003	85	38	72	58	69
SD2_4	0.081±0.03	0.102±0.09	0.135	72	38	68	42	60
SD1SD2_4	0.003±0.00	0.016±0.03	0.006	96	34	73	83	75
RATIO_4	0.473±0.20	0.677±0.24	0.000	72	66	80	56	70
SD1_5	0.040±0.02	0.080±0.09	0.003	85	38	72	58	69
SD2_5	0.080±0.03	0.101±0.09	0.133	70	38	68	41	59
SD1SD2_5	0.003±0.00	0.016±0.03	0.007	96	34	73	83	75
RATIO_5	0.514±0.21	0.710±0.24	0.000	70	69	81	56	70
SD1_6	0.041±0.02	0.080±0.09	0.004	83	38	71	55	67
SD2_6	0.079±0.03	0.101±0.09	0.122	70	38	68	41	59
SD1SD2_6	0.003±0.00	0.016±0.03	0.007	96	34	73	83	75
RATIO_6	0.546±0.22	0.733±0.24	0.001	69	69	80	54	69
SD1_7	0.042±0.02	0.081±0.09	0.004	81	38	71	52	66
SD2_7	0.078±0.03	0.100±0.09	0.112	70	38	68	41	59
SD1SD2_7	0.003±0.00	0.016±0.03	0.007	96	34	73	83	75
RATIO_7	0.572±0.22	0.739±0.23	0.002	69	66	79	53	67
SD1_8	0.043±0.02	0.080±0.08	0.006	81	38	71	52	66
SD2_8	0.078±0.03	0.102±0.09	0.093	70	38	68	41	59
SD1SD2_8	0.003±0.00	0.016±0.03	0.007	96	34	73	83	75
RATIO_8	0.591±0.23	0.730±0.21	0.010	69	69	80	54	69
SD1_9	0.044±0.02	0.079±0.08	0.005	81	38	71	52	66
SD2_9	0.077±0.03	0.102±0.09	0.091	70	38	68	41	59
SD1SD2_9	0.003±0.00	0.016±0.03	0.007	96	34	73	83	75
RATIO_9	0.602±0.23	0.743±0.22	0.009	69	69	80	54	69
SD1_10	0.044±0.02	0.081±0.08	0.005	81	38	71	52	66
SD2_10	0.077±0.03	0.101±0.09	0.093	70	38	68	41	59
SD1SD2_10	0.003±0.00	0.016±0.03	0.007	96	34	73	83	75
RATIO_10	0.610±0.23	0.752±0.20	0.007	69	69	80	54	69

5.1.5 Classification Stage

A k-nearest neighbor classifier was used to evaluate the performance of the feature combinations in classifying these two groups. The algorithm was run for three times. In the first run, all HRV measures (given in Tables 5.1, 5.2, and 5.3) and Poincare plot measures with only lag=1 (the first four measures listed in Table 5.4) were used and the heart rate normalization process was not applied. To find out the effect of wavelet entropy measures was aimed in this run. In the second run, all HRV measures (given in Tables 5.1, 5.2, and 5.3) and Poincare plot measures with only lag=1 (the first four measures listed in Table 5.4) were used and the heart rate normalization process was applied optionally. To obtain the effect of heart rate normalization process was aimed in this run. In the last run, all HRV measures (given in Tables 5.1, 5.2, 5.3, 5.4, and 5.5) were used and the heart rate normalization process was applied optionally. To find out the effect of lagged Poincare plot measures was aimed in this run. In each cases, KNN classifier was used with different number of nearest neighbors' k=1, 3, 5, 7, 9, 11, and 13.

5.1.6 Model Evaluation Stage

The first run of the study was performed for a total of 28 times using these configurations (7 (k values) × 4 (configurations)):

- No MINMAX normalization using all features,
- No MINMAX normalization using only GA-selected features,
- MINMAX normalization using all features, and
- MINMAX normalization using only GA-selected features.

The aim of using these different cases is to compare the performance of the feature sets determined by GA with that of including all features and the effect of using MINMAX normalization process. The performances of all the classifiers were calculated based on their SEN, SPE, POS, NEG, and ACC measures (see Table 5.6). As can be seen from this table, three of the feature combinations, selected by GA, provide the maximum performance in terms of the accuracy measure of 89.16%: (i) for a 1-

nearest neighbor classifier, the selected features were seen to be mean, SDNN, SD2, FFT algorithm-based PSD measures of LF/HF ratio, normalized HF power, normalized LF power, LS algorithm-based PSD measures of normalized LF power and normalized HF power, and wavelet entropy measures of LF power and normalized LF power with sensitivity rate of 79.31% and specificity rate of 94.44%, (ii) for a 3-nearest neighbor classifier, the selected features were seen to be mean, SDNN, SD2, FFT algorithm-based PSD measures of LF/HF ratio, normalized HF power, normalized LF power, LS algorithm-based PSD measures of normalized LF power and normalized HF power, and wavelet entropy measures of LF power and normalized LF power with sensitivity rate of 79.31% and specificity rate of 94.44%, and (iii) for a 5-nearest neighbor classifier, the selected features were found to be age, mean, RMSSD, SD1, FFT algorithm based PSD measures of LF/HF ratio, VLF power, normalized LF power, and wavelet entropy measure of normalized HF power with sensitivity rate of 75.86% and specificity rate of 96.30% (İşler & Kuntalp, 2006, 2007a, 2007b).

Table 5.6 Classifier results for the first run where k is the parameter of the KNN classifier, SEN is sensitivity (%), SPE is specificity (%), POS is positive predictivity, NEG is negative predictivity, and ACC is accuracy (%). In the algorithm (Alg.) column, algorithm column, "All" indicates that all the variables in the dataset is used, "GA" indicates that feature selection is done using "GA" (İşler & Kuntalp, 2007a).

Alg.	***k***	***without MINMAX***					***with MINMAX***				
		SEN	***SPE***	***POS***	***NEG***	***ACC***	***SEN***	***SPE***	***POS***	***NEG***	***ACC***
ALL	1	62.16	86.99	71.95	81.06	78.31	72.41	92.59	84.00	86.21	85.54
	3	72.41	92.59	84.00	86.21	85.54	75.86	92.59	84.62	87.72	86.75
	5	68.97	92.59	83.33	84.75	84.34	65.52	96.30	90.48	83.87	85.54
	7	72.41	94.44	87.50	86.44	86.75	65.52	96.30	90.48	83.87	85.54
	9	75.86	92.59	84.62	87.72	86.75	68.97	94.44	86.96	85.00	85.54
	11	41.38	98.15	92.31	75.71	78.31	68.97	94.44	86.96	85.00	85.54
	13	75.53	85.36	73.49	86.66	81.93	65.60	94.40	86.29	83.63	84.34
GA	1	79.31	88.89	79.31	88.89	85.54	79.31	94.44	88.46	89.47	89.16
	3	75.86	92.59	84.62	87.72	86.75	79.31	94.44	88.46	89.47	89.16
	5	72.41	94.44	87.50	86.44	86.75	75.86	96.30	91.67	88.14	89.16
	7	75.86	92.59	84.62	87.72	86.75	72.41	96.30	91.30	86.67	87.95
	9	65.52	92.59	82.61	83.33	83.13	75.86	92.59	84.62	87.72	86.75
	11	65.52	94.44	86.36	83.61	84.34	75.86	94.44	88.00	87.93	87.95
	13	72.41	87.04	75.00	85.45	81.93	72.41	92.59	84.00	86.21	85.54

The most important point revealed by this run is that the combinations of features that give the best discrimination accuracies include wavelet entropy measures in addition to the standard HRV indices. This shows that supporting the classical HRV indices with measures obtained from wavelet entropy calculations could significantly improve the performance of the HRV analysis in the diagnosis of CHF and could be used as a diagnostic tool for discriminating the patients with CHF from healthy normals.

The second run of the study was performed for a total of 28 times using only GA-selected features for these configurations (7 (k values) × 4 (configurations)):

- No MINMAX normalization, No HR normalization,
- No MINMAX normalization, HR normalization,
- MINMAX normalization, No HR normalization, and
- MINMAX normalization, HR normalization.

The aim of using these different cases is to compare the performance of the heart rate normalization process using only feature sets determined by GA. The performances of all the classifiers were calculated similar to the previous run (see Table 5.7). As can be seen from this table, two of the feature combinations, selected by GA, provide the maximum performance in terms of the accuracy measure of 93.98%: (i) for a 3-nearest neighbor classifier, the selected features were seen to be AGE, SDNN, SD1, SD2, PNN20, PNN50, SDSD, FFT algorithm based PSD measures of LF/HF ratio, VLF power, LF power, and wavelet entropy measures of LF power and normalized LF power with sensitivity rate of 82.76% and specificity rate of 100.0% and (ii) for a 5-nearest neighbor classifier, the selected features were found to be AGE, RMSSD, SD1, PNN20, PNN50, SDSD, LS algorithm based PSD measures of normalized LF power, FFT algorithm based PSD measures of LF/HF ratio, VLF power, LF power, and wavelet entropy measures of LF power and normalized LF power with sensitivity rate of 82.76% and specificity rate of 100.0% (İşler & Kuntalp, 2009a).

The results show that using both normalization procedures of MIN-MAX and HR improve the performance of the classification. Therefore, heart rate normalization seems to increase the effect of the heart rate variability analysis.

Table 5.7 Classifier results for the second run where k is the parameter of the KNN classifier, SEN is sensitivity (%), SPE is specificity (%), POS is positive predictivity (%), NEG is nagetive predictivity (%), and ACC is accuracy (%). In the algorithm (Alg.) column, HRV shows HRV analysis and HRN shows heart rate normalized HRV analysis (İşler & Kuntalp, 2009a).

Alg.	***k***	***without MINMAX***					***with MINMAX***				
		SEN	***SPE***	***POS***	***NEG***	***ACC***	***SEN***	***SPE***	***POS***	***NEG***	***ACC***
HRV	1	79.31	88.89	79.31	88.89	85.54	79.31	94.44	88.46	89.47	89.16
	3	75.86	92.59	84.62	87.72	86.75	79.31	94.44	88.46	89.47	89.16
	5	72.41	94.44	87.50	86.44	86.75	75.86	96.30	91.67	88.14	89.16
	7	75.86	92.59	84.62	87.72	86.75	72.41	96.30	91.30	86.67	87.95
	9	65.52	92.59	82.61	83.33	83.13	75.86	92.59	84.62	87.72	86.75
	11	65.52	94.44	86.36	83.61	84.34	75.86	94.44	88.00	87.93	87.95
	13	72.41	87.04	75.00	85.45	81.93	72.41	92.59	84.00	86.21	85.54
HRN	1	65.52	85.19	70.37	82.14	78.31	75.86	98.15	95.65	88.33	90.36
	3	72.41	96.30	91.30	86.67	87.95	82.76	100.0	100.0	91.53	93.98
	5	72.41	96.30	91.30	86.67	87.95	82.76	100.0	100.0	91.53	93.98
	7	75.86	98.15	95.65	88.33	90.36	75.86	100.0	100.0	88.52	91.57
	9	72.41	96.30	91.30	86.67	87.95	72.41	98.15	95.45	86.89	89.16
	11	72.41	90.74	80.77	85.96	84.34	75.86	100.0	100.0	88.52	91.57
	13	79.31	90.74	82.14	89.09	86.75	79.31	96.30	92.00	89.66	90.36

The third and last run of this part of the study was also performed for a total of 28 times using only GA-selected features for these configurations (7 (k values) × 4 (configurations)):

- No MINMAX normalization, No HR normalization,
- No MINMAX normalization, HR normalization,
- MINMAX normalization, No HR normalization, and
- MINMAX normalization, HR normalization.

The aim of using these different cases is to find out the possible improvement in the performance using lagged Poincare plots' measures. The performances of all the classifiers were calculated similar to the others (see Table 5.8). As can be seen from this table, three of the feature combinations, selected by GA, provide the maximum performance in terms of the accuracy measure of 93.98%: (i) for a 1-nearest neighbor classifier, the selected features were seen to be AGE, SDNN, SD1 (lag=1), RATIO (lag=1), SD1SD2 (lag=3), SD2 (lag=6), SD1SD2 (lag=7), LS algorithm based PSD measures of VLF power, normalized LF power, and normalized HF power, FFT

algorithm based PSD measures of VLF power and HF power, and wavelet entropy measures of LF/HF ratio, VLF power, normalized LF power, and normalized HF power with sensitivity rate of 89.66% and specificity rate of 96.30%, (ii) for a 3-nearest neighbor classifier, the selected features were seen to be AGE, SDNN, PNN50, SDSD, SD1 (lag=1), SD2 (lag=1), SD1SD2 (lag=3), LS algorithm based PSD measures of normalized LF power, FFT algorithm based PSD measures of VLF power and HF power, and wavelet entropy measures of LF/HF ratio, VLF power, and normalized LF power with sensitivity rate of 82.76% and specificity rate of 100.0%, and (iii) for a 5-nearest neighbor classifier, the selected features were found to be AGE, SDNN, RMSSD, PNN20, SDSD, SD1 (lag=1), SD1SD2 (lag=3), and SD2 (lag=6), LS algorithm based PSD measures of VLF power and normalized LF power, FFT algorithm based PSD measures of VLF power, LF/HF ratio, and HF power, and wavelet entropy measures of LF power, normalized LF power, and normalized HF power with sensitivity rate of 82.76% and specificity rate of 100.0%.

Table 5.8 Classifier results for the third run where k is the parameter of the KNN classifier, SEN is sensitivity (%), SPE is specificity (%), POS is positive predictivity (%), NEG is nagetive predictivity (%), and ACC is accuracy (%). In the algorithm (Alg.) column, HRV shows HRV analysis and HRN shows heart rate normalized HRV analysis.

Alg.	***k***	***without MINMAX***					***with MINMAX***				
		SEN	***SPE***	***POS***	***NEG***	***ACC***	***SEN***	***SPE***	***POS***	***NEG***	***ACC***
HRV	1	79.31	88.89	79.31	88.89	85.54	79.31	94.44	88.46	89.47	89.16
	3	72.41	92.59	84.00	86.21	85.54	75.86	96.30	91.67	88.14	89.16
	5	68.97	92.59	83.33	84.75	84.34	75.86	96.30	91.67	88.14	89.16
	7	72.41	94.44	87.50	86.44	86.75	72.41	96.30	91.30	86.67	87.95
	9	75.86	92.59	84.62	87.72	86.75	75.86	92.59	84.62	87.72	86.75
	11	41.38	98.15	92.31	75.71	78.31	75.86	94.44	88.00	87.93	87.95
	13	75.53	85.36	73.49	86.66	81.93	72.41	92.59	84.00	86.21	85.54
HRN	1	68.97	88.89	76.92	84.21	81.93	89.66	96.30	92.86	94.55	93.98
	3	72.41	96.30	91.30	86.67	87.95	82.76	100.0	100.0	91.53	93.98
	5	72.41	96.30	91.30	86.67	87.95	82.76	100.0	100.0	91.53	93.98
	7	75.86	98.15	95.65	88.33	90.36	75.86	100.0	100.0	88.52	91.57
	9	72.41	96.30	91.30	86.67	87.95	72.41	98.15	95.45	86.89	89.16
	11	72.41	90.74	80.77	85.96	84.34	75.86	100.0	100.0	88.52	91.57
	13	79.31	90.74	82.14	89.09	86.75	79.31	96.30	92.00	89.66	90.36

There was only improvement in the performance of the KNN classifier with k=1 by comparing the previous results (Table 5.7). Although the lagged Poincare measures were selected by GA for these classifiers, the maximum performance achieved was still unchanged (93.98%). Hence, lagged Poincare plots' measures seem to be useless to improve the classifier performance.

5.2 Discriminating Systolic versus Diastolic Dysfunction in CHF Patients

5.2.1 Data Acquisition Stage

The data used in this study were obtained from the Faculty of Medicine in Dokuz Eylül University. All data included in this database have been carefully reviewed and labeled by the experts. These data include long-term (~24 h) ECG recordings that were digitized at 128 samples per second. The systolic CHF has data from 8 patients (5 men, 3 women) with an age range of 20 to 66 years and the diastolic CHF has data from 4 patients (all women) with an age range of 39 to 65. Because the short-term analysis was of interest, only 5-minute ECG data were used.

5.2.2 Preprocessing Stage

The second stage of the system covers noise removal from ECG records, data transformation from ECG to HRV data, removing ectopic beats, heart rate normalization, interpolation, and detrending steps. In this part of the thesis, all these steps were used in a sequence.

Smoothness priors based detrending algorithm was used to isolate baseline wander from ECG signals in this study. The smooth approximation of the signal was calculated and subtracted from the original ECG. This algorithm was tested using a synthetically generated data (McSharry, Clifford, Tarrassenko, & Smith, 2003) with artificially added baseline like sinusoid at 0.35 Hz (Fig. 5.4a). Then, this signal was high-pass filtered with the cut-off frequency of 0.64 Hz (Fig. 5.4b) as offered in (Christov, Dotsinsky, &

Daskalov, 1992) and smoothness priors method with λ=1000 (Fig. 5.4c) (İşler & Kuntalp, 2008).

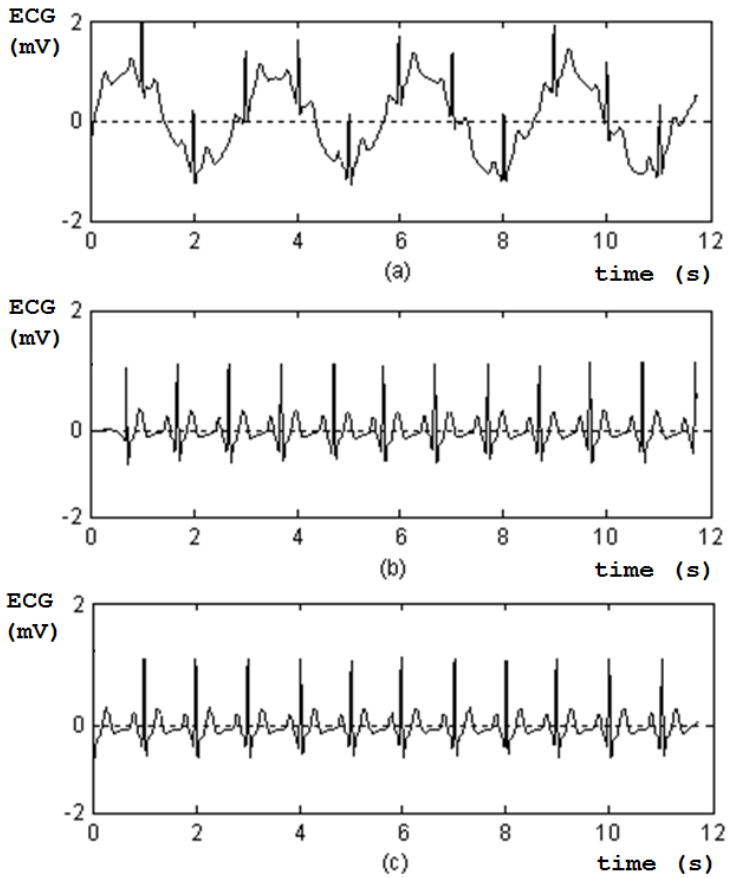

Figure 5.4 Baseline wander elimination from the synthetic ECG signal: (a) the corrupted signal with the sinusoid of 0.35 Hz, (b) baseline wander elimination using high-pass FIR filter, and (c) baseline wander elimination using smoothness priors (İşler & Kuntalp, 2008).

QRS complexes were obtained using the filtered and smoothed synthetic ECG signal. These values were compared to the original timing values (Table 5.9). The smoothness priors' based detrending method finds the correct QRS timings by comparing the classical high-pass filtering method. After detecting all R points using the QRS detection algorithm developed by Pan and Tompkins (Tompkins, 2000), RR interval (HRV data) were constructed using consequent R timing values. In addition, smoothness priors' method is able to determine all RR intervals correctly. The classical filtering method, on the other hand, has failed.

Table 5.9 QRS occurring timings and corresponding RR intervals for synthetically generated ECG (İşler & Kuntalp, 2008).

Synthetic ECG		After filtering		After smoothness priors	
QRS Occurring (s)	RR interval (s)	QRS Occurring (s)	RR interval (s)	QRS Occurring (s)	RR interval (s)
1.000	-	1.688	-	1.000	-
1.988	0.988	2.676	0.988	1.988	0.988
3.000	1.012	3.688	1.012	3.000	1.012
4.016	1.016	4.703	1.015	4.016	1.016
4.996	0.980	5.684	0.981	4.996	0.980
5.988	0.992	6.676	0.992	5.988	0.992
7.016	1.028	7.703	1.027	7.016	1.028
8.012	0.996	8.699	0.996	8.012	0.996
8.980	0.968	9.668	0.969	8.980	0.968
9.996	1.016	10.680	1.012	9.996	1.016
11.020	1.024	11.700	1.020	11.020	1.024

5.2.3 Feature Extraction Stage

The 71 features were calculated for this part of the thesis using the same methods described in Section 5.1.3. Patient information of age for all records in the data recorded was included into the study and summarized in Table 5.10. This feature seems to be statistically insignificant different between two groups.

Table 5.10 Patient age information for the patients with both systolic CHF and diastolic CHF. All values are presented as mean ± standard deviation.

Feature	***Systolic CHF***	***Diastolic CHF***	***p***	***SEN***	***SPE***	***POS***	***NEG***	***ACC***
Age	41.000±17.59	54.500±12.04	0.202	75	75	60	86	75

Time domain statistical measures were calculated using raw HRV data and heart rate normalized HRV data (Table 5.11). NaN values are used to indicate that there is no value for corresponding feature. Features related to NN50 measures were not presented because there were no HRV data that had successive differences more than ±50 ms. After heart rate normalization, NN20_2 (the number of HRV data that had successive differences less than -20ms) was also not presented. None of the time-domain measures showed statistically significant differences.

Table 5.11 Nominal 5-min time-domain metric values for the patients with both systolic CHF and diastolic CHF. All values are presented as mean ± standard deviation.

Feature	***Systolic CHF***	***Diastolic CHF***	***P***	***SEN***	***SPE***	***POS***	***NEG***	***ACC***
BEFORE HEART RATE NORMALIZATION								
MEAN	0.844±0.37	0.992±0.42	0.547	50	88	67	78	75
SDNN	0.528±1.35	1.489±1.99	0.340	50	88	67	78	75
RMSSD	0.661±1.74	1.713±2.23	0.387	50	88	67	78	75
NN20_1	0.125±0.35	0.500±1.00	0.348	25	88	50	70	67
NN20_2	0.125±0.35	0.500±1.00	0.348	25	88	50	70	67
NN20	0.250±0.71	1.000±2.00	0.348	25	88	50	70	67
PNN20	0.002±0.00	0.006±0.01	0.383	25	88	50	70	67
NN50_1	0.000±0.00	0.000±0.00	NaN	NaN	NaN	NaN	NaN	NaN
NN50_2	0.000±0.00	0.000±0.00	NaN	NaN	NaN	NaN	NaN	NaN
NN50	0.000±0.00	0.000±0.00	NaN	NaN	NaN	NaN	NaN	NaN
PNN50	0.000±0.00	0.000±0.00	NaN	NaN	NaN	NaN	NaN	NaN
SDSD	0.663±1.75	1.718±2.24	0.387	50	88	67	78	75
AFTER HEART RATE NORMALIZATION								
MEAN	0.800±0.00	0.800±0.00	0.019	50	75	50	75	67
SDNN	0.274±0.61	0.867±1.06	0.237	50	88	67	78	75
RMSSD	0.331±0.79	1.005±1.20	0.265	50	88	67	78	75
NN20_1	0.000±0.00	0.250±0.50	0.167	25	100	100	73	75
NN20_2	0.000±0.00	0.000±0.00	NaN	NaN	NaN	NaN	NaN	NaN
NN20	0.000±0.00	0.250±0.50	0.167	25	100	100	73	75
PNN20	0.000±0.00	0.001±0.00	0.167	25	100	100	73	75
NN50_1	0.000±0.00	0.000±0.00	NaN	NaN	NaN	NaN	NaN	NaN
NN50_2	0.000±0.00	0.000±0.00	NaN	NaN	NaN	NaN	NaN	NaN
NN50	0.000±0.00	0.000±0.00	NaN	NaN	NaN	NaN	NaN	NaN
PNN50	0.000±0.00	0.000±0.00	NaN	NaN	NaN	NaN	NaN	NaN
SDSD	0.332±0.79	1.008±1.21	0.265	50	88	67	78	75

Frequency domain measures have also been found common use in all the forms of signal processing field. These measures were calculated using the FFT-based PSD, Lomb-Scargle PSD, and Wavelet entropies (Table 5.12) similar to the previous part of the study. Because heart rate normalization process changed only the mean value of the data, the frequency domain measures were not affected from this process. In this table, LS algorithm based normalized LF power and normalized HF power, and wavelet entropy based HF power were found statistically different between two groups.

Table 5.12 Nominal 5-min frequency-domain metric values for the patients with both systolic CHF and diastolic CHF. All values are presented as mean ± standard deviation.

Feature	*Systolic CHF*	*Diastolic CHF*	*P*	*SEN*	*SPE*	*POS*	*NEG*	*ACC*
BEFORE HEART RATE NORMALIZATION								
LS_LFHF	2.715±2.97	0.454±0.14	0.169	100	50	50	100	67
LS_VLF	0.229±0.19	0.220±0.19	0.938	50	50	33	67	50
LS_LF	0.190±0.12	0.073±0.04	0.080	100	38	44	100	58
LS_HF	0.129±0.08	0.173±0.09	0.423	50	50	33	67	50
LS_NLF	0.599±0.22	0.308±0.06	0.030	100	63	57	100	75
LS_NHF	0.401±0.22	0.692±0.06	0.030	100	63	57	100	75
FFT_LFHF	9.31±14.79	115.82±224.39	0.189	25	100	100	73	75
FFT_VLF	401.61±1135.9	4.33±5.30	0.510	100	13	36	100	42
FFT_LF	90.346±255.53	19.893±36.06	0.604	75	13	30	50	33
FFT_HF	2.026±5.73	0.180±0.26	0.544	100	13	36	100	42
FFT_NLF	0.734±0.22	0.598±0.41	0.465	50	75	50	75	67
FFT_NHF	0.266±0.22	0.402±0.41	0.465	50	75	50	75	67
WS_LFHF	1.071±0.61	1.807±1.90	0.325	25	75	33	67	58
WS_VLF	0.390±0.49	1.034±0.77	0.103	50	88	67	78	75
WS_LF	1.031±0.87	0.583±0.72	0.398	75	50	43	80	58
WS_HF	0.847±0.49	0.265±0.13	0.044	100	63	57	100	75
WS_NLF	0.482±0.14	0.543±0.20	0.551	50	50	33	67	50
WS_NHF	0.518±0.14	0.457±0.20	0.551	50	50	33	67	50
AFTER HEART RATE NORMALIZATION								
LS_LFHF	2.715±2.97	0.454±0.14	0.169	100	50	50	100	67
LS_VLF	0.229±0.19	0.220±0.19	0.938	50	50	33	67	50
LS_LF	0.190±0.12	0.073±0.04	0.080	100	38	44	100	58
LS_HF	0.129±0.08	0.173±0.09	0.423	50	50	33	67	50
LS_NLF	0.599±0.22	0.308±0.06	0.030	100	63	57	100	75
LS_NHF	0.401±0.22	0.692±0.06	0.030	100	63	57	100	75
FFT_LFHF	9.31±14.79	115.82±224.39	0.189	25	100	100	73	75
FFT_VLF	84.658±239.45	1.602±1.87	0.514	100	13	36	100	42
FFT_LF	19.045±53.87	10.363±19.72	0.766	75	13	30	50	33
FFT_HF	0.427±1.21	0.059±0.07	0.565	100	13	36	100	42
FFT_NLF	0.734±0.22	0.598±0.41	0.465	50	75	50	75	67
FFT_NHF	0.266±0.22	0.402±0.41	0.465	50	75	50	75	67
WS_LFHF	1.071±0.61	1.807±1.90	0.325	25	75	33	67	58
WS_VLF	0.390±0.49	1.034±0.77	0.103	50	88	67	78	75
WS_LF	1.031±0.87	0.583±0.72	0.398	75	50	43	80	58
WS_HF	0.847±0.49	0.265±0.13	0.044	100	63	57	100	75
WS_NLF	0.482±0.14	0.543±0.20	0.551	50	50	33	67	50
WS_NHF	0.518±0.14	0.457±0.20	0.551	50	50	33	67	50

Poincare Plot measures were calculated using the ellipse-fitting method with ten different lag values from 1 to 10 for HRV data (Table 5.13) and heart rate normalized HRV data (Table 5.14). In both tables, no measures showed statistically significant differences although there were improvements in these measures of heart rate

normalized HRV analysis. In the heart rate normalized HRV analysis, all classifier performances were greater or equal than those of HRV analysis.

Table 5.13 Poincare plots' measures with 10 different lags for the patients with both systolic CHF and diastolic CHF using HRV data. All values are presented as mean ± standard deviation.

Feature	***Systolic CHF***	***Diastolic CHF***	***P***	***SEN***	***SPE***	***POS***	***NEG***	***ACC***
SD1_1	0.469±1.23	1.214±1.58	0.387	50	88	67	78	75
SD2_1	0.579±1.45	1.726±2.33	0.313	50	88	67	78	75
SD1SD2_1	1.842±5.20	4.857±7.87	0.440	25	88	50	70	67
RATIO_1	0.583±0.37	0.731±0.08	0.462	75	63	50	83	67
SD1_2	0.500±1.32	1.354±2.00	0.391	50	88	67	78	75
SD2_2	0.556±1.39	1.602±2.02	0.312	50	88	67	78	75
SD1SD2_2	1.876±5.30	5.103±8.60	0.434	25	88	50	70	67
RATIO_2	0.592±0.25	0.668±0.23	0.620	25	63	25	63	50
SD1_3	0.523±1.37	1.441±2.00	0.366	50	88	67	78	75
SD2_3	0.538±1.34	1.551±2.01	0.318	50	88	67	78	75
SD1SD2_3	1.891±5.34	5.228±8.60	0.421	25	88	50	70	67
RATIO_3	0.667±0.27	0.755±0.20	0.574	75	63	50	83	67
SD1_4	0.521±1.36	1.400±2.00	0.384	50	88	67	78	75
SD2_4	0.544±1.36	1.580±2.03	0.313	50	88	67	78	75
SD1SD2_4	1.902±5.37	5.206±8.67	0.428	25	88	50	70	67
RATIO_4	0.718±0.21	0.709±0.20	0.949	75	50	43	80	58
SD1_5	0.528±1.37	1.446±2.03	0.371	50	88	67	78	75
SD2_5	0.539±1.36	1.546±2.00	0.322	50	88	67	78	75
SD1SD2_5	1.914±5.41	5.256±8.71	0.426	25	88	50	70	67
RATIO_5	0.754±0.20	0.735±0.21	0.882	50	50	33	67	50
SD1_6	0.537±1.39	1.402±1.93	0.390	50	88	67	78	75
SD2_6	0.534±1.35	1.528±1.98	0.323	50	88	67	78	75
SD1SD2_6	1.925±5.44	4.999±8.19	0.450	25	88	50	70	67
RATIO_6	0.801±0.22	0.755±0.18	0.724	75	50	43	80	58
SD1_7	0.538±1.40	1.244±1.64	0.452	50	88	67	78	75
SD2_7	0.535±1.35	1.364±1.69	0.377	50	88	67	78	75
SD1SD2_7	1.937±5.47	3.766±5.76	0.603	50	88	67	78	75
RATIO_7	0.841±0.24	0.742±0.19	0.492	75	50	43	80	58
SD1_8	0.532±1.38	1.250±1.66	0.444	50	88	67	78	75
SD2_8	0.545±1.38	1.362±1.68	0.387	50	88	67	78	75
SD1SD2_8	1.950±5.51	3.777±5.80	0.606	50	88	67	78	75
RATIO_8	0.828±0.23	0.769±0.18	0.668	75	50	43	80	58
SD1_9	0.443±1.12	1.234±1.60	0.338	50	88	67	78	75
SD2_9	0.622±1.60	1.384±1.74	0.467	50	88	67	78	75
SD1SD2_9	1.847±5.21	3.799±5.81	0.568	50	88	67	78	75
RATIO_9	0.829±0.25	0.739±0.17	0.541	50	50	33	67	50
SD1_10	0.530±1.37	1.217±1.64	0.458	50	88	67	78	75
SD2_10	0.554±1.41	1.398±1.73	0.382	50	88	67	78	75
SD1SD2_10	1.974±5.57	3.791±5.87	0.612	25	88	50	70	67
RATIO_10	0.872±0.25	0.737±0.18	0.361	75	63	50	83	67

Table 5.14 Poincare plots' measures with 10 different lags for the patients with both systolic CHF and diastolic CHF using heart rate normalized HRV data. All values are presented as mean ± standard deviation.

Feature	***Systolic CHF***	***Diastolic CHF***	***P***	***SEN***	***SPE***	***POS***	***NEG***	***ACC***
SD1_1	0.235±0.56	0.713±0.85	0.265	50	88	67	78	75
SD2_1	0.304±0.65	1.001±1.24	0.220	50	88	67	78	75
SD1SD2_1	0.390±1.10	1.501±2.08	0.243	50	88	67	78	75
RATIO_1	0.583±0.37	0.731±0.08	0.462	75	63	50	83	67
SD1_2	0.251±0.60	0.765±1.03	0.291	50	88	67	78	75
SD2_2	0.294±0.62	0.950±1.11	0.211	50	88	67	78	75
SD1SD2_2	0.398±1.12	1.539±2.26	0.257	50	88	67	78	75
RATIO_2	0.592±0.25	0.668±0.23	0.620	25	63	25	63	50
SD1_3	0.263±0.62	0.829±1.05	0.260	50	88	67	78	75
SD2_3	0.284±0.60	0.912±1.09	0.218	50	88	67	78	75
SD1SD2_3	0.401±1.12	1.601±2.27	0.237	50	88	67	78	75
RATIO_3	0.667±0.27	0.755±0.20	0.574	75	63	50	83	67
SD1_4	0.264±0.61	0.799±1.04	0.281	50	88	67	78	75
SD2_4	0.286±0.61	0.932±1.10	0.213	50	88	67	78	75
SD1SD2_4	0.404±1.13	1.582±2.28	0.248	50	88	67	78	75
RATIO_4	0.718±0.21	0.709±0.20	0.949	75	50	43	80	58
SD1_5	0.268±0.62	0.829±1.06	0.267	50	88	67	78	75
SD2_5	0.283±0.61	0.909±1.08	0.220	50	88	67	78	75
SD1SD2_5	0.406±1.14	1.603±2.29	0.243	50	88	67	78	75
RATIO_5	0.754±0.20	0.735±0.21	0.882	50	50	33	67	50
SD1_6	0.273±0.63	0.808±1.02	0.280	50	88	67	78	75
SD2_6	0.280±0.60	0.898±1.07	0.221	50	88	67	78	75
SD1SD2_6	0.409±1.14	1.535±2.16	0.255	50	88	67	78	75
RATIO_6	0.801±0.22	0.755±0.18	0.724	75	50	43	80	58
SD1_7	0.274±0.63	0.727±0.88	0.325	50	88	67	78	75
SD2_7	0.280±0.61	0.813±0.94	0.257	50	88	67	78	75
SD1SD2_7	0.411±1.15	1.206±1.55	0.337	50	88	67	78	75
RATIO_7	0.841±0.24	0.742±0.19	0.492	75	50	43	80	58
SD1_8	0.271±0.62	0.728±0.89	0.320	50	88	67	78	75
SD2_8	0.285±0.62	0.814±0.94	0.264	50	88	67	78	75
SD1SD2_8	0.414±1.16	1.207±1.56	0.340	50	88	67	78	75
RATIO_8	0.828±0.23	0.769±0.18	0.668	75	50	43	80	58
SD1_9	0.231±0.50	0.725±0.87	0.233	50	88	67	78	75
SD2_9	0.320±0.72	0.821±0.96	0.331	50	88	67	78	75
SD1SD2_9	0.392±1.10	1.217±1.57	0.309	50	88	67	78	75
RATIO_9	0.829±0.25	0.739±0.17	0.541	50	50	33	67	50
SD1_10	0.271±0.62	0.707±0.87	0.335	50	88	67	78	75
SD2_10	0.288±0.63	0.835±0.97	0.260	50	88	67	78	75
SD1SD2_10	0.419±1.17	1.205±1.57	0.349	50	88	67	78	75
RATIO_10	0.872±0.25	0.737±0.18	0.361	75	63	50	83	67

5.2.4 Feature Selection and Classification Stages

These stages were applied similar to Section 5.1.4 and 5.1.5. The only differences were that the classification was performed using 1- and 3- nearest neighbor classifiers and the features that had NaN values in their accuracies of Table 5.11 were excluded from the study. Therefore, 67 features were used in HRV analysis and 66 features were used in heart rate normalized HRV analysis.

5.2.5 Model Evaluation Stage

The results, as can be seen from the Table 5.15, show that using both MINMAX and HR normalization procedures improves the performance of the classification. The maximum accuracy is found as 100.0% in the configuration of MINMAX and HR normalized features selected with GA using a KNN classifier with k=1 among the constructed classifiers. The selected features in this combination were AGE, SDNN, RMSSD, SD2 (lag=2), RATIO (lag=7), SD2 (lag=9), RATIO (lag=9), SD2 (lag=10), LS algorithm based PSD measures of LF/HF ratio, VLF power, and normalized HF power, FFT algorithm based PSD measures of VLF power and HF power, and wavelet entropy measure of normalized HF power (İşler & Kuntalp, 2009b). Although the results seem to be satisfactory, there are only 12 participants in this part of the study and there is need of extra data to enhance the validity of this part.

Table 5.15 Classifier results where k is the parameter of the KNN classifier, SEN is sensitivity (%), SPE is specificity (%), POS is positive predictivity (%), NEG is negative predictivity (%), and ACC is accuracy (%).In the algorithm (Alg.) column, HRV shows HRV analysis and HRN shows heart rate normalized HRV analysis (İşler & Kuntalp, 2009b).

Alg.	***k***	***without MINMAX***					***with MINMAX***				
		SEN	***SPE***	***POS***	***NEG***	***ACC***	***SEN***	***SPE***	***POS***	***NEG***	***ACC***
HRV	1	87.50	100.0	100.0	80.00	91.67	87.50	100.0	100.0	80.00	91.67
	3	100.0	0.0	66.67	0.0	66.67	100.0	0.0	66.67	0.0	66.67
HRN	1	87.50	100.0	100.0	80.00	91.67	100.0	100.0	100.0	100.0	100.0
	3	100.0	0.0	66.67	0.0	66.67	100.0	25.00	72.73	100.0	75.00

CHAPTER SIX
CONCLUSION

Congestive Heart Failure (CHF) is a decreased ability of the heart to either fill itself with blood or emptying it with the fluid accumulation in various parts of the body. Although the diagnosis of heart failure is straightforward, it often challenges physicians because particular aspects of the syndrome lead to confusion. When heart failure is suspected, certain elements of the physical examination aid in the diagnosis. Unfortunately, the examination often does not yield enough information for confirmation. Although several diagnostic criteria schemes are available, their clinical utility is still questionable. Clinical assessment is mandatory before detailed investigations are conducted in patients with suspected heart failure, although specific clinical features are often absent and the condition can be diagnosed accurately only in conjunction with more objective investigation, particularly echocardiography. Echocardiography has been accepted as a golden standard to make the diagnosis of CHF. However the echocardiography is relatively expensive and thus does not exist in every health facility. In addition, the average waiting time for echocardiography was 1 month. On the other hand, the ECG is a cheap and common device that it can be found in almost every health station. Moreover, an ECG study was performed at a local hospital with a usual waiting time of 48h. Therefore, if an optimal diagnostic strategy based on the ECG to detect CHF can be presented; this would help to enhance the rate of early diagnosis cases, notably by the every-day practice. In this study, the goal is to be able to use the ECG device for the diagnosis of CHF and discriminating between its two types, i.e. systolic vs diastolic CHF.

In addition to discriminate the patients with CHF, from normal subjects, to distinguish diastolic heart failure from systolic heart failure based on physical findings or symptoms is also an important issue. Echocardiography has been used as a primary tool in the noninvasive assessment of cardiac systolic and diastolic dysfunctioning and is used to confirm the diagnosis of CHF. Thus, simple and reliable diagnostic procedures are very important for primary care physicians, who are responsible for the early diagnosis of CHF and implementation of an adequate therapy.

A healthy heart rapidly adjusts heart rate (HR) and other autonomic parameters in response to internal and external stimuli. A heart that has been weakened is less able to make such adjustments and therefore exhibits lower heart rate variability (HRV), i.e. shows fewer variations in its beat-to-beat timing. In certain circumstances, the evaluation of HRV has been shown to provide an indication of cardiovascular health. CHF has been the subject of many studies using HRV analysis. Majority of the CHF studies use HRV measures as predictors of the risk of mortality (prognosis). However, only a few studies have been focused on using HRV measures for diagnosis purpose.

This dissertation contributes into different stages in HRV analysis for the diagnosis purpose in CHF. These contributions are removing baseline wandering using smoothness priors' method, removing the effects of different heart rates using the heart rate normalization method in the preprocessing stage, using Wavelet entropy measures, using Poincare plot measures with different lags in the feature extraction stage, and finding the optimal feature combinations using GA and KNN classifier in the following stages.

In the first contribution, it was shown that the smoothness priors based baseline removal method can be applied instead of classical filtering techniques. This method does not lead to the phase difference with the original ECG signal, which helps to the exact determination of the QRS timing. Nonetheless, this method causes extreme computational load when compared to the classical filtering methods. In addition, this method requires whole data, which makes realizing the real time applications using this method impossible.

In the second contribution, the wavelet entropy based frequency domain measures were shown to improve the discrimination power of the HRV analysis. Because of its nature, the Wavelet transform is even suitable for using in nonstationary signals. Although the HRV signal is a nonstationary signal, only short-term (5-minute long) HRV data has been used to assume it stationary as offered in the Task Force.

In addition, the Poincare plot measures with different lags were shown not to improve the discrimination power of the HRV analysis. Classical Poincare measures show only 2-D properties. Nonetheless, some studies showed that the HRV data had

properties of higher dimensional space. The results showed that using Poincare measures with different lags did not improve the classification performances in this work.

The effects of HR normalization over the HRV data were also studied in this study. The class discrimination power of different combinations of short-term HRV measures were investigated using HRV data obtained from an on-line and widely-used database. The hypothesis in this thesis was that using the heart normalization preprocessing technique would remove the effects of different heart rates. This would make the analysis independent from the mean heart rate consideration as discussed in the Task Force.

The best combinations of the features were selected by a GA. A KNN classifier was used to evaluate the performance of each feature set selected since this classification method does not depend on the data following any particular distribution. The six-stage system (Fig. 5.1), which visualizes the whole study, summarizes all the techniques used in the short-term HRV analysis, which will help the novice researchers.

The results in discriminating the normal subjects from the patients with CHF, as can be seen from the Tables 5.6, 5.7, and 5.8, show that using both MINMAX and HR normalization procedures improves the performance of the classification. The maximum accuracy is found as 93.98% using a KNN classifier with k=1, 3, and 5 among the constructed classifiers.

The results in discriminating the systolic CHF patients from the diastolic CHF patients, as can be seen from the Table 5.15, also show that using both MINMAX and HR normalization procedures improves the performance of the classification. The maximum accuracy is found as 100.00% in the configuration of MINMAX and HR normalized features selected with GA using a KNN classifier with k=1 among the constructed classifiers.

As a result, heart rate normalization process and using both patient information and wavelet entropy based measures in addition to the classical HRV indices seem to increase the effect of the heart rate variability analysis at least in diagnosing the patients

with CHF and discriminating the systolic CHF patients from the diastolic CHF patients. On the other hand, using lagged Poincare plots measures were found to be not much of help in improving the performance of discriminating CHF patients from normal subjects.

Obviously, the performances of different combinations of features depend on the type of the classifier used. In this study, only the KNN classifier was used. Using other classifier types such as multilayer perceptrons (MLP), radial basis functions (RBF), and support vector machines (SVM) could further improve the accuracy values. Moreover, using long-term HRV measures in addition to the short-term ones could also increase the diagnostic ability of the constructed classifier systems.

In addition, the AR-based frequency domain measures were not included in the study because of its limitation in selecting an adequate model order. Although there have been many papers on selecting an adequate model order, it is still an open question in studies related to the HRV analysis. After including these AR-based frequency-domain measures, the study may expose a higher classification power.

Although the classification results achieved in the thesis seem satisfactory, larger databases are needed to confirm the achieved results. In addition, there is a lack of information such as drug use, physical activity and emotional states, which should be considered during performing the HRV analysis. Because this information was not noted in the databases used, the studies covered in the thesis neglected these considerations. The performance of the classification systems is hoped to improve further if these additional parameters are taken into account.

REFERENCES

Acır, N. (2005). Classification of ECG beats by using a fast least square support vector machines with a dynamic programming feature selection algorithm. *Neural Computing and Applications*, 14, 299–309.

Adams, K.F., Baughman, K.L., Konstam, M.A., Dec, W.G., Liu, P., Elkayam, U., Massie, B.M., Forker, A.D., Patterson, J.H., Gheorghiade, M., Silver, M.A., Hermann, D., & Stevenson, L.W. (2000). Heart failure society guidelines: A model of consensus and excellence. *Pharmacotherapy*, 20(5), 495–522.

Akselrod, S., Gordon, D., Ubel, F.A., Shannon, D.C., Barger, A.C., & Cohen, R.J. (1981). Power spectrum analysis of heart rate fluctuation: a quantitative probe of beat–to–beat cardiovascular control. *Science*, 213, 220–222.

Albert, N.M. (2000). Implementation strategies to manage heart failure outcomes: Managing clinical and economic outcomes. *AACN Clinical Issues: Advanced Practice in Acute & Critical Care*, 11(3), 396–411 & 475–477.

Aldroubi, A., & Unser, M. (1996). *Wavelets in Medicine and Biology*. CRC Press, Inc.

American Heart Association (1975). Recommendations for standardization of lead and specifications for instruments in ECG/VCG. *Circulation*, 52, 11–25.

American Heart Association (2005). ACC/AHA 2005 guideline update for the diagnosis and management of chronic heart failure in the adult: a report of the American College of Cardiology / American Heart Association Task Force on practice guidelines (writing committee to update the 2001 guidelines for the evaluation and management of heart failure). *Journal of the American College of Cardiology*, 46, 1–82.

American Heart Association (2006). Heart disease and stroke statistics–2006 update: A report from the American heart association statistics committee and stroke statistics subcommittee. *Circulation*, 113, 85–151.

Anastasiou-Nana, M.I., Terrovitis, J.V., Athanasoulis, T., Karaloizos, L., Geramoutsos, A., Pappa, L., Tsagalou, E., Efentakis, S., & Nanas, J. (2005). Prognostic value of iodine-123-metaiodobenzylguanidine myocardial uptake and heart rate variability in chronic congestive heart failure secondary to ischemic or idiopathic dilated cardiomyopathy. *American Journal of Cardiology*, 96(3), 427–431.

Antila, K.J., Valimaki, I.A.T., Makela, M., Tuominen, J., Wilson, A.J., & Southall, D.P. (1990). Heart rate variability in infants subsequently suffering sudden infant death syndrome (SIDS). *Early Human Development*, 22, 57–72.

Aronson, D., Mittleman, M.A., & Burger, A.J. (2004). Measures of heart period variability as predictors of mortality in hospitalized patients with decompensated congestive heart failure. *American Journal of Cardiology*, 93, 59–63.

Artinian, N.T., Harden, J.K., Kronenberg, M.W., Vander Wal, J.S., Daher, E., Stephensa, Q., & Bazzia, R.I. (2003). Pilot study of a web–based compliance monitoring device for patients with congestive heart failure. *Heart & Lung: The Journal of Acute and Critical Care*, 32(4), 226–233.

Ashcroft, S., & Pereira, C. (2003). *Practical Statistics for the Biological Sciences: Simple Pathways to Statistical Analyses*. Palgrave Macmillan, 1st ed.

Asyalı, M.H. (2003). Discrimination power of long–term heart rate variability measures. *In Proceedings of the 25th Annual International Conference of the IEEE Engineering in Medicine and Biology Society*, Cancun.

Bakardjian, H., & Yamamoto, K. (1995). Dynamic non–deterministic characterization of HRV through multiresolution wavelet decomposition. *In Annual International Conference of the IEEE Engineering in Medicine and Biology – Proceedings*, 17(2), 1063–1064.

Barbieri, R., Triedman, J.K., & Saul, J.P. (2002). Heart rate control and mechanical cardiopulmonary coupling to assess central volume: a systems analysis. *American Journal of Physiology - Regulatory, Integrative and Comparative Physiology*, 283, R1210–R1220.

Barrett, C.J., Navakatikyan, M.A., & Malpas, S.C. (2001). Long–term control of renal blood flow: what is the role of the renal nerves? *American Journal of Physiology - Regulatory, Integrative and Comparative Physiology*, 280, R1534–R1545.

Berne, R., & Levy, M. (1997). *Cardiovascular Physiology*. 7th ed.

Berntson, G.G., Bigger, T., Eckberg, D.L., Grossman, P., Kaufmann, P.G., Malik, M., Nagaraja, H.N., Porges, S.W., Saul, J.P., Stone, P.H., & van der Molen, M.W. (1997). Heart rate variability: Origins, methods, and interpretive caveats. *Psychophysiology*, 34, 623–648.

Bigger, J.T., Albrecht, P., Steinman, R.C., Rolnitzky, L.M., Fleiss, J.L., & Cohen, R.J. (1989). Comparison of time– and frequency domain–based measures of cardiac parasympathetic activity in Holter recordings after myocardial infarction. *American Journal of Cardiology*, 64, 536–538.

Bigger, J.T., Fleiss, J.L., Steinman, R.C., Rolnitzky, L.M., Kleiger, R.E., & Rottman, J.N. (1992). Correlations among time and frequency domain measures of heart

period variability two weeks after acute myocardial infarction. *American Journal of Cardiology*, 69, 891–898.

Bilchick, K.C., Fetics, B., Djoukeng, R., Gross, F.S., Fletcher, R.D., Singh, S.N., Nevo, E., & Berger, R.D. (2002). Prognostic value of heart rate variability in chronic congestive heart failure. *American Journal of Cardiology*, 90, 24–28.

Binder, T., Frey, B., Porenta, G., Heinz, G., Wutte, M., Kreiner, G., Gössinger, H., Schmidinger, R., Packer, H., & Weber, H. (1992). Prognostic value of heart rate variability in patients awaiting cardiac transplantation. *Pacing and Clinical Electrophysiology*, 15, 2215–2220.

Binkley, P.F., Nunziata, E., Haas, G.J., Nelson, S.D., & Cody, R.J. (1991). Parasympathetic withdrawal is an integral component of autonomic imbalance in congestive heart failure: demonstration in human subjects and verification in a paced canine model of ventricular failure. *Journal of the American College of Cardiology* , 18, 464–472.

Blanco, S., Figliola, A., Quian, Q.R., Rosso, O.A., & Serrano, E. (1998). Time–frequency analysis of electroencephalogram series (iii): information transfer function and wavelet packets. *Physical Review E*, 57, 932–940.

Bonaduce, D., Petretta, M., Marciano, F., Vicario, M., Apicella, C., Rao, M., Nicolai, E., & Volpe, M. (1999). Independent and incremental prognostic value of heart rate variability in patients with chronic heart failure. *American Heart Journal*, 138(2), 273–284.

Boveda, S., Galinier, M., Pathak, A., Fourcade, J., Dongay, B., Benchendikh, D., Massabuau, P., Fauvel, J.M., Senard, J.M., & Bounhoure, J.P. (2001). Prognostic

value of heart rate variability in time domain analysis in congestive heart failure. *Journal of Interventional Cardiac Electrophysiology*, 5(2), 181–187.

Boyd, K.J., Murray, S.A., Kendall, M., Worth, A., Benton, T.F., & Clausen, H. (2004). Living with advanced heart failure: a prospective, community based study of patients and their carers. *European Journal of Heart Failure*, 6(5), 585–591.

Braga, A.N., da Silva Lemos, M., da Silva, J.R., Fontes, W.R., & dos Santos, R.A. (2002). Effects of angiotensions on day–night fluctuations and stress–induced changes in blood pressure. *American Journal of Physiology - Regulatory, Integrative and Comparative Physiology*, 282, R1663–R1671.

Braune, H.J., & Geisenorfer, U. (1995). Measurement of heart rate variations: influencing factors, normal values and diagnostic impact on diabetic autonomic neuropathy. *Diabetes Research and Clinical Practice*, 29, 179–187.

Brennan, M., Palaniswami, M., & Kamen, P. (2001). Do existing measures of Poincare plot geometry reflect nonlinear features of heart rate variability? *IEEE Transactions on Biomedical Engineering*, 48(11), 1342–1347.

Brouwer, J., van Veldhuisen, D.J., Veld, A.J., Haaksma, J., Dijk,W.A., Visser, K.R., Boomsma, F., & Dunselman, P.H. (1996). The dutch ibopamine multicenter trial study group prognostic value of heart rate variability during long-term follow-up in patients with mild to moderate heart failure. *Journal of the American College of Cardiology*, 28, 1183–1189.

Butler, G.C., Ando, S., & Floras, J.S. (1997). Fractal component of variability of heart rate and systolic blood pressure in congestive heart failure. *Clinical Science*, 92, 543–550.

Cao, H. (2004). *Linear and nonlinear approaches to heart rate analysis near the time of birth*. Ph.D. thesis, University of Virginia, Department of Biomedical Engineering, USA.

Casolo, G., Balli, E., Taddei, T., Amuhasi, J., & Gori, C. (1989). Decreased spontaneous heart rate variability on congestive heart failure. *American Journal of Cardiology*, 64, 1162–1167.

Casolo, G.C., Stroder, P., Sulla, A., Chelucci, A., Freni, A., & Zerauschek, M. (1995). Heart rate variability and functional severity of congestive heart failure secondary to coronary artery disease. *European Heart Journal*, 16, 360–367.

Chang, K.L., Monahan, K.J., Griffin, M.P., Lake, D.E., & Moorman, J.R. (2001). Comparison and clinical application of frequency domain methods in analysis of neonatal heart rate time series. *Annals of Biomedical Engineering*, 29, 764–774.

Chattipakorn, N., Incharoen, T., Kanlop, N., & Chattipakorn, S. (2007). Heart rate variability in myocardial infarction and heart failure. *International Journal of Cardiology*, 120, 289–296.

Chiarugi, F., Colantonio, S., Emmanouilidou, D., Moroni, D., & Salvetti, O. (2008). Biomedical signal and image processing for decision support in heart failure. *Computers in Cardiology*, 35, 649–652.

Christov, I.I., Dotsinsky, I.A., & Daskalov, I.K. (March 1992). High pass filtering of ECG signals using QRS elimination. *Medical & Biological Engineering & Computing*, 253–256.

Clark, D.O., Tu, W., Weiner, M., & Murray, M.D. (2003). Correlates of health–related quality of life among lower–income, urban adults with congestive heart failure. *Heart & Lung: The Journal of Acute and Critical Care*, 32(6), 391–401.

Clifford, G.D., Azuaje, F., & McSharry, P.E. (2006). *Advanced Methods and Tools for ECG Data Analysis*. Artech House, Inc., Norwood, MA.

Clifford, G.D., & Tarassenko, L. (2005). Quantifying errors in spectral estimates of HRV due to beat replacement and resampling. *IEEE Transactions on Biomedical Engineering*, 52(4), 630–638.

Contreras, P., Canetti, R., & Migliaro, E.R. (2007). Correlations between frequency-domain HRV indices and lagged Poincare plot width in healthy and diabetic subjects. *Physiological Measurement*, 28, 85–94.

Cooley, J.W., & Tukey, J.W. (1965). An algorithm for the machine computation of complex Fourier series. *Mathematical Computations*, 19, 297–301.

Cooper, P.J., Lei, M., Cheng, L.X., & Kohl, P. (2000). Selected contribution: axial stretch increases spontaneous pacemaker activity in rabbit isolated sinoatrial node cells. *Journal of Applied Physiology*, 89(5), 2099–2104.

Costa, M., Goldberger, A.L., & Peng, C.K. (2002). Multiscale entropy analysis of physiologic time series. *Physical Review Letters*, 89, 062102.

Costa, M., Goldberger, A.L., & Peng, C.K. (2005). Multiscale entropy analysis of biological signals. *Physical Review E*, 71, 021906.

Costa, M., & Healey, J.A. (2003). Multiscale entropy analysis of complex heart rate dynamics: Discrimination of age and heart failure effects. *Computers in Cardiology*, 30, 705–708.

Costa, O., Lago, P., Rocha, A.P., Carvalho, M.J., Freitas, A., Freitas, J., Puig, J., Brando, A., & de Freitas, F. (1994). Heart rate variability in 24–hour Holter recordings. Comparative study between short– and long –term time and frequency–domain analyses. *Journal of Electrocardiology*, 27, 251–254.

Coumel, P., Hermid, J.S., Wennerblom, B., Leenhardt, P., Blanche, M., & Cauchemez, B. (1991). Heart rate variability in left ventricular hypertrophy and heart failure, and the effects of beta-blockade. a non-spectral analysis of heart rate variability in the frequency domain and in the time domain. *European Heart Journal*, 12, 412–422.

Daskalov, I., & Christov, I. (1997). Improvement of resolution in measurement of electrocardiogram RR intervals by interpolation. *Medical Engineering & Physics*, 19(4), 375–379.

Davie, A.P., Francis, C.M., Caruana, L., Sutherland, G.R., & McMurray, J.J. (1997). Assessing diagnosis in heart failure: which features are any use? *QJM - An International Journal of Medicine*, 90, 335–339.

Davies, M.K., Gibbs, C.R., & Lip, G.Y.H. (2000). ABC of heart failure investigation. *British Medical Journal*, 320, 297–300.

de Jong, K.A. (1975). *Analysis of the behaviour of a class of genetic adaptive systems*. Ph.D. thesis, University of Michigan, Ann Arbor, USA.

Dionne, I., White, M., & Tremblay, M. (2002). The reproducibility of power spectrum analysis of heart rate variability before and after a standardized meal. *Physiology & Behavior*, 75(3), 267–270.

Dosh, S. A. (2004). Diagnosis of heart failure in adults. *American Family Physician*, 70(11), 2145–2152.

Duda, R.O., Hart, P.E., & Stork, D.G. (2001). *Pattern Classification*. New York: John Wiley & Sons, 2nd ed.

Eberhart, R.C., & Dobbins, R.W. (1990). *Neural network PC tools*. San Diego: Academic Press.

Eberhart-Phillips, J., Fenaughty, A., & Rarig, A. (2003). *The burden of cardiovascular disease in Alaska: Mortality, hospitalization and risk factors*. Anchorage, AK: Section of Epidemiology, Division of Public Health, Alaska Department of Health and Social Services.

Edlinger, G., Litscher, G., & Pfurtscheller, G. (1994). Analysis of cardio-respiratory signals – methodology and applications in infants. *Biomedizinische Technik*, 39, 274–278.

Engin, M. (2007). Spectral and wavelet based assessment of congestive heart failure patients. *Computers in Biology and Medicine*, 37(6), 820–828.

Ewing, D.J., Martin, C.N., Young, R.J., & Clarke, B.F. (1985). The value of cardiovascular autonomic function tests: 10 years' experience in diabetes. *Diabetes Care*, 8, 491–498.

Fei, L., Keeling, P.J., Gill, J.S., Bashir, Y., Statters, D.J., Poloniecki, J., McKenna, W. J., & Camm, A.J. (1994). Heart rate variability and its relation to ventricular arrhythmias in congestive heart failure. *British Heart Journal*, 71, 322–328.

Flavell, C., & Stevenson, L.W. (2001). Take heart with heart failure. *Circulation*, 104, e89.

Fonseca, C., Mota, T., Morais, H., Matias, F., Costa, C., Oliveira, A.G., Ceia, F., & on behalf of the EPICA Investigators (2004). The value of the electrocardiogram and chest X-ray for confirming or refuting a suspected diagnosis of heart failure in the community. *European Journal of Heart Failure*, 6(6), 807–812.

Galinier, M., Pathak, A., Fourcade, J., Androdias, C., Curnier, D., Varnous, S., Boveda, S., Massabuau, P., Fauvel, M., Senard, J.M., & Bounhoure, J.P. (2000). Depressed low frequency power of heart rate variability as an independent predictor of sudden death in chronic heart failure. *European Heart Journal*, 21, 475–482.

General Electric Company, G.H. (2009). *Diagnostic ECG*. Available on the web at http://www.gehealthcare.com/euen/cardiology/products/diagnostic_ecg/algorithms/index.html.

Gibbons, R.J., Balady, G.J., Beasley, J.W., Bricker, J.T., Duvernoy, W.F., Froelicher, V.F., Mark, D.B., Marwick, T.H., McCallister, B.D., Thompson, P.D.J., Winters, W.L., Yanowitz, F.G., Ritchie, J.L., Cheitlin, M.D., Eagle, K.A., Gardner, T.J., Garson, A.J., Lewis, R.P., O'Rourke, R.A., & Ryan, T.J. (July, 1997). ACC/AHA guidelines for exercise testing, a report of the American College of Cardiology/ American Heart Association Task Force on practice guidelines (committee on exercise testing). *Journal of the American College of Cardiology*, 30(1), 260–311.

Gillespie, N.D. (2006). The diagnosis and management of chronic heart failure in the older patient. *British Medical Bulletin*, 75–76(1), 49–62.

Goldberg, D.E. (1989). *Genetic algorithms in search, optimization, and machine learning*. New York: Addison Wesley Pub. Comp. Inc.

Goldberg, D.E., & Deb, K. (1991). A comparison of selection schemes used in genetic algorithms. *In Foundation of Genetic Algorithms*, 69–93.

Goldberger, A.L., Amaral, L.A.N., Glass, L., Hausdorf, J.M., Ivanov, P.C., Mark, R.G., Mietus, J.E., Moody, G.B., Peng, C.K., & Stanley, H.E. (2000). Physiobank, physiotoolkit, and physionet: Components of a new research resource for complex physiologic signals. *Circulation*, 101(23), e215–e220.

Goldstein, B., Fiser, D.H., Kelly, M.M., Mickelsen, D., Ruttimann, U., & Pollack, M.M. (1998). Decomplexification in critical illness and injury: relationship between heart rate variability, severity of illness, and outcome. *Critical Care Medicine*, 26, 352–357.

Grossman, P. (1992). Breathing rhythms of the heart in a world of no steady state: a comment on weber, molenaar, and van der molen. *Psychophysiology*, 29(1), 66–72.

Gura, M.T., & Foreman, L. (2004). Cardiac resynchronization therapy for heart failure management. *AACN Clinical Issues: Advanced Practice in Acute & Critical Care*, 15(3), 326–339.

Gutierrez, C., & Blanchard, D.G. (2004). Diastolic heart failure: Challenges of diagnosis and treatment. *American Family Physician*, 69(11), 2609–2616.

Guzzetti, S., Cogliati, C., Turiel, M., Crema, C., Lombardi, F., & Malliani, A. (1995). Sympathetic predominance followed by functional denervation in the progression of chronic heart failure. *European Heart Journal*, 16, 1100–1107.

Guzzetti, S., La Rovere, M.T., Pinna, G.D., Maestri, R., Borroni, E., Porta, A., Mortara, A., & Malliani, A. (2005). Different spectral components of 24 h heart rate variability are related to different modes of death in chronic heart failure. *European Heart Journal*, 26, 357–362.

Güler, İ., & Übeyli, E.D. (2005a). ECG beat classifier designed by combined neural network model. *Pattern Recognition*, 38(2), 199–208.

Güler, İ., & Übeyli, E.D. (2005b). An expert system for detection of electrocardiographic changes in patients with partial epilepsy using wavelet-based neural networks. *Expert Systems*, 22(2), 62–71.

Hadase, M., Azuma, A., Zen, K., Asada, S., Kawasaki, T., Kamitani, T., Kawasaki, S., Sugihara, H., & Matsubara, H. (2004). Very low frequency power of heart rate variability is a powerful predictor of clinical prognosis in patients with congestive heart failure. *Circulation Journal*, 68(4), 343–347.

Hallstrom, A.P., Stein, P.K., Schneider, R., Hodges, M., Schmidt, G., & Ulm, K. (2004). Structural relationships between measures based on heart beat intervals: Potential for improved risk assessment. *IEEE Transactions on Biomedical Engineering*, 51(8), 1414–1420.

Hamilton, R., Mckenchnie, P., & Macfarlane, P. (2004). Can cardiac vagal tone be estimated from the 10-second ECG? *International Journal of Cardiology*, 95(1), 109–115.

Harper, R.M., Hoppenbrouwers, T., Sterman, M.B., McGinty, D.J., & Hodgman, J. (1976). Polygraphic studies of normal infants during the first six months of life. I: Heart rate and variability as a function of state. *Pediatric Research*, 10, 945–951.

Hirsh, J.A., & Bishop, B. (1981). Respiratory sinus arrhythmia in humans: how breathing pattern modulates heart rate. *American Journal of Physiology*, 241, H620–H629.

Ho, K.K.L., Moody, G.B., Peng, C.K., Mietus, J.E., Larson, M.G., Levy, D., & Goldberger, A.L. (1997). Predicting survival in heart failure cases and controls using fully automated methods for deriving nonlinear and conventional indices of heart rate dynamics. *Circulation*, 96, 842–848.

Hobbs, F.D.R., Korewicki, J., Cleland, J.G.F., Eastaugh, J., & Freemantle, N. (2005). The diagnosis of heart failure in European primary care: The IMPROVEMENT programme survey of perception and practice. *European Journal of Heart Failure*, 7, 768–779.

Holland, J. (1975). *Adaptation in Natural and Artificial Systems*. Univ. of Michigan Press, Ann Arbor, Mich.

Hombach, V. (2006). Electrocardiography of the failing heart. *Cardiology Clinics*, 24, 413–426.

Hon, E.H., & Lee, S.T. (1965). Electronic evaluations of the fetal heart rate patterns preceding fetal death: further observations. *American Journal of Obstetrics and Gynecology*, 814–826.

Hu, K., Ivanov, P.C., Chen, Z., Carpena, P., & Stanley, H.E. (2001). Effect of trends on detrended fluctuation analysis. *Physical Review E*, 64, 1–19.

Huikuri, H.V., Makikallio, T.H., Raatikainen, P., Perkiomaki, J., Castellanos, A., & Myerburg, R.J. (2003). Prediction of sudden sudden cardiac death: appraisal of the studies and methods assessing the risk of sudden arrhythmic death. *Circulation*, 108(1), 110–115.

Ingle, V.K., & Proakis, J.G. (2000). *Digital Signal Processing Using Matlab*. Pacific Grove, USA: Brooks/Cole Publishing Company.

Izard, C.E., Simons, R.F., Haynes, O.M., Porges, S.W., & Cohen, B. (1991). Infant cardiac activity: Developmental changes and relations with attachment. *Developmental Psychology*, 27(3), 432–439.

İşler, Y., Özyürek, S., Çobanoğlu, O., and Kuntalp, M. (2008). The Performance Effects of the Cut-Off Frequencies of the Filters Used In QRS Detection Algorithms, *XIV. Biyomedikal Mühendisliği Ulusal Toplantısı BIYOMUT 2008*, Ankara / Turkey.

İşler, Y., Avcu, N., Kocaoğlu, A., & Kuntalp, M. (2008). Investigating the effects of the methods used in frequency domain measures in heart rate variability analysis. *In Proceedings of SIU2008, IEEE 16th Signal Processing and Communications Applications Conference*, Didim, Aydın, Turkey.

İşler, Y., & Kuntalp, M. (2006). Investigating the effects of wavelet entropy in heart rate variability analysis for diagnosing of congestive heart failure. *In Proceedings of SIU2006, IEEE 14th Signal Processing and Communications Applications Conference*, Antalya, Turkey.

İşler, Y., & Kuntalp, M. (2007a). Combining classical HRV indices with wavelet entropy measures improves to performance in diagnosing congestive heart failure. *Computers in Biology and Medicine*, 37(10), 1502–1510.

İşler, Y., & Kuntalp, M. (2007b). Investigating effects of wavelet entropy detailed measures in heart rate variability analysis. *In Proceedings of SIU2007, IEEE 15th Signal Processing and Communications Applications Conference*, Eskisehir, Turkey.

İşler, Y., & Kuntalp, M. (2008). ECG baseline wander elimination using smoothness priors based detrending method. *In 13. Biyomedikal Mühendisliği Ulusal Toplantısı,* Ankara, Turkey.

İşler, Y., & Kuntalp, M. (2009a). Heart rate normalization in the analysis of heart rate variability in congestive heart failure. *Proceedings of the Institution of Mechanical Engineers, Part H: Journal of Engineering in Medicine*, in press, available online from http://dx.doi.org/10.1243/09544119JEIM642.

İşler, Y., & Kuntalp, M. (2009b). Systolic and Diastolic Dysfunction Discrimination in Congestive Heart Failure Patients using Heart Rate Variability Analysis. *IEEE Transactions on Biomedical Engineering*, under review.

İşler, Y., Selver, M.A., & Kuntalp, M. (2005). Effects of detrending in heart rate variability analysis. *In II. Mühendislik Bilimleri Genç Araştırmacılar Kongresi: MBGAK2005*, İstanbul, Turkey, 213–219.

Jain, A.K., Duin, R.P.W., & Mao, J. (2000). Statistical pattern recognition: A review. *IEEE Transactions on Pattern Analysis and Machine Intelligence*, 22(1), 4–37.

Jain, A.K., & Zongker, D. (1997). Feature selection evaluation, application, and small sample performance. *IEEE Transactions on Pattern Analysis and Machine Intelligence*, 19(2), 153–158.

Jiang, M., Hathaway, W.R., McNulty, M., Larsen, P.C., Hansley, R., Zhang, M., & O'Connor, M. (1997). Ability of heart rate variability to predict prognosis in patients with advanced congestive heart failure. *American Journal of Cardiology*, 80(6), 808–811.

John, G.H., Kohavi, R., & Pfleger, K. (1994). Irrelevant features and the subset selection problem. *In Proceedings of 11th International Conference on Machine Learning*, 121–129.

Kamen, P.W. (1996). Heart rate variability. *Australian Family Physician*, 25, 1087–1094.

Kamen, P.W., Krum, H., & Tonkin, A.M. (1996). Poincare plot of heart rate variability allows quantitative display of parasympathetic nervous activity. *Clinical Science*, 92, 201–208.

Kamen, P.W., & Tonkin, A.M. (1995). Application of the Poincare plot to heart rate variability: a new measure of functional status in heart failure. A*ustralian & New Zealand Journal of Medicine*, 25(1), 18–26.

Kantelhardt, J.W., Koscielny-Bunde, E., Rego, H.H.A., Havlin, S., & Bunde, A. (2001). Detecting long–range correlations with detrended fluctuation analysis. *Physica A*, 295, 441–454.

Kienzle, M.G., Ferguson, D.W., Birkett, C.L., Myers, G.A., Berg, W.J., & Mariano, D.J. (1992). Clinical hemodynamic and sympathetic neural correlates of heart rate

variability in congestive heart failure. *American Journal of Cardiology*, 69, 482–485.

Kingwell, B.A., Thompson, J.M., Kaye, D.M., McPherson, G.A., Jennings, G.L., & Elser, M.D. (1994). Heart rate spectral analysis, cardiac norepinephrine spillover, and muscle sympathetic nerve activity during human sympathetic nervous activation and failure. *Circulation*, 90, 234–240.

Kleiger, R.E., Bigger, J.T., Bosner, M.S., Chung, M.K., Cook, J.R., Rolnitzky, L.M., Steinman, R., & Fleiss, J.L. (1991). Stability over time of variables measuring heart rate variability in normal subjects. *American Journal of Cardiology*, 68, 626.

Kleiger, R.E., Miller, J.P., Bigger, J.T., & Moss, A.J. (1987). Decreased heart rate variability and its association with increased mortality after acute myocardial infarction. *American Journal of Cardiology*, 59(4), 256–262.

Kohler, B.-U., Hennig, C., & Orglmeister, R. (2002). The principles of software QRS detection: Reviewing and comparing algorithms for detecting this important ECG waveform. *IEEE Engineering in Medicine and Biology Magazine*, 21(1), 42–57.

Kotsiantis, S.B., Kanellopoulos, D., & Pintelas, P.E. (2006). Data preprocessing for supervised learning. *Transactions on Engineering, Computing and Technology*, 12, 277–282.

Koza, R.J. (1992). *Genetic programming, on the programming of computers by means of natural selection*. Cambridge Massachusetts: MIT Press.

Kreyzig, E. (1993). *Advanced Engineering Mathematics*. Wiley, New York, 7th ed.

La Rovere, M.T., Pinna, G.D., Maestri, R., Mortara, A., Capomolla, S., Febo, O., Ferrari, R., Franchini, M., Gnemmi, M., Opasich, C., Riccardi, P.G., Traversi, E., & Cobelli, F. (2003). Short-term heart rate variability strongly predicts sudden cardiac death in chronic heart failure patients. *Circulation*, 107(4), 565.

Laguna, P., Moody, G.B., & Mark, R.G. (1998). Power spectral density of unevenly sampled data by least–square analysis: Performance and application to heart rate signals. *IEEE Transactions on Biomedical Engineering*, 45(6), 698–715.

Landes, R.A., Scher, M.S., Sun, M., & Sclabassi, R.J. (1996). Characterization of heart rate dynamics in infants as a probe for neural state and age. *In 18th Annual International Conference of the IEEE Engineering in Medicine and Biology Society*, 1662–1663.

Lanfranchi, P.A., & Somers, V.K. (2002). Arterial baroreflex function and cardiovascular variability: interactions and implications. *American Journal of Physiology - Regulatory, Integrative and Comparative Physiology*, 283, R815–R826.

Langer, G.A., Frank, J.S., & Brady, A.J. (1976). *Cardiovascular physiology*. Baltimore: University Park.

Langley, P., di Bernardo, D., Allen, J., Bowers, E., Smith, F.E., Vecchietti, S., & Murray, A. (2001). Can paroxysmal atrial fibrillation be predicted? *Computers in Cardiology*, 28, 121–124.

Leistner, H.L., Haddad, G.G., Epstein, R.A., Lai, T.L., Epstein, M.F., & Mellins, R.B. (1980). Heart rate and heart rate variability during sleep in aborted sudden infant death syndrome. *The Journal of Pediatrics*, 97(1), 51–55.

Levy, D., Kenchaiah, S., Larson, M.G., Benjamin, E.J., Kupka, M.J., Ho, K.K.L., Murabito, J.M., & Vasan, R.S. (2001). Long–term trends in the incidence of and survival with heart failure. *The New England Journal of Medicine*, 347(18), 1397–1402.

Liao, D., Barnes, R.W., Chambless, L.E., & Heiss, G. (1996). A computer algorithm to impute interrupted heart rate data for the spectral analysis of heart rate variability–the ARIC study. *Computers and Biomedical research*, 29, 140–151.

Lippman, N., Stein, K.M., & Lerman, B.B. (1993). Nonlinear predictive interpolation: a new method for the correction of ectopic beats for heart rate variability analysis. *Journal of Electrocardiology*, 26, S14–S19.

Lippman, N., Stein, K.M., & Lerman, B.B. (1994). Comparison of methods for removal of ectopy in measurement of heart rate variability. *American Journal of Physiology*, 267(1), H411–H418.

Litvack, D.A., Oberlander, T.F., Carney, L.H., & Saul, J.P. (1995). Time and frequency domain methods for heart rate variability analysis: a methodological comparison. *Psychophysiology*, 32, 492–504.

Lomb, N.R. (1976). Least–squares frequency analysis of unequally spaced data. *Astrophysical and Space Science*, 39, 447–462.

Lombardi, F., Makikallio, T.H., Myerburg, R.J., & Huikuri, H. (2001). Sudden cardiac death: role of heart rate variability to identify patients at risk. *Cardiovascular Research*, 50, 210–217.

Lucreziotti, S., Gavazzi, A., Scelsi, L., Inserra, C., Klersy, C., Campana, C., Ghio, S., Vanoli, E., & Tavazzi, L. (2000). Five-minute recording of heart rate variability in

severe chronic heart failure: Correlates with right ventricular function and prognostic implication. *American Heart Journal*, 139(6), 1088–1095.

Luczak, H., & Lauring, W.J. (1973). An analysis of heart rate variability. *Ergonomics*, 16, 85–97.

Lynn, K.S., & Chiang, H.D. (2001). A two–stage solution algorithm for paroxysmal atrial fibrillation prediction. *Computers in Cardiology*, 28, 405–407.

Macfarlane, P.W. (1992). Recent developments in computer analysis of ECGs. *Clinical Physiology and Functional Imaging*, 12(3), 313–317.

MacFarlane, P.W., Peden, J., Lennox, J., Watts, M.P., & Lawrie, T.D. (1977). The Glasgow system. *In Proceedings Of Trends in Computer-Processed Electrocardiograms*, North-Holland, 143–150.

Makikallio, T.H., Huikuri, H.V., Hintze, U., Videbaek, J., Mitrani, R.D., Castellanos, A., Myerburg, R.J., & Moller, M. (2001). Fractal analysis and time- and frequency-domain measures of heart rate variability as predictors of mortality in patients with heart failure. *American Journal of Cardiology*, 87, 178–182.

Malik, M., & Camm, A.J. (1995). *Heart Rate Variability*. Futura Publishing Company.

Malik, M., Cripps, T., Farrell, T., & Camm, A.J. (1989). Prognostic value of heart rate variability after myocardial infarction. a comparison of different data–processing methods. *Medical & Biological Engineering & Computing*, 27, 603–611.

Malik, M., Farrell, T., Cripps, T., & Camm, A.J. (1989). Heart rate variability in relation to prognosis after myocardial infarction: selection of optimal processing techniques. *European Heart Journal*, 10, 1060–1074.

Malpas, S.C. (2002). Neural influences on cardiovascular variability: possibilities and pitfalls. *American Journal of Physiology – Heart & Circulatory Physiology*, 282, H6–H20.

Marciano, M.L., Migaux, F., Acanfora, D., Furgi, G., & Rengo, F. (1994). Quantification of Poincare maps for the evaluation of heart rate variability. *Computers in Cardiology*, 557–580.

Mateo, J., & Laguna, P. (2003). Analysis of heart rate variability in the presence of ectopic beats using the heart timing signal. *IEEE Transactions on Biomedical Engineering*, 50(3), 334–343.

Mazursky, J.E., Birkett, C.L., Bedell, K.A., Ben-Haim, S.A., & Segar, J.L. (1998). Development of baroreflex influences on heart rate variability in preterm infants. *Early Human Development*, 53(1), 37–52.

McNames, J., & Aboy, M. (2006). Reliability and accuracy of heart rate variability metrics versus ECG segment duration. *Medical & Biological Engineering & Computing*, 44, 747–756.

McSharry, P.E., Clifford, G.D., Tarassenko, L., & Smith, L. (2003). A dynamical model for generating synthetic electrocardiogram signals. *IEEE Transactions On Biomedical Engineering*, 50(3), 289–294.

Medigue, C., Bestel, J, Renard, S., Garrido, M., Pizarro O'Ryan, F., & Peirano, P. (1997). Discrete wavelet transform applied to heart rate variability analysis in iron–deficient anemic infant. *In Proceedings of 19th International Conference on IEEE/EMBS*, 1613–1616.

Merri, M., Farden, D.C., Mottley, J.G., & Titlebaum, E.L. (1990). Sampling frequency of the electrocardiogram for spectral analysis of the heart rate variability. *IEEE Transactions on Biomedical Engineering*, 37(1), 99–106.

Meyer, C.R., & Kelser, H.N. (1977). Electrocardiogram baseline noise estimation and removal using cubic splines and state-space computation techniques. *Computers and Biomedical Research*, 10, 459–470.

Mietus, J.E., Peng, C.K., Henry, I., Goldsmith, R.L., & Goldberger, A.L. (2002). The pNNx files: re–examining a widely used heart rate variability measure. *Heart*, 88, 378–380.

Mitchell, T.M. (1997). *Machine Learning*. McGraw–Hill Companies Press.

Mitov, I.P. (1998). A method for assessment and processing of biomedical signals containing trend and periodic components. *Medical Engineering & Physics*, 20(9), 660–668.

Mokikallio, T.H., Seppanen, T., Airaksinen, J.K.E., Koistinen, J., Tulppo, M.P., Peng, C.K., Goldberger, A.L., & Huikuri, H.V. (1997). Dynamical analysis of heart rate may predict subsequent ventricular tachycardia after myocardial infarction. *American Journal of Cardiology*, 80, 779–783.

Moody, G.B., Goldberger, A.L., McClennen, S., & Swiryn, S. (2001). Predicting the onset of paroxysmal atrial fibrillation. *Computers in Cardiolody*, 28, 113–116.

Mortara, A., La Rovere, M.T., Signorini, M.G., Pantaleo, P., Pinna, G., Martinelli, L., Ceconi, C., Cerutti, S., & Tavazzi, L. (1994). Can power spectral analysis of heart rate variability identify a high risk subgroup of congestive heart failure patients with excessive sympathetic activation? *British Heart Journal*, 71, 422–430.

Mozaffary, B., & Tinati, M.A. (2005). ECG baseline wander elimination using wavelet packets. *Proceedings of World Academy of Science, Engineering and Technology*, 3, 22–24.

Mrowka, R., Schluter, B., Gerhardt, D., & Patzak, A. (1996). Heart rate control in infants at high risk for sudden infant death syndrome SIDS. *Computers in Cardiology*, 173–176.

Myers, G.A., Martin, G.J., Magid, N.M., Barnett, P.S., Schaad, J.W., Weiss, J.S., Lesch, M., & Singer, D.H. (1986). Power spectral analysis of heart rate variability in sudden cardiac death: comparison to other methods. *IEEE Transactions on Biomedical Engineering*, 33(12), 1149–1156.

Nixon, M.S. & Aguado, A.S. (2002). *Feature extraction & image processing*. Newness Butterworth-Heinemann, Woburn, 1st ed.

Ori, Z., Monir, G., Weiss, J., Sayhouni, X., & Singer, D.H. (1992). Heart rate variability frequency domain analysis. *Cardiology Clinics*, 10(3), 499–533.

Osowski, S., Hoai, L.T., & Markiewicz, T. (2004). Support vector machine-based expert system for reliable heartbeat recognition. *IEEE Transactions on Biomedical Engineering*, 51(4), 582–589.

Pagani, M. (2000). Heart rate variability and autonomic diabetic neuropathy. *Diabetes Nutrition Metabolism*, 13(6), 341–346.

Pagani, M., Lombardi, F., Guzzetti, S., Rimoldi, O., Furlan, R., Pizzinelli, P., Sandrone, G., Malfatto, G., Dell'Orto, S., Piccaluga, E., Turiel, M., Baselli, G., Cerutti, S., & Malliani, A. (1986). Power spectral analysis of heart rate and arterial pressure

variabilities as a marker of sympathovagal interaction in man and conscious dog. *Circulation Research*, 59, 178–193.

Pahlm, O., & Sornmo, L. (1984). Software QRS detection in ambulatory monitoring – a review. *Medical & Biological Engineering & Computing*, 22, 289–297.

Pakhomov, S.V., Buntrock, J., & Chute, C.G. (2003). Identification of patients with congestive heart failure using a binary classifier: a case study. *In Proceedings of the ACL 2003 Workshop on Natural Language Processing in Biomedicine*, 89–96, Cancun.

Pan, J., & Tompkins, W.J. (1985). A real–time QRS detection algorithm. *IEEE Transactions on Biomedical Engineering*, 32(3), 230–236.

Panina, G., Khot, U.N., Nunziata, E., Cody, R.J., & Binkley, P.F. (1995). Assessment of autonomic tone over a 24-hour period in patients with congestive heart failure: relation between mean heart rate and measures of heart rate variability. *American Heart Journal*, 129, 748–753.

Penaz, J., Roukenz, J., & Van der Waal, H.J. (1968). Spectral analysis of some spontaneous rhythms in the circulation. *In Leipzig, Germany: Biokybernetik, Karl Marx University*, 233–241.

Peng, C.K., Buldyrev, S.V., Havlin, S., Simons, M., Stanley, H.E., & Goldberger, A.L. (1994). Mosaic organization of DNA nucleotides. *Physical Review E*, 49, 1685-1689.

Pernkopf, F. (2005). Bayesian network classifiers versus selective kNN classifier. *Pattern Recognition*, 38(1), 1–10.

Pichot, V., Gaspoz, J.M., Molltex, S., Antoniadis, A., Busso, T., Roche, F., Costes, F., Quintin, L., Lacour, J.R., & Barthelemy, J.C. (1999). Wavelet transform to quantify heart rate variability and to assess its instantaneous changes. *Journal of Applied Physiology,* 86(3), 1081–1091.

Pikkujamsa, S.M., Makikallio, T.H., Sourander, L.B., Raiha, I.J., Puukka, P., Skytta, J., Peng, C.-K., Goldberger, A.L., & Huikuri, H.V. (1999). Cardiac interbeat interval dynamics from childhood to senescence: Comparison of conventional and new measures based on fractals and chaos theory. *Circulation*, 100, 393-399.

Pincus, S.M. (1991). Approximate entropy as a measure of system complexity. *Proceedings of the National Academy of Sciences*, 88, 2297–2301.

Pinna, G.D., Maestri, R., Di Cesare, A., Colombo, R., & Minuco, G. (1994). The accuracy of power–spectrum analysis of heart–rate variability from annotated RR lists generated by Holter systems. *Physiological Measurement*, 15, 163–179.

Pomeranz, M., Macaulay, R.J.B., Caudill, M.A., Kutz, I., Adam, D., Gordon, D., Kilborn, K.M., Barger, A.C., Shannon, D.C., Cohen, R.J., & Benson, M. (1985). Assessment of autonomic function in humans by heart rate spectral analysis. *American Journal of Physiology*, 248, H151–H153.

Ponikowski, P., Anker, S.D., Chua, T.P., Szelemej, R., Piepoli, M., Adamopoulus, K., Webb-Peploe, S., Harrington, D., Banasiak, W., Wrabec, K., & Coats, A.J. (1997). Deppressed heart rate variability as an independent predictor of death in chronic congestive heart failure secondary to ischemic or idiopathic dilated cardiomyopathy. *American Journal of Cardiology,* 79, 1645–11650.

Ponikowski, P., Chua, T.P., Amadi, A.A., Piepoli, M., Harrington, D., Volterrani, M., Colombo, R., Mazzuero, G., Giordano, A., & Coats, A.J. (1996). Detection and

significance of a discrete very low frequency rhythm in RR interval variability in chronic congestive heart failure. *American Journal of Cardiology*, 77, 1320–1326.

Porter, G.A. J., & Rivkees, S.A. (2004). Ontogeny of humoral heart rate regulation in the embryonic mouse. *American Journal of Physiology – Heart & Circulatory Physiology*, 281, R401–R407.

Proakis, J.G., & Manolakis, D.G. (1996). *Digital signal processing: principles, algorithms, and applications*. New Jersey: Prentice Hall.

Raymer, M.L., Punch, W.F., Goodman, E.D., Kuhn, L.A., & Jain, A.K. (2000). Dimensionality reduction using genetic algorithms. *IEEE Transactions on Evolutionary Computation*, 4(2), 164–171.

Rentero, N., Cividjian, A., Trevaks, D., Pequignot, J.M., Quintin, L., & McAllen, R.M. (2002). Activity patterns of cardiac vagal motoneurons in rat nucleus ambiguous. *American Journal of Physiology - Regulatory, Integrative and Comparative Physiology*, 283, R1327–R1334.

Richard, G., Sandercock, H., & Brodie, D.A. (2006). The role of heart rate variability in prognosis for different modes of death in chronic heart failure. *Pacing and Clinical Electrophysiology*, 29, 892–904.

Rompelman, O. (1993). Rhythms and analysis techniques, *In The Physics of Heart and Circulation*, 101–120. Institute of Physics Publishing, Bristol.

Rosenstock, E.G., Cassuto, Y., & Zmora, E. (1999). Heart rate variability in the neonate and infant: Analytical methods, physiological and clinical observations. *Acta Paediatrica*, 88, 477–482.

Rosso, O.A., Blanco, S., Yordanova, J., Kolev, V., Figliola, A., & Başar, E. (2001). Wavelet entropy: a new tool for analysis of short duration brain electrical signals. *Journal of Neuroscience Methods*, 105, 65–75.

Rosso, O.A., Quian, Q.R., Blanco, S., Figliola, A., & Başar, E. (1998).Wavelet–entropy applied to brain signal analysis. *In Proceedings of the IX European Signal Processing Conference, EUSIPCO–98*, IV, 2445–2448.

Rottman, J.N., Steinman, R.C., Albrecht, P., Bigger, J.T.J., Rolnitzky, L.M., & Fleiss, J.L. (1990). Efficient estimation of the heart period power spectrum suitable for physiologic or pharmacologic studies. *American Journal of Cardiology*, 66, 1522–1523.

Sanderson, J.E. (1998). Heart rate variability in heart failure. *Heart Failure Reviews*, 2, 235–244.

Sanderson, J.E., Yeung, L.Y.C., Yeung, D.T.K., Kay, R.L.C., Tomlinson, B., Critchley, J.A.J.H., Woo, K.S., & Bernardi, L. (1996). Impact of changes in respiratory frequency and posture on power spectral density analysis of heart rate and systolic blood pressure variability in normal subjects and patients with heart failure. *Clinical Science*, 90, 1–9.

Saul, J.P., Arai, Y., Berger, R.D., Lily, L.S., Wilson, S., Colucci, W.S., & Cohen, R.J. (1988). Assessment of autonomic regulation in chronic congestive heart failure by heart rate spectral analysis. *American Journal of Cardiology*, 61, 1292–1299.

Sayers, B.M. (1973). Analysis of heart rate variability. *Ergonomics*, 16, 17–32.

Scargle, J.D. (1982). Studies in astronomical time series analysis. II. statistical aspects of spectral analysis of unevenly spaced data. *Astrophysical Journal*, 263, 835–853.

Schechtman, V.L., Henslee, J.A., & Harper, R.M. (1998). Developmental patterns of heart rate variability in infants with persistent apnea of infancy. *Early Human Development*, 50, 251–262.

Schilling, R.J., & Sandra, L.H. (1999). *Applied Numerical Methods for Engineers*. Pacific Grove, CA, USA: Brooks/Cole Publishing Company.

Shamsham, F., & Mitchell, J. (2000). Essentials of the diagnosis of heart failure. *American Family Physician*, 61, 1319–1328.

Shannon, C.E. (1948). A mathematical theory of communication. *Bell Systems Technology Journal*, 27, 379–423 & 623–656.

Shimazu, M., Ojima, S., Takasugi, S.-I., Nejime, T., & Kamishima, T. (1999). Time–frequency analysis of heart rate variability using complex discrete wavelet transform. *In Annual International Conference of the IEEE Engineering in Medicine and Biology – Proceedings*, 958.

Siedlecki,W., & Sklansky, J. (1989). A note on genetic algorithms for large–scale feature selection. *Pattern Recognition Letters*, 10, 335–347.

Smith, A.L., Reynolds, K.J., & Owen, H. (2007). Correlated Poincare indices for measuring heart rate variability. *Australasian Physical & Engineering Sciences in Medicine*, 30(4), 336–341.

Sornmo, L. (1993). Time varying digital filtering of ECG baseline wander. *Medical & Biological Engineering & Computing*, 31, 503–508.

Soyadi, O., & Shamsollahi, M.B. (2008). Model-based fiducial points extraction for baseline wandered electrocardiograms. *IEEE Transactions on Biomedical Engineering*, 55(1), 347–351.

Spicer, C.C., & Lawrence, C.J. (1987). Statistical analysis of heart rates in subsequent victims of sudden infant death syndrome. *Statistics in Medicine,* 6, 159–166.

Stein, P.K., Le, Q., & Domitrovich, P.P. (2008). Development of more erratic heart rate patterns is associated with mortality post-MI. *Journal of Electrocardiology,* 41(2), 110–115.

Stevens, V.G., Wilson, A.J., Franks, C.I., & Southall, D.P. (1988). Techniques for the analysis of long–term cardio-respiratory recordings from infants. *Medical & Biological Engineering & Computing*, 26, 282–288.

Syswerda, G. (1989). Uniform crossover in genetic algorithms. *In Proceedings of 3rd International Conference on Genetic Algorithms*, 2–9.

Szabo, D.J., van Veldhuisen, B.M., van der Veer, N., Brouwer, J., De Graeff, P.A., & Crijns, H.J. (1997). Prognostic value of heart rate variability in chronic congestive heart failure secondary to idiopathic or ischemic dilated cardiomyopathy. *American Journal of Cardiology*, 79, 978–980.

Şahan, S., Polat, K., Kodaz, H., & Güneş, S. (2007). A new hybrid method based on fuzzy–artificial immune system and k–NN algorithm for breast cancer diagnosis. *Computers in Biology and Medicine,* 37, 415–423.

Şeker, R., Saliu, S., Birand, A., & Kudaiberdieva (2000). Validity test for a set of nonlinear measures for short data length with reference to short-term heart rate variability signal. *Journal of Systems Integration,* 10, 41–53.

Tanabe, T., Iwamoto, T., Fusegawa, Y., Yoshioka, K., & Shina, Y. (1995). Alterations of sympathovagal balance in patients with hypertrophic and dilated cardiomyopathies assessed by spectral analysis of RR interval variability. *European Heart Journal*, 16, 799–807.

Taqqu, M.S., Teverovsky, V., & Willinger, W. (1995). Estimators for long range dependence: An empirical study. *Fractals*, 3, 785–798.

Tarvainen, M.P., Ranta-aho, P.O., & Karjalainen, P.A. (2002). An advanced detrending method with application to HRV analysis. *IEEE Transactions on Biomedical Engineeering*, 49(2), 172–175.

Task Force [of the European Society of Cardiology and the North American Society of Pacing and Electrophysiology] (1996). Heart rate variability: Standards of measurement, physiological interpretation, and clinical use. *European Heart Journal*, 17, 354–381.

Thakre, T.P., & Smith, M.L. (2006). Loss of lag-response curvilinearity of indices of heart rate variability in congestive heart failure. *BMC Cardiovascular Disorders*, 6, 27.

Tompkins, W. J. (2000). *Biomedical Digital Signal Processing*. Prentice Hall, Upper Saddle River, New Jersey.

Torrence, C., & Compo, G.P. (1998). A practical guide to wavelet analysis. *Bulletin of the American Meteorological Society*, 79(1), 61–78.

Übeyli, E.D. (2007). ECG beats classification using multiclass support vector machines with error correcting output codes. *Digital Signal Processing*, 17, 675–684.

Übeyli, E.D. (2009). Combining recurrent neural networks with eigenvector methods for classification of ECG beats. *Digital Signal Processing*, 19, 320–329.

Vafaie, H., & De Jong, K. (1995). Genetic algorithms as a tool for restructuring feature space representations. *In Proceedings, 7th International Conference on Tools with Artificial Intelligence*, 8–11.

Valafar, F. (2001). Applications of Neural Networks in Medicine and Biological Sciences. In *Intelligent Control Systems Using Soft Computing Methodologies*. CRC.

Van Aleste, J.A., & Schilder, T.S. (1985). Removal of baseline wander and power-line interference from the ECG by an efficient FIR filter with a reduced number of taps. *IEEE Transactions on Biomedical Engineering*, 32(12), 1052–1060.

Van de Borne, P., Montano, N., Pagani, M., Oren, R., & Somers, V.K. (1997). Absence of low-frequency variability of sympathetic nerve activity in sever heart failure. *Circulation*, 95, 1449–1454.

Vatanabe, S. (1985). *Pattern recognition: human and mechanical*. New York: JohnWiley & Sons Inc.

Vornanen, M., Ryokkynen, A., & Nurmi, A. (2002). Temperature–dependent expression of sarcolemmal K+ currents in rainbow trout atrial and ventricular myocytes. *Journal of Physiology - Regulatory, Integrative and Comparative Physiology*, 282, R1191–R1199.

Wang, X., & Paliwal, K.K. (2003). Feature extraction and dimensionality reduction algorithms and their applications in vowel recognition, pattern recognition. *Journal of the Pattern Recognition Society*, 36, 2429–2439.

Warner, M., & Loeb, J. (1986). Beat-by-beat modulation of AV conduction I. heart rate and respiratory influences. *American Journal of Physiology – Heart & Circulatory Physiology*, 251, 1126–1133.

Weber, E.J.M., Molenaar, C.M., & van der Molen, M.W. (1992). A nonstationarity test for the spectral analysis of physiological time series with an application to respiratory sinus arrhythmia. *Psychophysiology*, 29(1), 55–65.

Webster, J. G. (1993). *Design of cardiac pacemakers*. TAB–IEEE Press.

Webster, J. G. (1998). *Medical instrumentation–application and design*. Houghton Mifflin Company, 3rd ed.

Wiklund, U., Akay, M., & Niklasson, U. (1997). Short–term analysis of heart–rate variability by adapted wavelet transforms. *IEEE Engineering in Medicine and Biology*, 16(5), 113–118 & 138.

Wilbur, J., & James, P. (2005). Diagnosis and management of heart failure in the outpatient setting. *Primary Care: Clinics in Office Practice*, 32, 1115–1129.

Williams, T.D., Chambers, J.B., Henderson, R.P., Rashotte, M.E., & Overton, J.M. (2002). Cardiovascular responses to caloric restriction and thermo–neutrality in C57BL/6J mice. *American Journal of Physiology - Regulatory, Integrative and Comparative Physiology*, 282, R1459–R1467.

Wolf, M. M., Varigos, G. A., Hunt, D., & Sloman, J. G. (1978). Sinus arrhythmia in acute myocardial infarction. *Medical Journal of Australia*, 2, 52–53.

Woo, M.A., Stevenson, W.G., & Middlekauff, H.R. (1994). Complex heart rate variability and serum norepinephrine levels in patients with advanced heart failure. *Journal of the American College of Cardiology*, 23, 565–569.

Woo, M.A., Stevenson, W.G., Moser, D.K., Trelease, R.B., & Harper, R.H. (1992). Patterns of beat–to–beat heart rate variability in advanced heart failure. *American Heart Journal*, 123, 704–710.

Yanowitz, F.G. (2006). *ECG learning center in cyberspace*. Available on the web at http://library.med.utah.edu/kw/ecg/index.html.

Yeragani, V.K., Sobolewski, E., Jampala, V.C., Kay, J., Yeragani, S., & Igel, G. (1998). Fractal dimension and approximate entropy of heart period and heart rate: Awake versus sleep differences and methodological issues. *Clinical Science*, 95, 295–301.

Zambroski, C.H. (2003). Qualitative analysis of living with heart failure. *Heart & Lung: The Journal of Acute and Critical Care*, 32(1), 32–40.

Zongker, D., & Jain, A.K. (1996). Algorithms for feature selection: an evaluation. *In ICPR'96: International Conference on Pattern Recognition*, 18–22.

APPENDIX A
STATISTICAL ANALYSIS

A.1 Hypothesis Testing

Hypothesis testing is the use of statistics to determine the probability that a given hypothesis is true. There are four general steps to test (Ashcroft & Pereira, 2003):

- Formulate the null hypothesis H_0 (commonly, that the observations are the result of pure chance) and the alternative hypothesis H_1 (commonly, that the observations show a real effect combined with a component of chance variation).
- Identify a test statistic that can be used to assess the truth of the null hypothesis.
- Compute the *p*-value, which is the probability that a statistic at least as significant as the one observed would be obtained assuming that the null hypothesis were true. The smaller *p*-value, the stronger the evidence against the null hypothesis.
- Compare the *p*-value to an acceptable significance value, α. If $p \leq \alpha$, that the observed effect is statistically significant, and the alternative hypothesis is valid. The most commonly used significance level is $\alpha = 0.05$ (for a two-sided test, α/2).

Hypotheses are generally defined as:

$$H_0: \mu_1 = \mu_2 \tag{A.1}$$

and

$$H_1: \mu_1 \neq \mu_2 \tag{A.2}$$

where μ_1 and μ_2 are the mean values of two groups.

A.1.1 General t-Testing

A t-test is a statistical hypothesis test in which the test statistic has a Student's t distribution if the null hypothesis is true. It is applied when the population is assumed to

be normally distributed but the sample sizes are small enough that the statistic on which inference is based is not normally distributed because it relies on an uncertain estimate of standard deviation rather than on a precisely known value. The general formula for t-test is as follows:

$$t = \frac{(Statistics) - (Hypothesized\ value\ of\ parameter)}{(Estimated\ standard\ error\ of\ statistics)} \tag{A.3}$$

Among the t tests, the unpaired t-Test with Unequal Variance method, which is given in the following subsection, is used in the thesis.

A.1.2 Unpaired t-Test with Unequal Variance

The difference from the previous test is that the variance in two samples is extremely different, meaning samples are very different in size. The two sample t test for unpaired data is defined as:

$$t = \frac{\bar{x}_1 - \bar{x}_2}{\sqrt{\frac{s_1^2}{n_1} + \frac{s_2^2}{n_2}}} \tag{A.4}$$

where n_1 and n_2 are the sample sizes, $\bar{x}_1$ and $\bar{x}_2$ are the sample means, and s_1^2 and s_2^2 are the sample variances. It assumes that the degree of freedom (*d.f.*) is calculated by:

$$d.f. = \frac{\left(\frac{s_1^2}{n_1} + \frac{s_2^2}{n_2}\right)^2}{\frac{\left(\frac{s_1^2}{n_1}\right)^2}{n_1 - 1} + \frac{\left(\frac{s_2^2}{n_2}\right)^2}{n_2 - 1}} \tag{A.5}$$

where *d.f.* is rounded to an integer value after this calculation is completed.